

RESPONSE CHARACTERISTICS OF PULMONARY
MECHANORECEPTORS OF THE FROG

by


Thomas A. McKean, B. A.

A THESIS


Presented to the Department of Physiology
and the Graduate Division of the University of Oregon Medical School
in partial fulfillment of
the requirements for the degree of
Doctor of Philosophy

April 1968

APPROVED:



(Professor in Charge of Thesis)



(Chairman, Graduate Council)

ACKNOWLEDGEMENTS

Three people rose above and beyond the call of duty in assisting with this thesis. Their names are, in alphabetical order, John M. Brookhart, Cynthia F. McKean, and Shigemi Mori.

I also wish to acknowledge The National Institutes of Health for the financial support of my work and my family.

TABLE OF CONTENTS

1. INTRODUCTION	1
What is a receptor and why is it needed?	1
To what do receptors respond?	2
Are receptors of a class physiologically homogeneous?	3
Membrane phenomena	6
Transmission through surrounding tissues	17
Transfer function	32
Pulmonary mechanoreceptors in mammals	36
Anatomy and physiology of frog pulmonary mechanoreceptors	45
Prospectus	51
2. MATERIALS AND METHODS.	56
Acquisition and housing of frogs	56
Gross dissection	56
Microdissection	59
Input	60
Recording	63
Signal processing	64
Data reduction	66
Experimental procedure	67
Miscellaneous Procedures	69
3. RESULTS	
Pressure-volume characteristics of the frog lung	72
Initial lung volume	75
Threshold	76
Conduction velocity	76
Discharge patterns	76
The relationship between discharge frequency and lung volume and rate of change of lung volume	87
Decay times	89
Model of the three receptor types	90
Simulation	92
Sinusoidal forcing	97

4. DISCUSSION	112
Pressure-volume characteristics	112
Threshold	115
Conduction velocity	117
Model	117
Components of the response and their origin	121
5. SUMMARY AND CONCLUSIONS	126
6. BIBLIOGRAPHY	127
7. APPENDIX	135
Justification of Toyama's model	135
Instantaneous frequency meter	136
Response histogram	143

LIST OF ILLUSTRATIONS

Figure 1.	Muscle Spindle of the Frog.	8
Figure 2.	Schematic Diagram of a Pacinian Corpuscle	10
Figure 3.	Schematic Diagram of the Crayfish Stretch Receptor.	12
Figure 4.	A. Schematic Illustration of the Innervation of the Muscle Spindle; B. Mechanical Model of Spindle Receptor.	20
Figure 5.	Comparison Between the Theoretical and the Actual Time Courses of the Spindle Response	24
Figure 6.	Generator Potential of the Pacinian Corpuscle Before and After Removal of Connective Tissue.	25
Figure 7.	Mechanical Analog of a Pacinian Corpuscle.	27
Figure 8.	A Schematic Drawing of the Relation of a Tendon Organ to Muscle	30
Figure 9.	A, Slowly Adapting and B, Rapidly Adapting Stretch Receptor of the Cat Lung.	39
Figure 10.	Adaptation Index Histogram	41
Figure 11.	Nerve Endings in the Lungs of Puppies.	44
Figure 12.	Nerve Endings as They Appear in the Frog Lung	46
Figure 13.	Lung Interior of Bullfrog Showing Smooth Muscle Lattice.	48
Figure 14.	Diagrammatic Representation of the Response of a Rate, a Rate Plus Proportional, and a Proportional Receptor to Half-trapezoid Input.	53

Figure 15.	Block Diagram of Preparation and Apparatus	62
Figure 16.	Calibration Curve of Pressure Recording System.	65
Figure 17.	Relationship Between Action Potential Input and Computer Output.	68
Figure 18.	Pressure-volume Characteristics of the Frog Lung	73
Figure 19.	Intertrial Variability of the Response.	78
Figure 20.	Discharge Pattern of Rate Receptor.	80
Figure 21.	Discharge Pattern of Rate Receptor.	81
Figure 22.	Discharge Pattern of Rate Plus Proportional Receptor.	82
Figure 23.	Discharge Pattern of Rate Plus Proportional Receptor.	84
Figure 24.	Discharge Pattern of Proportional Receptor	85
Figure 25.	Discharge Pattern of Proportional Receptor	86
Figure 26.	Rate and Proportional Responses of Frog Lung Receptors	88
Figure 27.	Model of the Frog Lung Receptor and Surround- ing Tissue.	91
Figure 28.	Patch Diagram for Model Shown in Figure 27	93
Figure 29.	Model Response to Half-trapezoid Volume Change Input	94
Figure 30.	Receptor Response to Sinusoidal Inflation.	99
Figure 31.	Rate Plus Proportional Receptor Response to Sinusoidal Inflation.	100
Figure 32.	Mass Discharge Response to Rapid Half- trapezoidal Inflation	102

Figure 32.	Phase Angle Data for Eleven Receptors	105
Figure 33.	Phase Angle Data for Rate and Rate Plus Proportional Receptors	106
Figure 34.	Phase Angle Versus Frequency of a System with a Transfer Function of the Form $(S + b)/(S + a)$	107
Figure 35.	Phase Angle Data for Proportional Receptor	109
Figure 36.	Model Response to Sinusoidal Forcing	110
Figure 37.	Triggering System for Instantaneous Frequency Meter.	137
Figure 38.	Discharge Network for Instantaneous Frequency Meter	139
Figure 39.	Recording of Nerve Discharge Using Instantaneous Frequency Meter.	140
Figure 40.	Calibration Curve for Instantaneous Frequency Meter.	142
Figure 41.	Patch Diagram for Action Potential Counting. . . .	144

LIST OF TABLES

Table I.	Composition of Ringer's Solution.	57
Table II.	Repeatability of Onset and Cessation of Discharge Times During Sinusoidal Inflation of a <u>Typical</u> Receptor	103
Table III.	Phase Relationship (Lag) Between Simulated Input and Simulated Output at Different Fre- quencies of Sinusoidal Model Forcing.	111

INTRODUCTION

What is a Receptor and Why is it Needed?

During the latter half of the nineteenth century Claude Bernard (1) promulgated the doctrine of the constancy of the milieu interne whereby evolution of the higher forms of life was possible only because of the stable and regulated conditions of their body fluids. However before an organism can regulate its internal environment it must first make measurements concerning the state of what is to be regulated. Thus if an organism is to regulate blood pressure or plasma osmolarity it must make measurements of its blood pressure or osmolarity so that appropriate action may be taken toward the maintenance of desired values. An organism must also continuously sample its external environment in order to seek food, avoid predators and seek shelter from extreme temperature if species survival is to continue.

Organisms sample their internal and external environments by means of nerve endings where the membrane is functionally specialized; these areas of terminal membrane are called receptors. (2) Receptors function as transducers in that they transform one form of energy into a second form of energy. No matter what form of energy the receptor is measuring - heat, light, pressure,

chemical concentrations - the receptor changes this energy into electrical energy (3). This transducer output takes the form of a change in the electrical potential in the specialized nerve ending membrane and is called a generator potential. The magnitude of the generator potential is directly related to intensity of the stimulus (4, 5). The generator potential, if of sufficient magnitude, may cause one or more action potentials in the nerve fiber with which the endings are associated (4, 5, 6). These action potentials traverse the length of the nerve fiber and, in the case of the vertebrate, enter the central nervous system. The time interval between successive action potentials varies inversely, in a non-linear fashion, with the magnitude of the generator potential. Thus the magnitude of the stimulus determines the magnitude of the generator potential which in turn determines the frequency of discharge of the nerve fiber (4).

To What Do Receptors Respond?

Sherrington believed that a given receptor responded to a specific form of energy and in his words "The main function of the receptor is . . . to lower the threshold of excitability . . . for one kind of stimulus and to heighten it for all others." (7) There are receptors which appear to have a specific response to heat (8), light (9), pressure (10), sound (11), chemicals (12), elongation (13) and electricity (14). Thus each receptor has an adequate stimulus which

is the particular energy form to which the receptor responds.

Are Receptors of a Given Class Physiologically Homogeneous?

Although it is possible to categorize receptors on the basis of the quality of environmental change to which they are selectively sensitive, such a classification does not reveal the nature or the degrees of functional variability among members of these large groups. Inhomogeneity within a population may appear as differences in threshold, as differences in sensitivity to various sub-qualities to a given form of energy, or as differences in range of susceptibility to a given form of environmental change.

Variation in threshold among receptors of a given class were detected by one of the earliest students of receptor function. Adrian and Zotterman (13) suggested that differences in the threshold for excitation among receptors in a given class was an additional means of detecting stimulus intensity. These authors recorded action potentials from nerve fibers associated with receptors which were contained in, and were sensitive to elongation of, the sterno-cutaneous muscle of the frog. As the muscle was elongated experimentally, not only did the frequency of discharge of individual sensory units increase, but additional sensory units were recruited into activity. Therefore the magnitude of stretch could be signalled by the frequency of discharge of individual nerve fibers associated with

receptors as well as the total number of active fibers.

Visual receptors have been shown to be responsive to particular portions of the visible spectrum. Granit (15) introduced different wavelengths of light into the retina of the cat and found that the receptors exhibited differential spectral sensitivities. Granit's measurement of receptor activity was indirect in that he recorded action potentials from single ganglion cells which are one cell removed from the receptor cells, yet on the basis of anatomical and chemical evidence it was likely that the responses represented the activity of single classes of retinal receptors. The ganglion cell responses were generated by three different populations of receptors; the first showed a maximum sensitivity about a wavelength of 450 m μ and was overlapped by the second population which had its maximum sensitivity at 525 m μ and was in turn overlapped by the third population which had a response most easily evoked by incident light of 600 m μ wavelength.

Cones which are a class of light detecting receptors of the eye have been shown to contain one of three visual pigments (16). A reversible chemical reaction in these pigments occurs when the pigments are exposed to certain wavelengths of light (17) and electrical activity may be initiated in the receptor as a result of the chemical breakdown. The three visual pigments which have been found in cones are blue, green, and red sensitive pigment. The spectral

sensitivity of the ganglion cell response and the corresponding spectral sensitivity of the visual pigments suggest that cones function as color detectors and single ganglion cells are influenced by cones selectively sensitive to one of the three colors of light.

Mechanoreceptors activated by joint motion are all activated by a similar process occurring in their environment, but the range over which they respond may be quite limited. Skogland (18) in an examination of the receptors of the knee joint of the cat found that a given receptor was not active over the entire range of joint movement. He used as an index of receptor activity the frequency of discharge of action potentials in a single afferent fiber associated with a joint receptor. He found a given receptor may be active for only a 30 degree arc and remain quiescent for the remaining 100 degree angle which the tibia may make with the femur. There were few active receptors when the tibia was neither flexed nor extended while the majority of joint angle receptors were active at either extreme flexion or extreme extension. Thus when the tibia was extended from a flexed position there were receptors which were initially active and as extension proceeded over the initial 30 degree arc these receptors became silent at the same time that a new population of receptors became active. Although a single joint angle receptor was active over a discreet range of joint angles its response was not uniform and constant over the entire angle, but

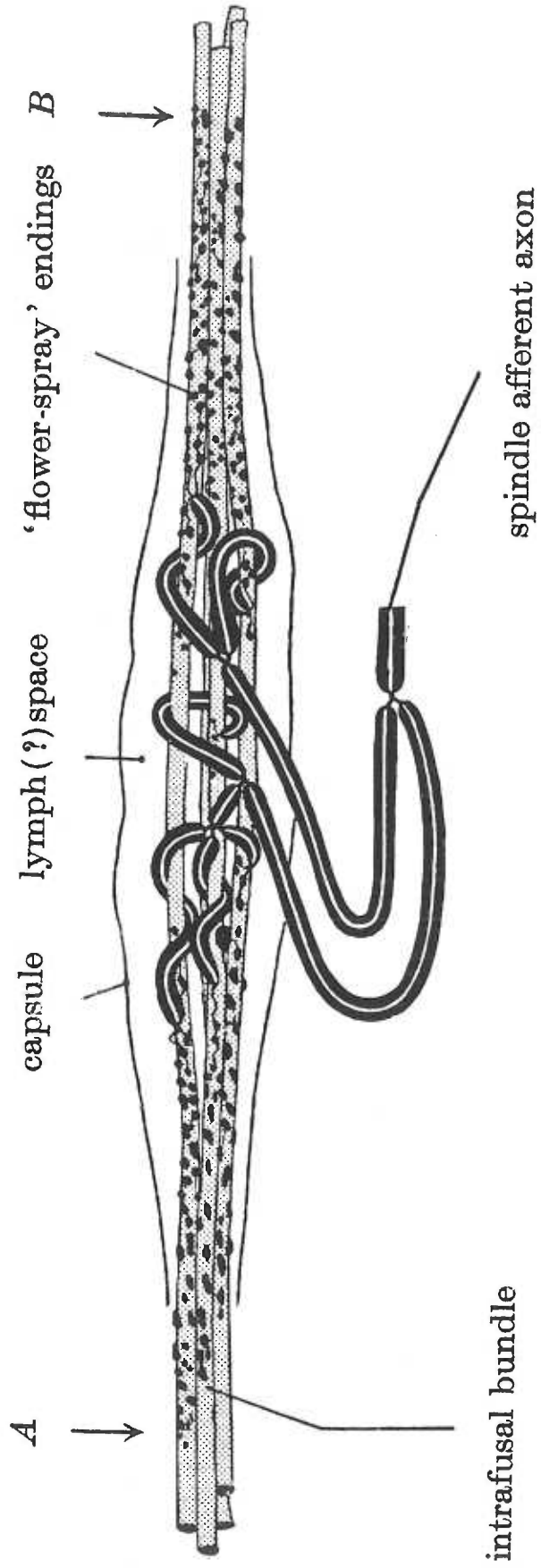
longus dig. IV muscle of the frog was first investigated by Katz (5). The muscle spindle (fig. 1) of the frog toe consists of a variable number of muscle fibers called intrafusal fibers which are segregated from the remainder of the muscle fibers (extrafusal muscle fibers) by a connective tissue capsule. The spindle is often innervated by a single afferent and single efferent nerve fiber. After entering the capsule the sensory axon loses its myelin sheath, branches, and wraps around the intrafusal muscle fibers. The nerve endings are generally found within one millimeter of the point of entrance into the capsule. The spindle itself rarely exceeds 1 mm in length.

Katz mounted the muscle in an apparatus so that he could stretch the muscle at will and simultaneously record from the sensory axon at a point no more than several millimeters from the sensory terminals. He observed that each single action potential elicited by muscle stretch was preceded by a small electrical potential. If a train of action potentials was elicited by sustained muscle stretch there was a persistent electrical potential between spikes. This interspike potential increased in a nonlinear fashion with increasing muscle length. Application of procaine solution (0.3%) abolished the action potentials yet the small potential which normally preceded the action potential remained and in the absence of action potentials became continuous with what were the interspike

Figure 1. Muscle spindle of the frog.

From Gray, Proc. Roy. Soc. (Biol.), 1956-1957.

146, 416-430. (19)



'flower-spray' endings B

lymph (?) space

capsule

A

intrafusal bundle

spindle afferent axon

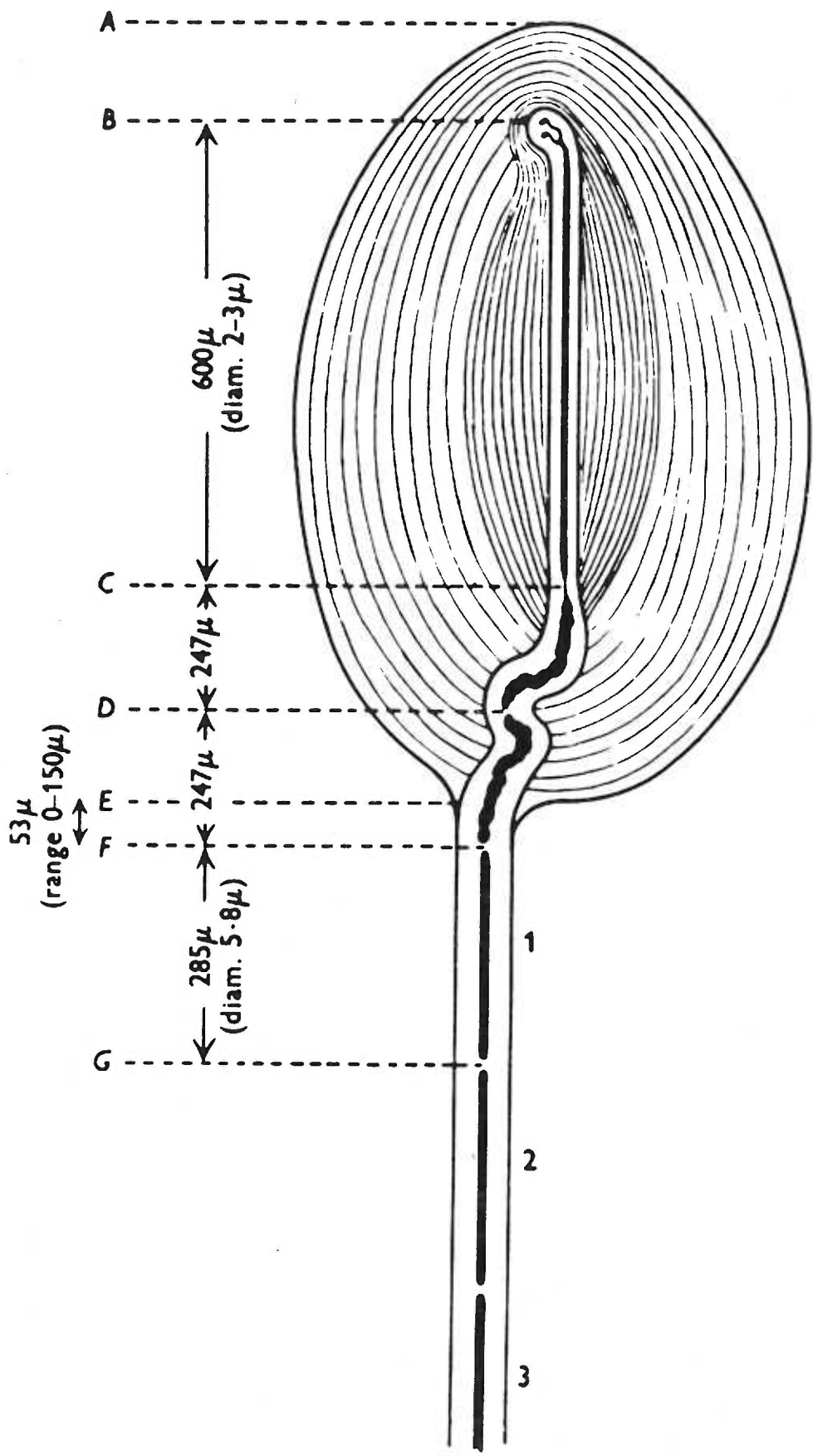
potentials. Since the magnitude of procaine resistant depolarization varied directly with stretch and velocity of stretch Katz believed that there was a causal relationship between muscle stretching and the spindle potential as he called it.

In addition Katz found a linear ($R=0.97$, $n=91$) relationship between the magnitude of the generator potential and the frequency of discharge in the sensory axon. Earlier Hodgkin (20) had shown that repetitive action potentials occurred as a consequence of passing current into unmyelinated nerve fibers of Carcinus and each action potential was preceded by an initial depolarization of the nerve membrane. Therefore Katz proposed that stretching the muscle caused a graded potential which originated in the sensory nerve endings and which was passively propagated away from the terminals. If of sufficient magnitude, this potential caused action potentials in the sensory axon of the spindle.

Although subsequent work confirms Katz's hypothesis Katz did not directly demonstrate the origin of a generator potential nor the electrotonic spread of the generator potential. Loewenstein (6) experimentally examined the origin of the generator potential and confirmed its electrotonic spread in the Pacinian corpuscle. But before considering his work it is first necessary to appreciate the anatomy of this receptor. (fig. 2)

The Pacinian corpuscle of the cat mesentery consists of a

Figure 2. Schematic diagram of a Pacinian Corpuscle.
From Goldman, Cold Spring Harbor Symposia
on Quantitative Biology, 1965. 30, 59-68.



fluid filled capsule of concentric lamellae in which a sensory axon terminates. Shortly following the axon's entrance into the corpuscle the myelin sheath is lost. As will be shown later the corpuscle has an internal vascular system which is supplied by arteries of the mesentery (21).

Loewenstein was able to isolate the relatively large capsule and remove the lamellae thus exposing the core of the capsule which consists of the unmyelinated nerve ending and a surrounding sheath of adventitious tissue. Punctate stimuli were applied to the core and electrical activity was monitored via electrodes placed on either the myelinated portion of the axon or on the central core. Punctate stimulation of the myelinated portion of the nerve including that part found within the capsule failed to produce electrical response. Punctate stimulation applied to the distal end of the core, coupled with stepwise movement of the recording electrode away from the site of stimulus application yielded an exponential decline in the magnitude of the generator potential with respect to the distance from the site of stimulus application. This finding suggested that the generator potential originated at the site of stimulation and was passively propagated along the nerve according to the properties of transmission along a cable. However, these results did not rule out the possibility that the surrounding adventitious tissue was responsible for generation of the electrical potential. To test this possibility

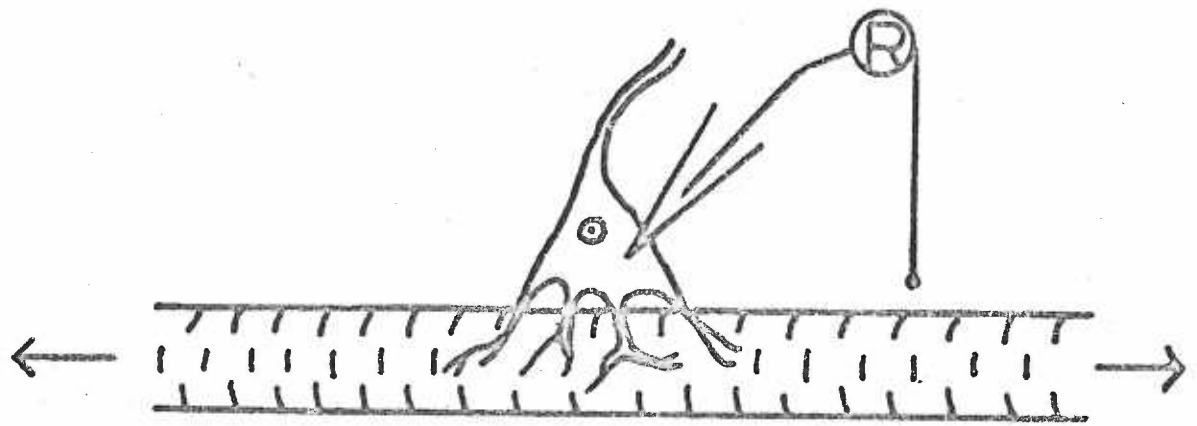
Loewenstein (22) cut the axon of the corpuscle in the living animal, allowed several days for the degeneration of the axon, removed the corpuscle and repeated the experiment. No electrical activity was detected. Thus by creating an "endless core" Loewenstein demonstrated that the origin of the generator potential was the unmyelinated nerve ending.

The Site of Initiation of the Action Potential

The abdominal stretch receptor (fig. 3) found in a number of crustacea consists of dendrites which are entwined in the muscles bridging the abdominal segments. These dendrites originate from a large cell body which is accessible to microelectrode impalement and from which originates a sensory axon.

In an attempt to find the site of origin of action potentials Edwards and Ottoman (23) recorded the latencies of muscle stretch evoked responses in several regions of the cell body and along the axon of the crustacean stretch receptor. Although action potentials invaded both the cell body and axon these authors believed the action potential originated in the axon near the cell body and spread antidromically to the cell body. The action potentials did not invade the smaller dendrites of the receptor (4). Loewenstein (6) electrically stimulated the myelinated portion of the axon of the Pacinian

Figure 3. Schematic diagram of the crayfish stretch receptor.
Arrows denote the direction in which stretch is normally applied. From Eyzaguirre & Kuffler, J. Gen. Physiol., 1955. 39, 87-119.



corpuscle in order to produce action potentials. As in the crustacean stretch receptor, the action potentials did not invade the receptor terminal. Loewenstein applied gentle compression to the first node of Ranvier while mechanically stimulating the core of the corpuscle. He found that action potentials were abolished as a result of the compression procedure while the generator potential was unaffected. He interpreted these findings to mean that electrotonic spread of the generator potential to the region of the first node of Ranvier may cause action potentials which are then confined to the myelinated portion of the axon. In both the crustacean stretch receptor and the Pacinian corpuscle, the action potential is initiated some distance away from the receptor terminals and these action potentials do not invade the receptor terminals.

Generator Potential in Crustacean Stretch Receptor

Terzuolo and Washizu (4) studied the generator potential - discharge frequency relationship in the crustacean stretch receptor. These authors altered the generator potential by means of muscle stretch. They monitored action potentials via an intracellular microelectrode. As did Katz (5) these authors recorded a generator potential attenuated by spatial decrement. Nevertheless the generator potential actually recorded was proportional to the generator potential at its site of origin. The generator potential of the

crustacean stretch receptor could not be determined directly in the presence of spike activity as in the muscle spindle, therefore these authors passed just sufficient current into the cell to prevent the occurrence of action potentials. The magnitude of the current required to prevent spike activity was known and the membrane resistance was determined during the procedure. Thus the change in membrane potential from resting to spike threshold potential plus the product of applied current and membrane resistance yielded the generator potential. Eyzaguirre and Kuffler (24) had previously determined that the threshold potential for discharge in this same receptor was nearly constant for discharge frequencies up to 20 discharges per second. Thus the determination of the threshold potential allowed Terzuolo and Washizu to indirectly determine the generator potential under a variety of stretch conditions. The crustacean stretch receptor like the amphibian muscle spindle exhibited a linear relationship between generator potential and impulse frequency. The proportionality constant relating impulse frequency to generator potential was 2 impulses / sec / mv. This proportionality constant was valid for generator potentials ranging from zero to 15 mv. The relationship was nonlinear outside of this range of generator potentials.

Origin of Generator Potential

In an attempt to determine if the unmyelinated portion of the Pacinian corpuscle nerve was a single transducer or consisted of many discontinuous transducers, Loewenstein (6) crushed various segments of the unmyelinated portion of the nerve. Whenever there was an undamaged region central to the region of crushing, stimulation of this region produced a generator potential. However, stimulation distal to the crushed tissue did not produce a generator potential which could be measured in the primary afferent fiber. Furthermore, if two spatially separated punctate stimuli were applied simultaneously to the unmyelinated portion of the nerve, summation of the two responses occurred. If instead of near simultaneous application of two spatially separated stimuli, two brief stimuli separated by one millisecond were applied to the area of the membrane, summation did not occur. In light of these findings Loewenstein developed a model of the transducer system consisting of 20 independently activated "all or nothing" units. A comparison of experimental data and model behavior indicated that the generator potential resulting from stretch of the unmyelinated nerve ending and as measured in the primary afferent could be explained by a number of discrete "all or nothing" units located on the sensory ending membrane.

It had been shown in giant lobster axons (25) that compression of the axon was accompanied by a decrease in membrane resistance. Furthermore, mechanical stimulation in the form of compression led to the depolarization of the membrane (cf. generator potential). If this depolarization were of sufficient magnitude an action potential resulted. Goldman (26) argued that rapid compression of cylindrical fluid filled structures such as the lobster axon and the unmyelinated core of the Pacinian corpuscle produced a stretching of the nerve membrane. Since stretching a membrane must increase the intermolecular distance an increased permeability follows as a natural consequence. An increase in ionic permeability as a consequence of stretch is compatible with the increased membrane conductance observed during experimental compression. Goldman applied the constant field potential equation to the lobster axon to find what change would result in the membrane potential if sodium permeability were suddenly doubled. Experimentally this change in membrane potential was found to occur when the axon was compressed to 80% of its original diameter. Calculation of the change in surface area due to such a compression assuming a thin and weak nerve membrane yielded an area change of only 0.5% of the original area. Goldman completed his argument by stating that such a small change in membrane area could easily double sodium permeability. Thus Goldman believes on theoretical grounds, and his views are

supported by Hubbard (27), that the generator potential is caused by an increase in permeability of ions to the nerve membrane as a consequence of the membrane stretching during the application of radial stress.

Since Goldman proposed that an increase in sodium permeability caused by membrane stretch could be responsible for the generator potential, this potential should not be elicited in a sodium free medium. Diamond, Gray, and Inman (21) perfused a Pacinian corpuscle with an is osmotic but sodium free solution and monitored electrical activity in the primary afferent fiber. Action potentials were abolished within two minutes following perfusion of the sodium free solution and within 11 to 30 minutes the generator potential fell to a constant minimum value which was about 10% of the initial value. These authors concluded that although the sodium ion is involved in the production of a normal generator potential other ions are probably involved also.

Terzuolo and Washizu (4) found the equilibrium potential of the crustacean stretch receptor was near zero volts and therefore the origin of the generator potential represented a nonselective increase in ion permeability.

Transmission Through Surrounding Tissues

It was previously stated that information concerning the state

of the receptor's surround is encoded as a frequency modulated series of action potentials in the afferent fiber associated with the receptor. It was shown in several mechanoreceptors that stretching of the receptor membrane occurs as a consequence of the mechanical stimulus and that this stretching causes a nonselective increase in ion permeability of the receptor membrane. A local depolarization of the membrane occurs as a result of the permeability increase and the magnitude of depolarization of the receptor membrane diminishes with the distance from its site of origin. If this depolarization or generator potential is of sufficient magnitude at a particular region of the nerve, action potentials occur as a consequence of membrane depolarization in this region and these action potentials are then propagated along the afferent fiber. The frequency with which these action potentials occur is linearly related over a limited range to the magnitude of the generator potential.

The following section of this introduction will deal with the processes which precede the initiation of the generator potential, namely the transmission of mechanical energy, from the receptor's surround to the receptor itself. These processes have been studied directly by means of high speed cinematography of tissue strain in response to externally applied stress and they have been studied indirectly. Indirect studies have involved electrical recording of either generator potentials or action potentials during the application

of controlled stress to the tissues surrounding the receptor. Knowledge of the input to the tissue, and the output of the receptor or nerve, in conjunction with anatomical observations has led to proposals concerning the mechanisms of the intervening process by which mechanical energy is transmitted through the surrounding tissue to the receptor.

Muscle Spindle

Katz (5) found in the muscle spindle of the frog toe that the frequency of discharge of the spindle afferent and the magnitude of the generator potential reflected not only the load applied to the muscle but the rate at which that load was changing. That is the muscle spindle receptor could perform the task of differentiation in the mathematical sense. Earlier B. H. C. Matthews (28) had stated that the ability of the cat's muscle spindle to differentiate could be explained by the mechanical properties of the spindle tissue. If the nerve endings were located in a region of low viscosity relative to the remainder of the spindle the strain around these endings at a given muscle load would be greater if there was a positive rate of change of load than if the rate of change of load was negative or zero. Katz (29) in an electron microscopic investigation of the frog muscle spindle found the terminal branches of a single afferent axon were distributed in two anatomically distinct regions of the spindle (Fig. 4).

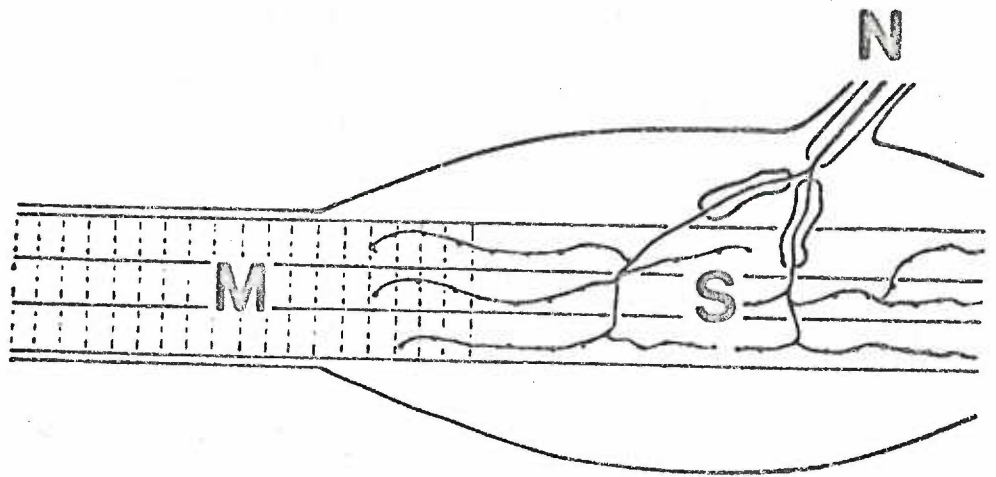
Figure 4. A. Schematic illustration of the innervation of the muscle spindle; M, compact region; S, reticular region.

B. Mechanical model of spindle receptor; G_1 , spring representing elasticity of the reticular region; G_2 , spring representing elasticity of compact region; b , dashpot representing viscosity of compact region; L, muscle length (input); P, tension in spring one (output).

From Toyama, Jap. J. Physiol., 1966. 116,

113-125.

A



B

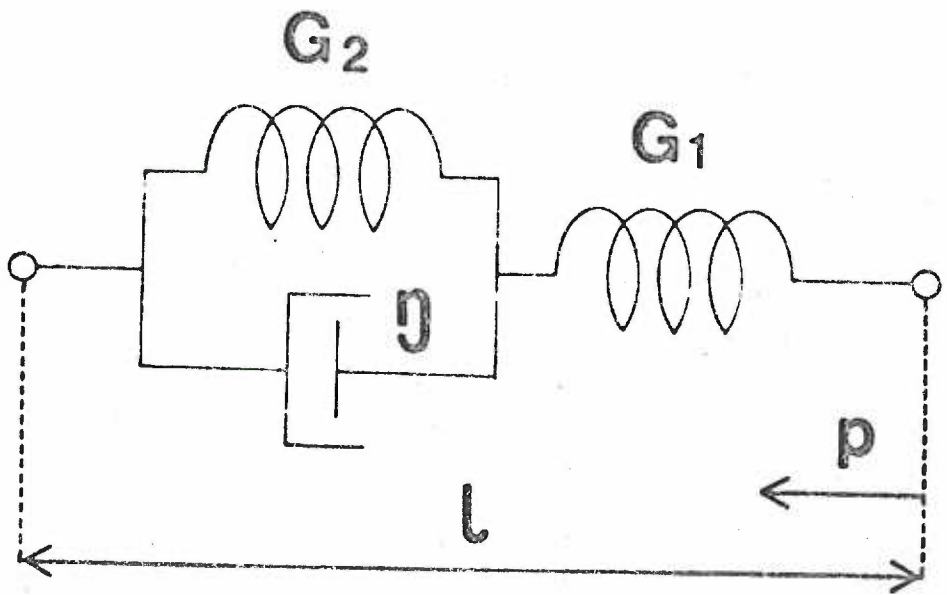
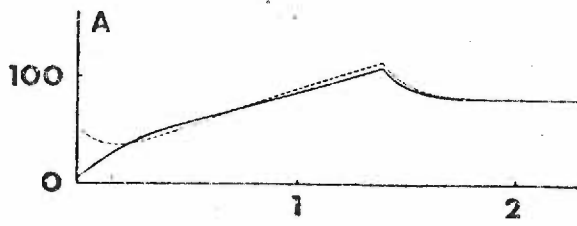


Figure 5. Comparison between the theoretical (solid lines) and the actual (dotted lines) time courses of the spindle response.

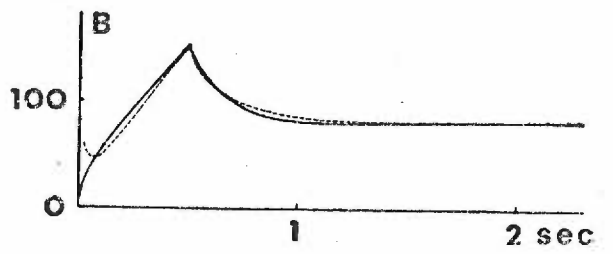
From Toyama, *Jap. J. Physiol.*, 1966. 16, 113-125.

Recent evidence by Schäfer (32) suggests a response to acceleration in the mammalian primary muscle spindle. The response is most easily seen with the onset of the ramp in half-trapezoid elongation of the extrafusal muscle. The initial burst of activity seen in this figure with the onset of the ramp suggests an acceleration component in the response of the frog muscle spindle.

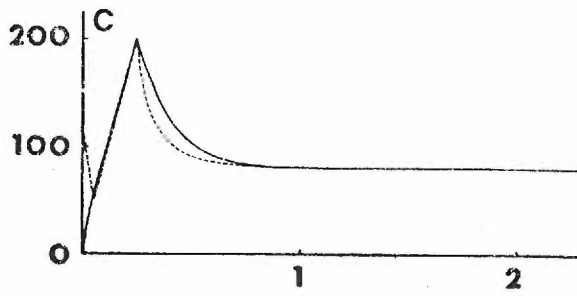
imp./sec



Imp./sec



200
100
0



200
100
0

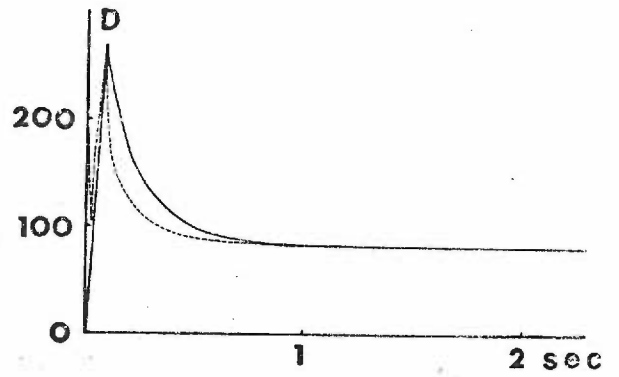
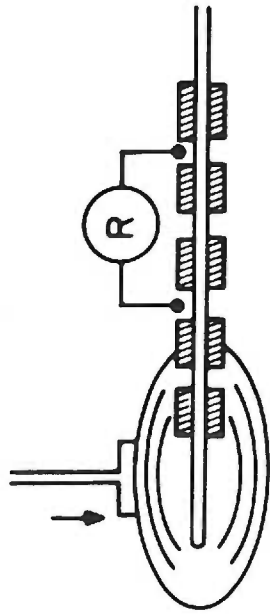


Figure 6. Generator potential of the Pacinian corpuscle before (A) and after (B) removal of connective tissue; e, generator potential; m, mechanical stimulus.

From Mendelson and Loewenstein, *Science*, 1964.
144, 554-555. (35)

A

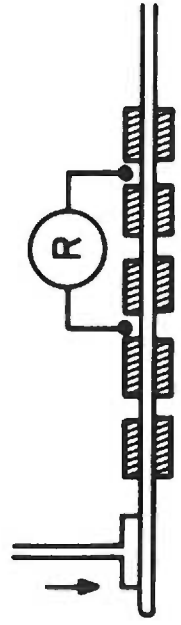


e



m

B



e



m

10 msec.

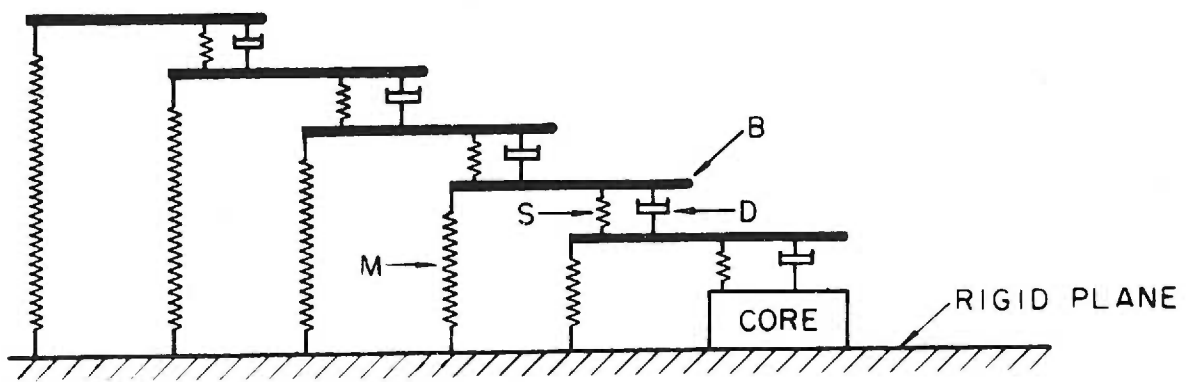
movement of the inner lamellae was similar to the time course of the generator potential recorded from the myelinated axon (33) during the application of a similar stimulus. Yet the time required for decay from the peak amplitude to the prestimulus condition was somewhat longer in the generator potential than in the lamellar movement. Although a displacement of the sensory region of the corpuscle was not observed, Hubbard and others, (26, 34) suggested that the generator potential was produced as a consequence of strain in the central core of the corpuscle. The stress to which the central core was subjected was dependent upon the stimulus waveform and the filtering characteristics of the tissue surrounding the nerve membrane.

Loewenstein (30) developed a mechanical analog of the tissue surrounding the receptor as a means of predicting the response of the receptor to various stimuli. Loewenstein's model (fig. 7) contains the equivalent of 30 lamellae, the number which normally occurs in a mesenteric corpuscle. He assigned values to the various springs and dashpots and placed certain constraints on the model. The end result was close agreement between model behavior and the actual behavior which had been determined by Hubbard. Loewenstein's work went beyond Hubbard's work in that the interlamellar pressures as well as central core stress could be predicted. The model predicted that elastic forces were not transmitted to the core while viscous forces were transmitted to the central core with little

Figure 7. Mechanical analog of a Pacinian Corpuscle.

B, Lamella; S, spring representing interlamellar compliance; M, spring representing compliance of the individual lamellae; D, dashpot representing interlamellar viscosity.

From Loewenstein, Cold Spring Harbor Symposia on Quantitative Biology, 1965. 30, 29-43.



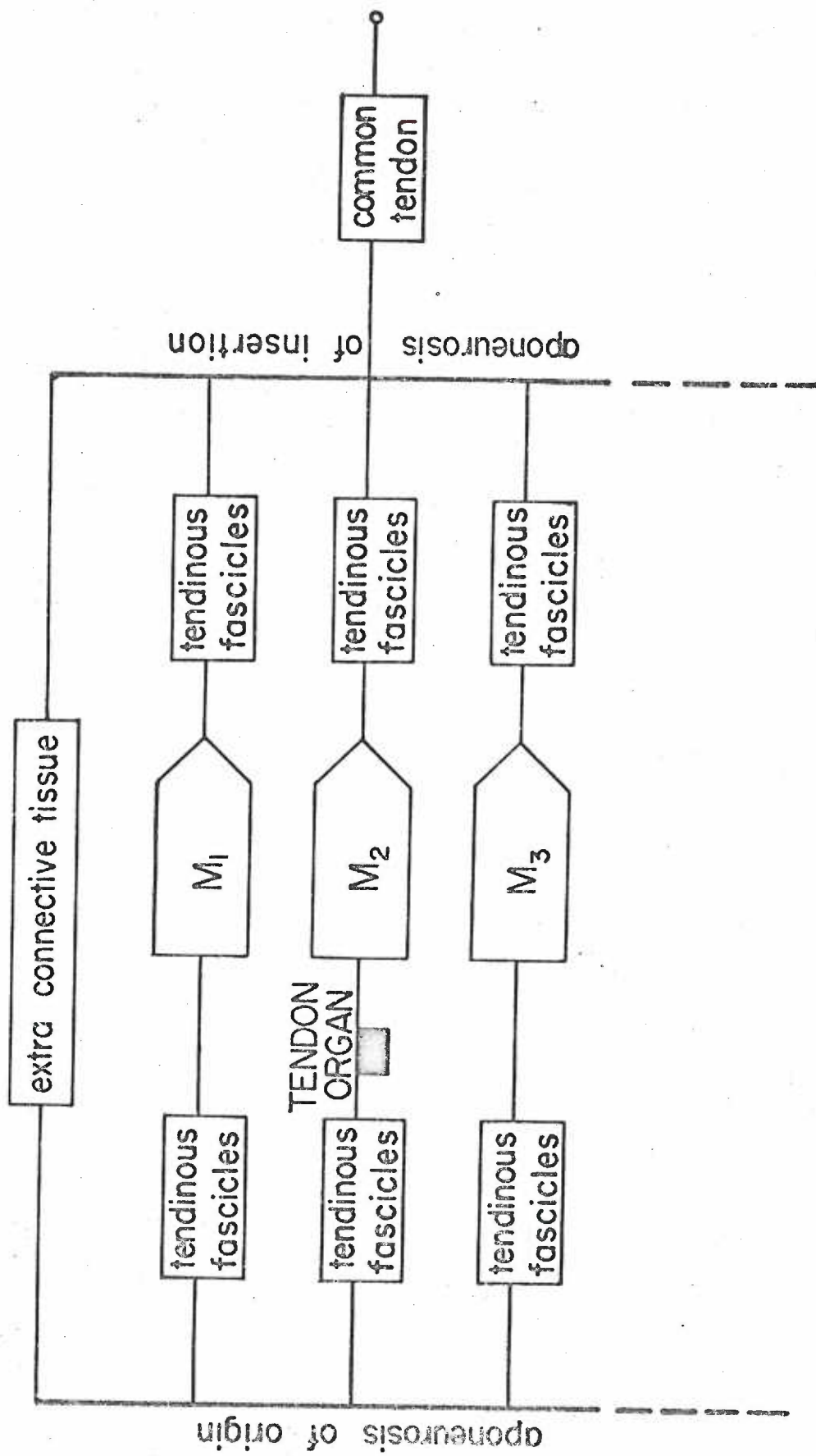
attenuation. Recording of the generator potential in the encapsulated corpuscle had necessarily been accomplished external to the capsule on the myelinated axon. The generator potential recorded in this region was not a faithful reproduction or miniature of the generator potential but was altered by the "cable" properties of the membrane. Taking into account the properties of the nerve membrane and their effect on the transmission of the generator potential, Loewenstein showed that the theoretical generator potential at its site of origin and the predicted stress on the central core had similar time courses.

The Loewenstein model predicted that a sudden release in compression would reverse the viscous forces which appeared during stimulus onset. Since strain was predicted to occur in the central core during the release of compression a generator potential should accompany this strain. Figure 6 shows the characteristic response of the Pacinian corpuscle when compression is suddenly released.

On the basis of the direct evidence submitted by Hubbard and the model developed by Loewenstein the rate receptor characteristics of the Pacinian corpuscle may be explained: the peripheral lamellae possess physical characteristics which permit transmission of only rate of change of mechanical energy to the receptor site.

Figure 8. A schematic drawing of the relation of a tendon organ to muscle.

From Houk, J. Neurophysiol., 1967. 30, 1482-1493.



in both the receptor's and the muscle's response to stretch were identical. Houk and Henneman (38) had previously reported that the tendon organ's raison d'être was the detection of tension in a muscle. If this is the case then following the step increase in length the muscle tension has a slow decay component with a time constant of 2.94 seconds (0.34^{-1}) presumably caused by the visco-elastic properties of the muscle. The frequency response characteristics of the receptor are such that this low frequency tension decay is detected by the receptor and causes the first exponential term to appear in the receptor's response to a step increase in muscle length. Houk did not discuss the origin of the more rapid decay terms.

The above studies indicate that an important aspect of the transduction process is the transmission of mechanical energy through the tissues which surround the receptor. It may be through the mechanical properties of this surrounding tissue that a receptor's response is determined. Thus a Pacinian corpuscle's response is correlated with rate of change of applied force because the surrounding tissues may only transmit rate of change of applied pressure to the nerve membrane. The tendon organ and muscle spindle receptors have a steady state (d. c.) response because the surrounding tissues transmit steady stretch to the nerve membrane of the receptor. Experimental evidence will be presented in the body of

this thesis which lends further support to this hypothesis.

Transfer Function

There have been recent attempts to incorporate the process of energy transmission, transduction, and F.M. encoding into a single processing unit for which an analytical expression may be determined which relates output in the afferent fiber (e. g., discharge frequency) to the input (e. g., tension). Many of these attempts have been directed toward the determination of a general input-output relationship, general in that the expression relates the output to any input provided that the input is expressed in mathematical terms. The general input-output relationship is called a transfer function and the term transfer function signifies that the processing unit or "system" is linear and may be described by linear differential equations.

Biologists have taken two approaches to the experimental determination of the transfer function of receptor systems. The more common approach has been the determination of the system response ($y(t)$) to a step function input $z(t')$. The input and output are then related by the convolution integral

$$y(t) = \int_{-\infty}^t z(t')h(t-t')dt'$$

where $h(t)$ represents the system's response to a unit impulse and t' is a dummy variable. Additional insight into the use of this integral can be gained by considering the Laplace transformation of a

determined the transfer function of the tendon organ in this fashion as did Brown and Stein (39), Chapman and Smith (40), and Pringle and Wilson (41) for insect mechanoreceptors.

Houk (42) and Borsellino, Poppele, and Terzuolo (43) experimentally determined the transfer function of the muscle spindle and crayfish receptor respectively by means of sinusoidal stimulation and log magnitude-frequency diagrams. The technique first involves establishing system linearity then the determination of the ratio of output to input, and the phase relationship between output and input all at different frequencies of sinusoidal input. The resulting Bode plot of gain and phase angle versus the logarithm of input frequency is a kind of "fingerprint" for the system in that each system has a unique Bode plot. Conversely if the Bode plot has been determined experimentally it is often possible to determine the transfer function from these data if the system is second order or even less complex.

The transfer functions of many biological systems (44, 45, 46) other than receptors have been determined utilizing sinusoidal input and Bode plots whereas this technique has not been applied extensively to receptor physiology. The reason for this is due to the impossibility for the frequency of discharge in the nerve to assume a value less than zero. Consider a IA afferent associated with a muscle spindle under unstretched conditions. The discharge frequency will be zero or near zero and with the onset of sinusoidal elongation the

discharge frequency will rise and reach a peak. However during the downswing of elongation the rate of change component of the generator potential is being driven negative with respect to the resting membrane potential and since it sums algebraically with the proportional component the resultant may be of insufficient magnitude to initiate action potentials and the discharge in the afferent ceases. Clearly this results in nonlinear behavior since the sinusoidal output does not occur. The nonlinearity may be circumvented by increasing the mean discharge frequency by muscle elongation and applying low amplitude sinusoidal stretch about this new level. If however the receptor is a rate receptor or a rate plus proportional receptor with small proportional response this attempt to circumvent the nonlinearity will fail. The use of step function or other monotonic increasing input waveforms has been prevalent in the determination of transfer functions because with these inputs the receptor may exhibit linear behavior.

The above was intended to be a brief description of some of the techniques which have been utilized for the purpose of transfer function determination in receptors. It is anticipated that the theory and method for generation of Bode plots and transfer functions will become clear during the experimental portion of this thesis. In these sections problems concerning threshold, rate sensitivity, proportional sensitivity, tissue-receptor interactions, and transfer

functions will be presented for a pulmonary mechanoreceptor and then discussed and whenever possible compared with studies cited above. Before describing the methods and materials which were used in this investigation it is first necessary to consider the previously established anatomical and physiological aspects of pulmonary mechanoreceptors.

Pulmonary Mechanoreceptors in Mammals

The study of the properties of pulmonary mechanoreceptors has progressed at a slower rate than studies concerned with muscle spindle, tendon organ, crustacean stretch receptor, and the Pacinian corpuscle. Pulmonary mechanoreceptors were first postulated in order to explain a reflex where lung inflation inhibited further lung inflation. This reflex was first observed at a time when there was no electrophysiological evidence for these receptors. Even now there is only indirect evidence for precise anatomical localization of the pulmonary receptor under study. Anatomists have described at least five anatomically identifiable receptor classes each diffusely distributed throughout the lung parenchyma. Because of the diffuse receptor distribution, the exact site and the class of the receptor associated with the afferent fiber under study has not been determined. The physiology of the Pacinian corpuscle and previously discussed mechanoreceptors has progressed more rapidly than

pulmonary mechanoreceptor physiology primarily because of the relative ease in which the receptor "system" of the former has been isolated and subsequently identified.

The pulmonary mechanoreceptors were proposed as a result of two early physiological investigations. In 1868 Hering (47) and Breuer (48) observed a decrease in the frequency of inspiratory efforts during maintained distention of the lungs of anesthetized animals. Maintained lung deflation produced an increase in the frequency of inspiratory efforts. Cervical vagotomy abolished the responses. This reflex is now known as the inflation reflex of Hering-Breuer. Later investigations (49, 50) indicated that the afferent limb of the reflex ascended with the pulmonary branch of the vagus nerve and that interruption of the carotid and aortic chemoreceptors and baroreceptors had no effect on the reflex.

Near the turn of the last century Einthoven (51) and others (52, 53) established electrophysiological evidence for the existence of these proposed receptors. They observed that the electrical activity recorded in the peripheral end of a cut vagus nerve increased with increasing volume of the lung. Later Adrian (54) was able to isolate from the cervical vagus of the cat, single active fibers which had discharge frequencies that were linearly related to lung volume. The proportionality constant for this relationship varied according to the size of the animal with larger animals exhibiting a smaller

proportionality constant than small animals. Adrian also found that there was considerable variability in the amount of inflation needed to recruit different fibers into activity. In addition Adrian found that hypoxia, hypercapnea, and 2.5% chloroform in air did not alter the response characteristics to pulmonary volume changes. Because the adequate stimulus for the receptor appeared to be stretching or expansion of the lung tissue, Adrian described the receptors as pulmonary stretch receptors.

Davis, Fowler, and Lambert (55) proposed that the receptor response was directly related to the total transpulmonary pressure rather than to lung volume. They found that the frequency of discharge of a single afferent fiber increased as volume increased and also increased as inspiratory airflow was increased.

The work of Knowlton and Larabee (56) indicated that there were two types of pulmonary stretch receptors in the mammalian lung. Discharge recorded from the afferent associated with one type of receptor was transient and was seen only during the inflation procedure (fig. 9). Furthermore relatively large lung inflations were needed in order to recruit this receptor into activity. The receptors studied by Adrian (54) and Davis et al. (55) were often times active at relatively small lung volumes. Furthermore the discharges in single afferent fibers associated with this second type of receptor were maintained as long as the pulmonary volumes were maintained

Figure 9. A, slowly adapting and B, rapidly adapting stretch receptor of the cat lung. Upper trace in both A and B depicts transpulmonary pressure.

From Knowlton and Larrabee, *Am. J. Physiol.*, 1946. 147, 100-114.

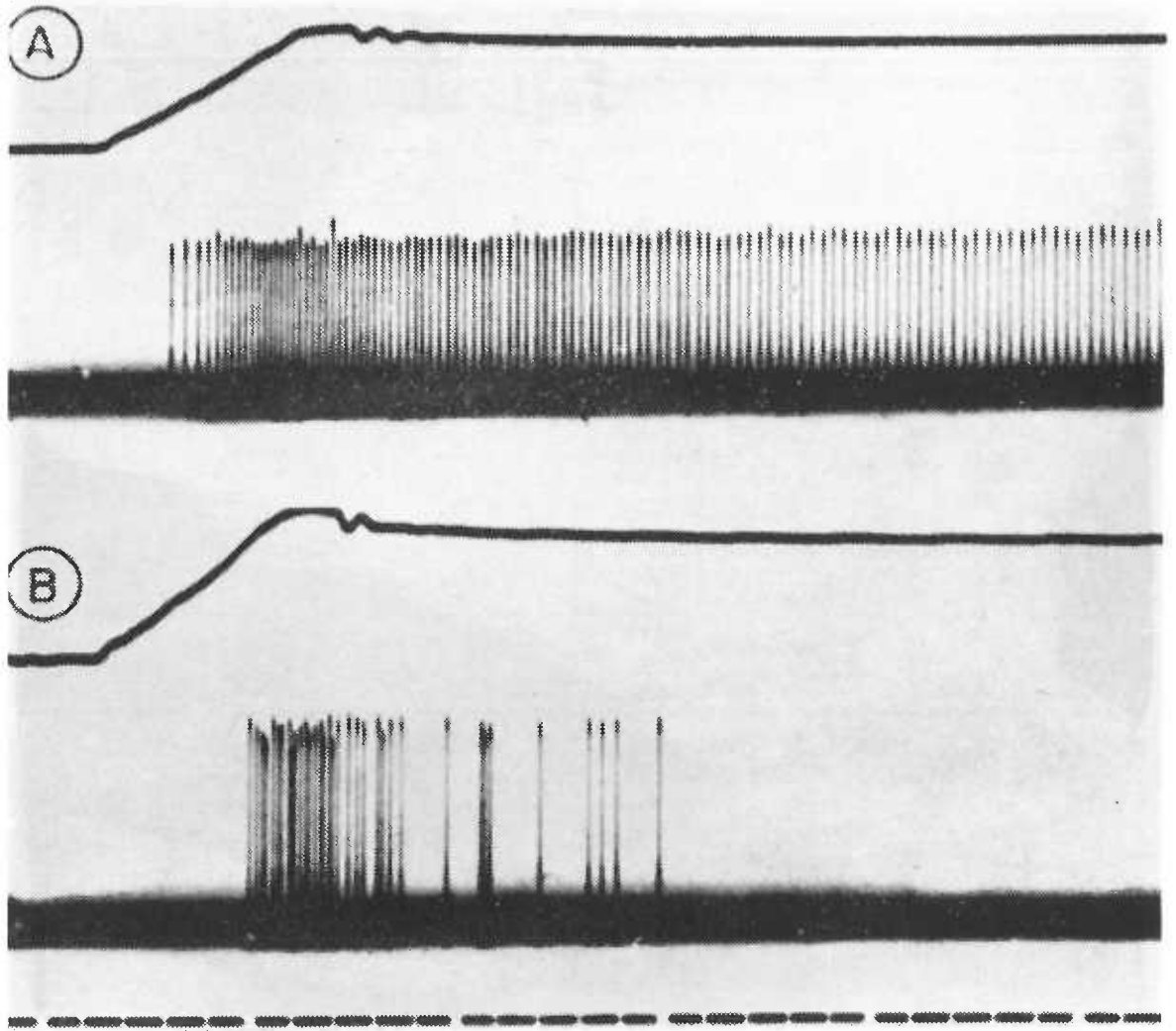


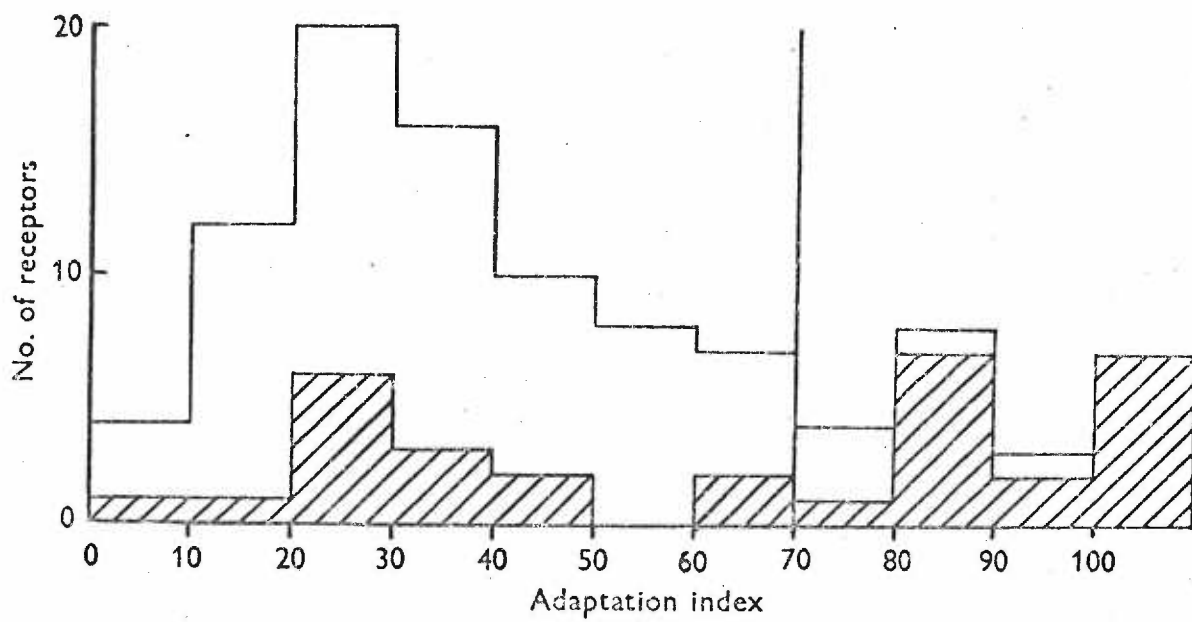
(fig. 9). The discharge frequency during constant volume did not remain constant but diminished slightly with time. This slow (5% in ten seconds) decline in discharge frequency during constant volume prompted Adrian to describe the receptor as a slowly adapting pulmonary receptor. The more rapid rate of decline in discharge frequency of the sensory unit described by Knowlton and Larrabee prompted these investigators to name their receptor the rapidly adapting pulmonary stretch receptor.

The experiments of Widdecombe (57) indicate that the slowly adapting and rapidly adapting pulmonary stretch receptors do not exist as distinct groups, but there is a blending of one group into another. Widdecombe examined the afferent discharge in one hundred vagal fibers associated with receptors which were located in the tracheobronchial trees of cats. The waveform was a half-trapezoid volume increase applied via the trachea. Fibers were classified as rapidly adapting or slowly adapting according to their adaptation index which was given by $\frac{100(A-B)}{A}$ where A = peak discharge frequency and B = discharge frequency two seconds following peak discharge. According to this formula the rapidly adapting receptor has a large adaptation index and the slowly adapting receptor has an adaptation index near zero. Figure 10 shows the adaptation indices of one hundred receptors which were studied. Although there does not appear to be a multimodal distribution of fibers

Figure 10. Adaptation index histogram. The indices are in groups of ten, except 100% which is shown separately. Receptors to the right of the vertical line were "rapidly adapting." The cross hatched areas represent receptors which responded to lung deflation.

From Widdecombe, J. *Physiol. (London)*, 1954.

123, 71-104.

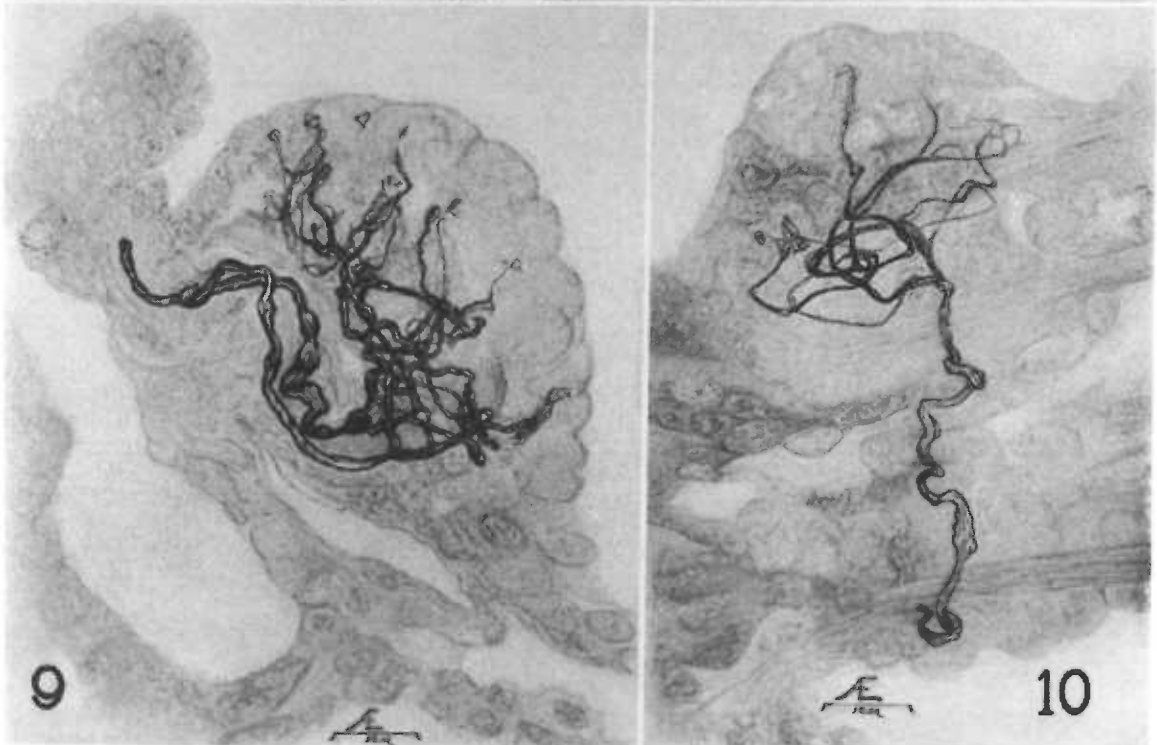
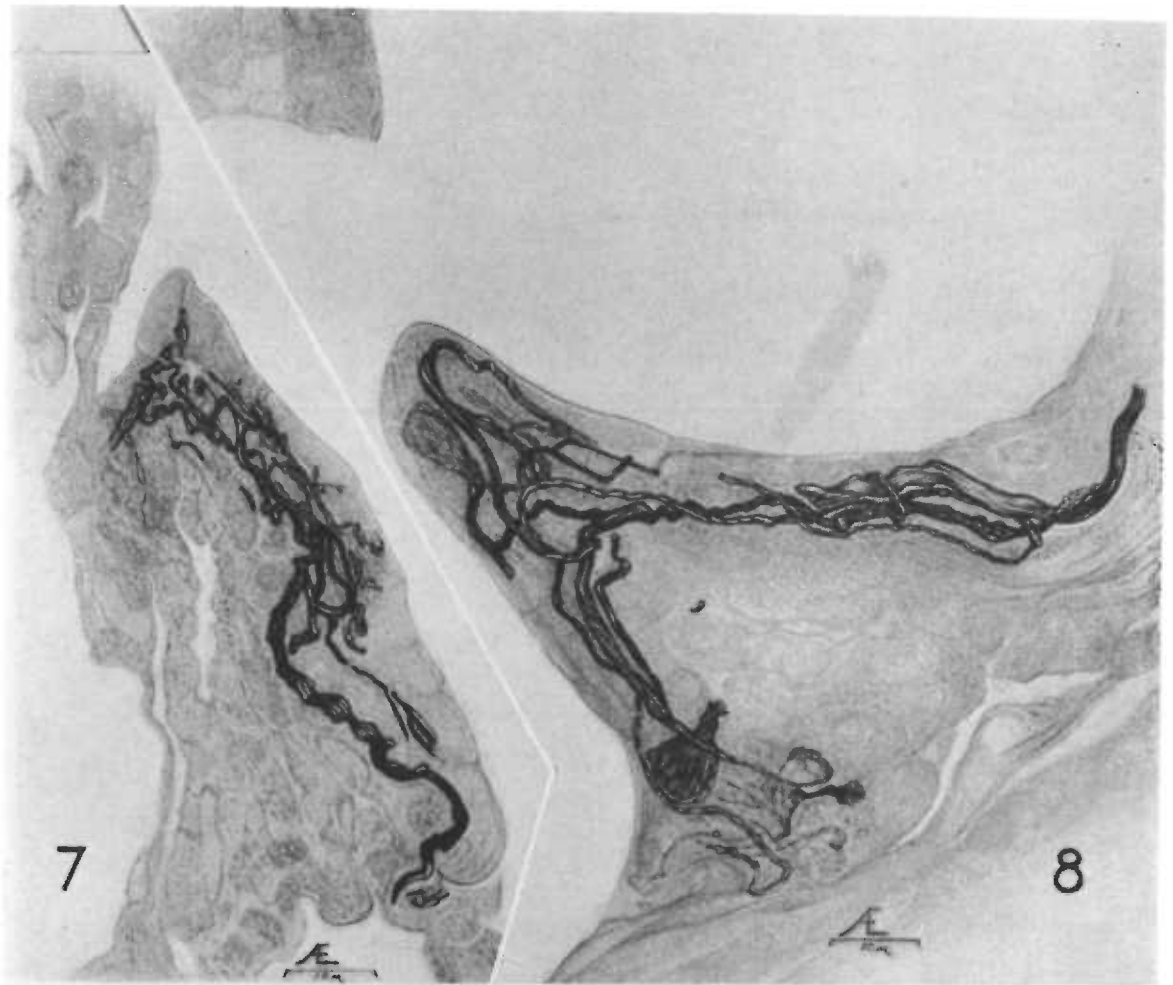


had described endings in the more terminal portions of the lung. During the histological examination of one lobe of a six week old dog Elftman encountered a total of 155 afferent nerve endings of which 46 or 30% were found distal to respiratory bronchioles and were not of the smooth muscle type. The histological appearance of these receptors is shown in figure 11. Whether those receptors are of the rapidly adapting type, the slowly adapting type, or whether they are even stretch receptors has not yet been established.

Adrian (54), Knowlton and Larrabee (56), and Widdecombe (57) have described an increased afferent nerve activity during deflation of the lung. To explain a deflation reflex Head (60) postulated that lung deflation activated a class of receptors which had a central influence of increasing the respiratory drive for inflation. Adrian, Knowlton and Larrabee, and Widdecombe used negative pressure ventilation in open chest animals as a means of exciting the deflation receptors. Only one of the twenty deflation sensitive receptors studied by Widdecombe had a pressure threshold less than -1 mm Hg across the tracheal wall while three of the twenty had a threshold greater than -100 mm Hg. Adrian stated that "forcible deflation (of the lungs) . . . by compressing the thorax by hand" was insufficient to excite the deflation receptors. Although there may be a deflation reflex, recording the afferent discharge associated with lung deflation has been accomplished only through procedures which very

Figure 11. Nerve endings in the lungs of puppies. 7, Flattened nerve ending beneath basement membrane in wall of alveolar duct; 8, nerve ending at the bifurcation of two air sacs; 9, nerve ending in a nodule in the wall of an air sac; 10, nerve ending in the wall of an alveolus.

From Elftman, *Am. J. Anat.*, 1943. 72, 1-28.



seldom if ever occur in the life span of the animal.

It is to be concluded from the above that there is a host of histologically distinct afferent nerve endings found in the mammalian lung. There is physiological evidence for two types of receptors, a rapidly adapting and a slowly adapting stretch receptor. The discharge frequency in the afferent fiber associated with the slowly adapting receptor has been shown to be closely related to both pulmonary volume and transpulmonary pressure. During eupnea deflation sensitive receptors are not active.

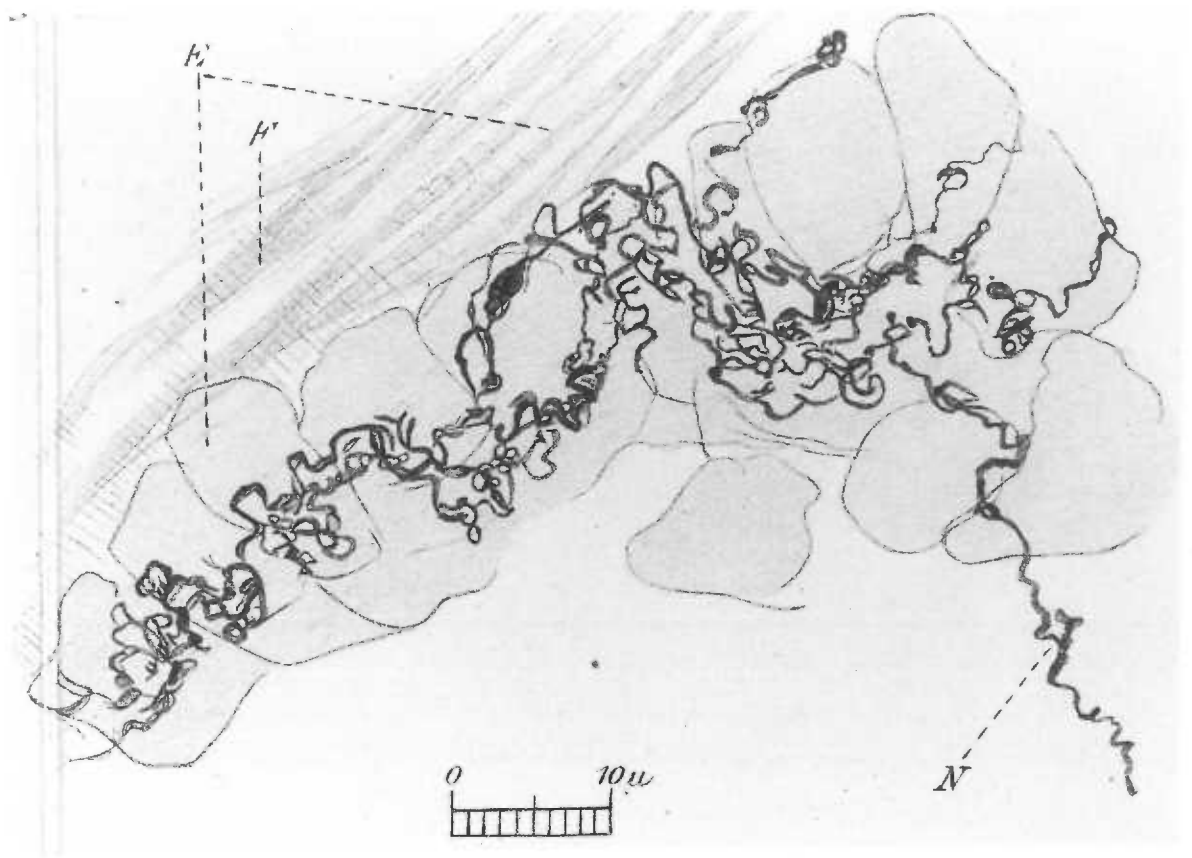
Anatomy and Physiology of Frog Pulmonary Mechanoreceptors

Following a histological examination of the nerve endings in the frog lung Wolff (61) stated that the position of these endings was ideal for the detection of stretch or tension within the lung. Wolff found a class of nerve endings which were dispersed throughout the inner epithelial lining of the lung (fig. 12). In addition Wolff was able to confirm findings of Cuccati (62) who demonstrated a network of nerve endings which was subepithelial and lay upon the underlying connective tissue and smooth muscle. Gaupp (63) reported nerve endings within the smooth muscle. However, his report did not contain illustrations of these nerve endings nor did he provide evidence that these endings were associated with afferent fibers. Gaupp also stated that most of the nerve endings of the lung were located in

Figure 12. Nerve endings as they appear in the frog lung.

N, nerve fiber; E, epithelial cells; F, smooth muscle fibers.

From Wolff, Arch. Anat. Entwickl, 1902. 5,
155-183.



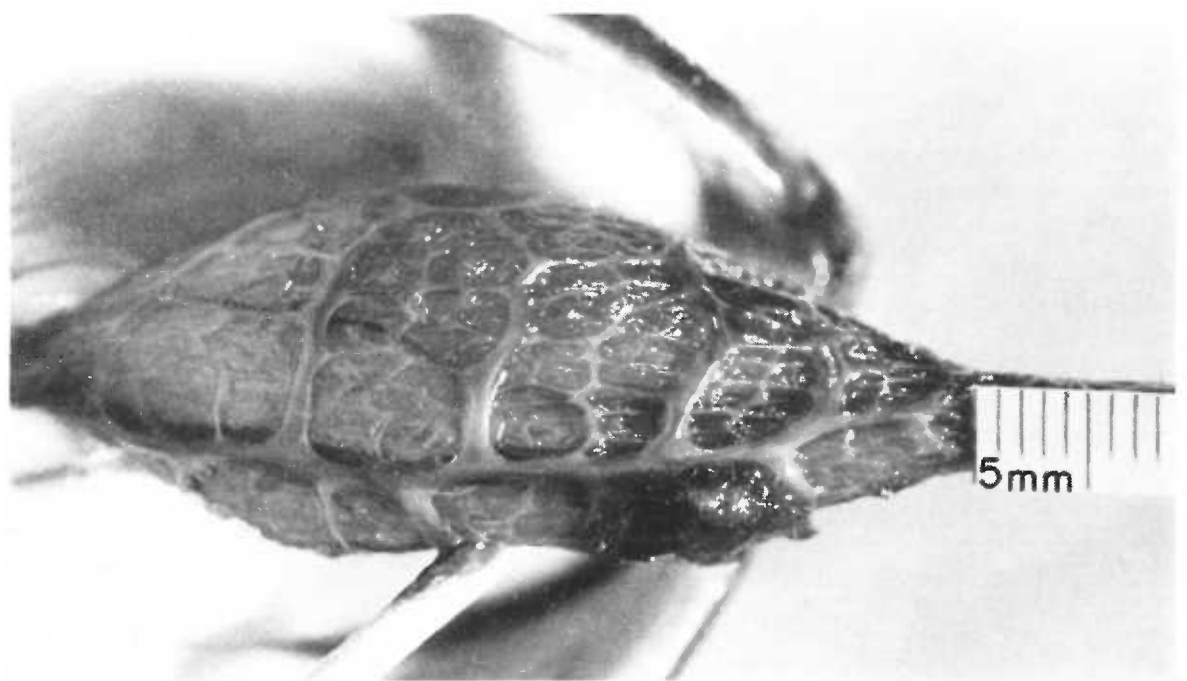
the neck of the lung near the bronchus.

The gross anatomy of the frog lung is substantially less complex than that of the mammalian lung. ". . . the lung is a . . . muscular sac [with] numerous septa on the interior surface dividing this [surface] into small spaces or alveoli. The septa extend only a few millimeters from the lung wall, so that the larger part of the lung cavity is a single air space." (64) (fig. 13). The receptors are contained in or below the epithelial lining which surrounds the smooth muscle lattice of the lung.

Electrophysiological investigation of the frog pulmonary mechanoreceptors began with the recording of action potentials in the pulmonary branch of the vagus nerve in response to lung inflation (65). This introductory work was followed by a quantitative study of the receptor in which Bonhoeffer and Kollat (66) found a linear relationship between discharge frequency and lung volume. The results were based on a total of ten single fiber experiments. The discharge frequency observed five seconds following inflation to a given lung volume was used as the discharge frequency in the discharge frequency-lung volume relationship. Pulmonary volume was increased in steps of one milliliter to a maximum lung volume of five milliliters. During the experimental volume increase the value of the intrapulmonic pressure was in excess of 100 cm water in some instances. Carlson and Luckhardt (64) found the intrapulmonic

Figure 13. Lung interior of bullfrog showing smooth muscle lattice. Lung has been everted.

From Kilburn, J. Appl. Physiol., 1967. 23,
804-810. (67)



pressure in a spontaneously breathing frog ranged from 3 to 5 cm of water with 10 cm of water being maximum value of intrapulmonic pressure which they recorded. Bonhoeffer and Kollat observed a nonlinear decrease in discharge frequency with time following the termination of inflation (cf. adaptation). Had these authors chosen for their discharge frequency determination a time other than 5 seconds following inflation, the relationship between discharge frequency and volume would not have been linear. So clearly the linear relationship between discharge frequency and volume was dependent upon the measurement of discharge frequency at a particular time following inflation. Furthermore, there was no indication of a statistical treatment of data. Rather the results from a single receptor were presented in graphic form. The findings of these authors must be interpreted with care in light of the intrapulmonic pressures which were attained and the lack of statistical treatment of data.

Taglietti and Casella (68) challenged the linear discharge frequency-volume relationship as they proposed a linear relationship between discharge frequency and tension in the wall of the lung. They could not measure the tension in the wall of the lung at the particular site of the receptor but certain assumptions allowed the computation of the total wall tension. If the receptors were linear transducers and were homogeneously distributed throughout the lung, the

frequency of discharge of all the pulmonary mechanoreceptors should be linearly related to the total wall tension. The total tension was computed according to

$$T = \int_{V_0}^V P dV / \Delta S$$

where P, V, and S signify pressure, volume, and surface area respectively. The integral was evaluated graphically and ΔS was computed by assuming the lung to be ellipsoidal in shape; the measurement of both major and minor axes would allow the calculation of

S. Since tension in a particular region of the lung would not necessarily be linearly related to total wall tension these authors chose to record from not one but many afferent fibers associated with pulmonary mechanoreceptors (mass discharge recording). The authors felt it reasonable to neglect the surface area of the septa because the septa ". . . completely disappear even by moderate inflation." However the authors did not comment on the previously established heterogeneous distribution of the receptors. The discharge frequency was taken as a total number of discharges which were electronically counted during the fifth to fifteenth second following inflation to a given volume. The discharge was also determined during the fiftieth to sixtieth second following inflation and these discharge frequencies were compared with the tensions which were realized during the appropriate time interval. In both time intervals the

discharge frequency was linearly related ($p < 0.001$) to wall tension. The results were based on four different lung volumes (0.5, 1.0, 2.0, 3.0 ml) with eight trials at each lung volume. The pressures which were attained following the inflation were within the "physiological" range. However, the pressures recorded during and just following inflation were not presented in the text. It is during this period that intrapulmonic pressure is greatest (65).

These authors also challenged the term adaptation as applied to the frog pulmonary stretch receptors. Even though the discharge frequency decreased with time following inflation it was still linearly related to tension and had the same proportionality constant throughout. Thus if tension were the adequate stimulus adaptation to this stimulus did not occur.

There are several other facets of frog lung and frog lung receptor physiology which were discussed by the German (66) and Italian (68) investigators. However, these points will be presented in the discussion portion of this thesis and in that context will have more meaning.

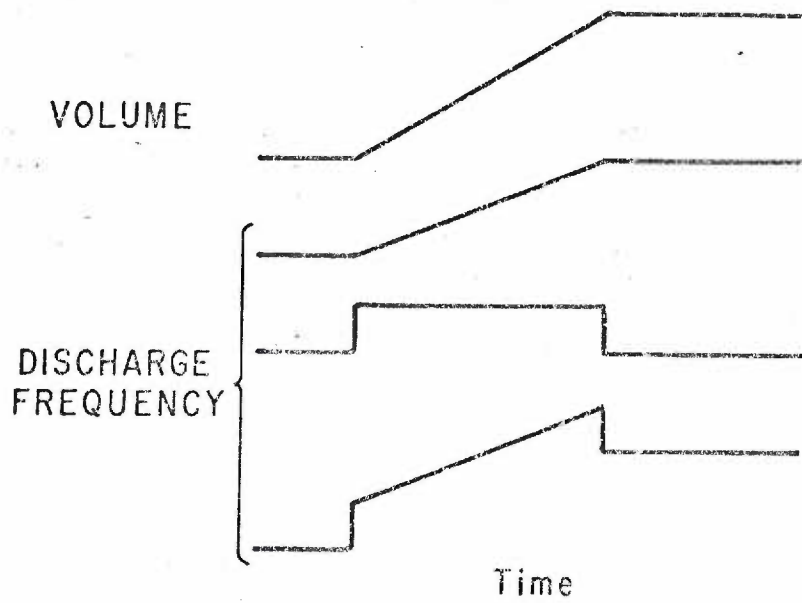
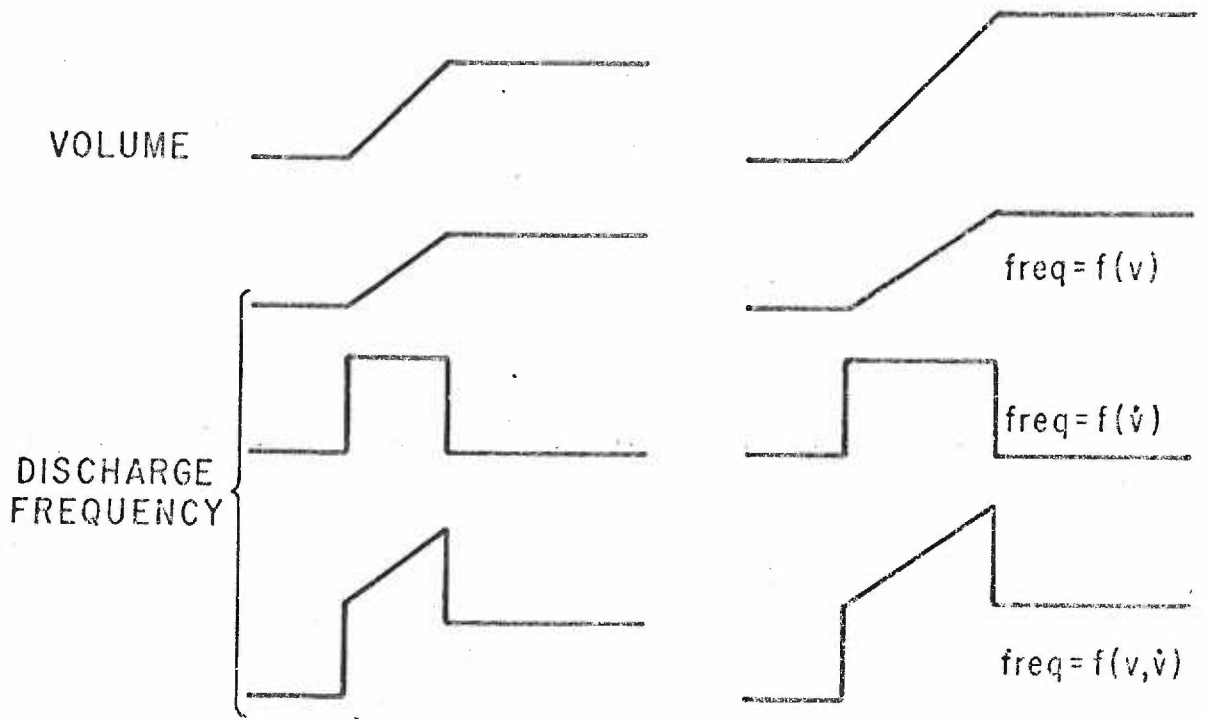
Prospectus

The goal of the experimental portion of this thesis was the determination of the transfer function of the pulmonary stretch receptors of the frog. The transfer function is defined as the output-

input ratio. The output, for the purposes of this study, was the frequency of discharge generated by pulmonary stretch receptors in single afferent fibers of the vagus nerve. Although there is evidence that tissue tension is the adequate stimulus for the receptor, pulmonary volume rather than pulmonary wall tension was used as the input metric for the determination of the transfer function. Pulmonary volume in comparison to pulmonary wall tension is more easily controlled and measured. Furthermore, two volume controlling devices became available for use in this investigation; the availability and simplicity of these devices provided a strong argument for the use of volume as the input metric.

Initial efforts involved the development of an isolated lung-single fiber preparation. Following the development of the preparation a population of receptors was examined to determine the response of these receptors to pulmonary volume changes. An input waveform consisting of the leading edge of a trapezoid was considered especially suited for the determination of response characteristics. The threshold for discharge, rate response, proportional response, lung pressure-volume characteristics and input-output delay were determined through the use of this input waveform. Figure 14 shows diagrammatically the responses of a rate, rate plus proportional, and proportional receptors to this half-trapezoid input. The proportional response of a receptor was determined by relating

Figure 14. Diagrammatic representation of the response of a rate, a rate plus proportional, and a proportional receptor to half-trapezoid input. Reading from top to bottom the four traces represent volume change input, proportional receptor response, rate receptor response, and rate plus proportional receptor response. The top two groups show the effect of increasing lung volume. The bottom group of responses shows the effect of decreasing the rate of inflation.



the discharge frequency to volume during the constant volume portion of the waveform. The rate response of a receptor was determined by subtracting the proportional response during the plateau from the response during the terminal portion of the ramp. Pressure-volume relationships were determined by measuring intrapulmonic pressure during the constant volume portion of the waveform and relating this pressure to the pulmonary volume. The thresholds of receptors which were not active during initial conditions were determined by noting the pulmonary volume necessary for the excitation of discharge activity in these receptors' afferent fibers. Finally the time delay between the initiation of a half-trapezoid volume change of very steep slope and initiation of a change of discharge activity in the afferent was determined. Later discussion will show the importance of this time delay.

The results of half-trapezoid inflation were used to develop a model which exhibited behavior similar to the behavior of the receptors. The differential equations which describe the model were used to develop an analog computer program of the model. Since the computer response to half-trapezoid inputs closely approximated the receptors' response to the half-trapezoid inputs, the coefficients of the transfer function could be determined. However, the transfer function describes the output to any known input. Only the half-trapezoid input was used in the determination of the transfer function,

therefore a second input waveform to the receptor was needed to confirm this transfer function. A sinusoidal volume change was used as the input waveform to test the uniqueness of the previously found transfer function. A phase angle versus log frequency diagram was obtained from the sinusoidal data. The phase angle portion of the Bode plot did not deny the uniqueness of the previously found transfer function but only weakly confirmed the relationship.

The results of the study suggested that the receptors' response may be influenced by the mechanical properties of the lung as a whole as well as the mechanical properties of the tissue immediately surrounding the receptor.

MATERIALS AND METHODS

Acquisition and Housing of Frogs

Unrefrigerated summer and winter frogs (Rana pipiens) were obtained from a local biological outlet and used throughout the study. The animals were housed in a 12" by 14" plastic tub to which tap water, small amounts of Ringer's solution (Table I), and moss were added. The moss was obtained from the biological outlet and accompanied the frogs during mail delivery. During the winter when "red leg" was present 300 mg. Chloromycetin was added to the housing tub.

Gross Dissection

Prior to dissection the animals were rendered unconscious by a sharp blow to the head, decapitated, and their spinal cords destroyed by pithing. The internal organs of the frog were exposed by skin incision followed by clavicular and sternal resection. 0.1 ml of heparin in 0.1 ml Ringer's solution was injected into the ventricle of the heart. It was felt that heparinization facilitated the dissection of single fibers from the nerve trunk. The liver, stomach, intestine, and ovaries were removed. Following evisceration the animal was placed under a binocular dissecting microscope. Dissection was performed under 10x magnification and was aided by a high intensity

TABLE I
Composition of Ringer's Solution

NaCl	6.5 grams/liter
KCl	0.14 grams/liter
CaCl ₂	0.12 grams/liter
NaHCO ₃	0.20 grams/liter
Na ⁺	114.4 m moles/liter
K ⁺	1.9 m moles/liter
Ca ⁺⁺	1.5 m moles/liter
Cl ⁻	115.4 m moles/liter
HCO ₃ ⁻	2.4 m moles/liter
	<hr/> 235.6 m moles/liter

light source located in front of the dissecting microscope and behind the preparation. The preparation was enclosed in a Faraday cage which was used to diminish outside electrical interference and improve the signal to noise ratio of the nerve recording.

Gross dissection of the vagus nerve began with removal of the heart and proximal aorta. Jewler's forceps and iridectomy scissors proved useful in this procedure. These same instruments were used to separate the vagus nerve from the pulmonary artery and following separation the artery was cut. The lung was reflected medially and the gastric, cardiac, and esophageal branches of the vagus nerve were cut. The remaining portion of the nerve was separated from the sternocutaneous artery and was traced laterally and dorsally and freed from surrounding tissue. The nerve was then cut just above its junction with the laryngeal branch of the vagus nerve. Fine silk was passed under the dorsal aspect of the larynx. A small (5 mm) slit was cut in the ventral aspect of the larynx and a blunted and shortened 13 gauge needle was passed through the slit and into the lung cavity. A shallow (< 1 mm) groove had been etched around the needle 5 mm from the needle tip. The silk was drawn tightly around the larynx so that the silk fit into the groove of the needle. Prior to the tightening of the ligature, traction in the caudal direction was placed on the nerve since the ligature was only a few millimeters cephalad to the nerve as it entered the lung tissue. The nerve was

easily damaged during this procedure and great care had to be exercised at this point in the procedure. After the cannula was placed in the lung, the lung and vagus nerve were dissected from the remainder of the animal and excess connective tissue was trimmed from the lung-nerve preparation. The preparation was placed on the male fitting of a side arm adapter which was supported by a clamp attached to a ring stand. The needle which was inserted into the lung cavity pointed downward and made an angle of approximately 30 degrees with the vertical. A culture dish was placed under the preparation and was filled with Ringer's solution to a level of the neck of the lung. The bottom of the culture dish was painted black to provide a dark background for the white nerve. This aided microdissection of the nerve.

Microdissection

Single fiber dissection was accomplished in the following manner. The vagus nerve was placed on the recording electrodes which had been previously flamed. The lung was inflated with several tenths of a milliliter of Ringer's solution which was contained in a tuberculin syringe. If activity indicative of nerve activity was present on the face of the oscilloscope used for visual display, 60 ml of mineral oil was poured into the culture dish. The mineral oil was used to prevent the nerve from drying. The inflation procedure was

also used to clear the lung of air and parasites (Pneumonices) and to test for leaks. If nerve activity was absent or if the lung was damaged or excessively parasitized the experiment was terminated. The cut end of a viable nerve was crushed with jeweler's forceps and then divided longitudinally into two roughly equal parts. One of these nerve strands was grasped at the cut end and this strand was subdivided into smaller strands. Following each division the smaller of the divided strands was placed on the electrodes and the lung was inflated to assay for nerve activity. This procedure was followed until a single active unit was isolated. Single active units were most easily isolated if the jeweler's forceps were both sharp and symmetrical. It was felt that very fine filaments should not be stripped from a nerve strand as these fine filaments (2-3 fibers) were almost always unviable. Neither should large filaments (20-30 fibers) be stripped from a nerve strand as more than one active fiber was usually present in them. Action potentials seen on the scope face that were of constant magnitude and rhythmicity were thought to represent unitary discharge. These criteria of constant magnitude and rhythmicity were applied later in the experimental procedure as a check.

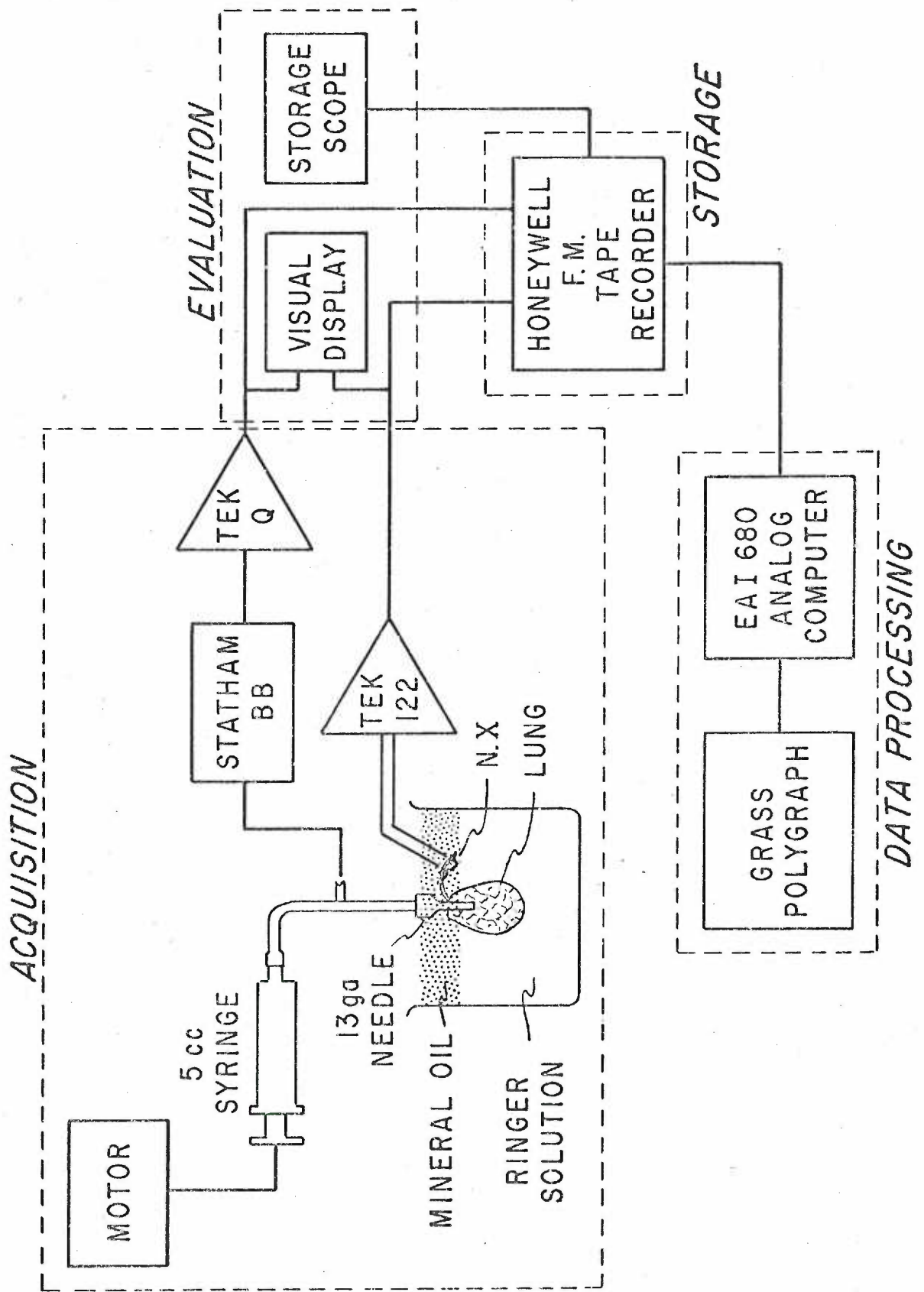
Input

The lung was inflated by means of a motor-driven, fluid-filled

syringe connected to the lung by a 35 cm length of polyethelene tubing (PE 320) (figure 15). Ringer's solution rather than air inflation was desirable for two reasons. With a fluid-filled system there was no air-fluid interface with the resultant surface forces which have been shown to influence the pressure-volume relationships of the mammalian lung (69). Secondly, since Ringer's solution is present in both the lung cavity and the culture dish, the lung was not distorted by having to support its own weight or by buoyancy forces.

The half-trapezoid volume change was carried out in the following manner. A Harvard infusion pump (model 600-910/920) was switched on and the motor and gear assembly pushed the plunger of a 5.0 ml glass syringe forward (or pulled it backward) at a constant rate. When the desired volume change had been accomplished the motor was switched off and the movement of the plunger was abruptly terminated by applying an opposing force with the thumb. It was felt that with practice this technique produced a close approximation of a half-trapezoid waveform. The rates of inflation used in the study were 0.34, 0.14, and 0.07 ml/sec. The volume changes were limited to a maximum volume change of 1.0 ml so that intrapulmonic pressure remained within the physiological range. The sinusoidal inflation was accomplished through the use of a scotch yoke apparatus connected to the plunger of a plastic 1 ml syringe. The wheel of the apparatus was turned by a Bodine (type NSE-11-R) electric motor.

Figure 15. Block diagram of preparation and apparatus.



The speed of the motor was varied by changing the input voltage to the motor. A Variac was used for this purpose. The frequency of the sinusoidal waveform could be varied from 0.2 Hz to 2.0 Hz. A linear potentiometer was used to measure the position of the syringe plunger. The potentiometer was used in conjunction with a Tektronix type Q plug in unit.

Due to the small diameter of the neck of the lung, intrapulmonic pressure was not measured directly but was measured several centimeters above the fluid level of the culture dish (figure 15). If the appropriate hydrostatic pressure correction is made, the recorded pressure is identical to intrapulmonic pressure when no flow is present in the system. During the most rapid half-trapezoid inflations the indicated pressure exceeded intrapulmonic pressure by 0.5 cm of water. Pressure records were not corrected for this error. The compliance of the syringe, tubing, and pressure transducer system was approximately 10^{-3} ml/cm H₂O. This was several orders of magnitude less than the compliance of the lung and was therefore neglected.

Recording

The pressure measuring device was a Statham P-5 pressure transducer used in conjunction with a Grass 5P1 preamplifier. The transducer was connected to the side arm adapter with a ten cm

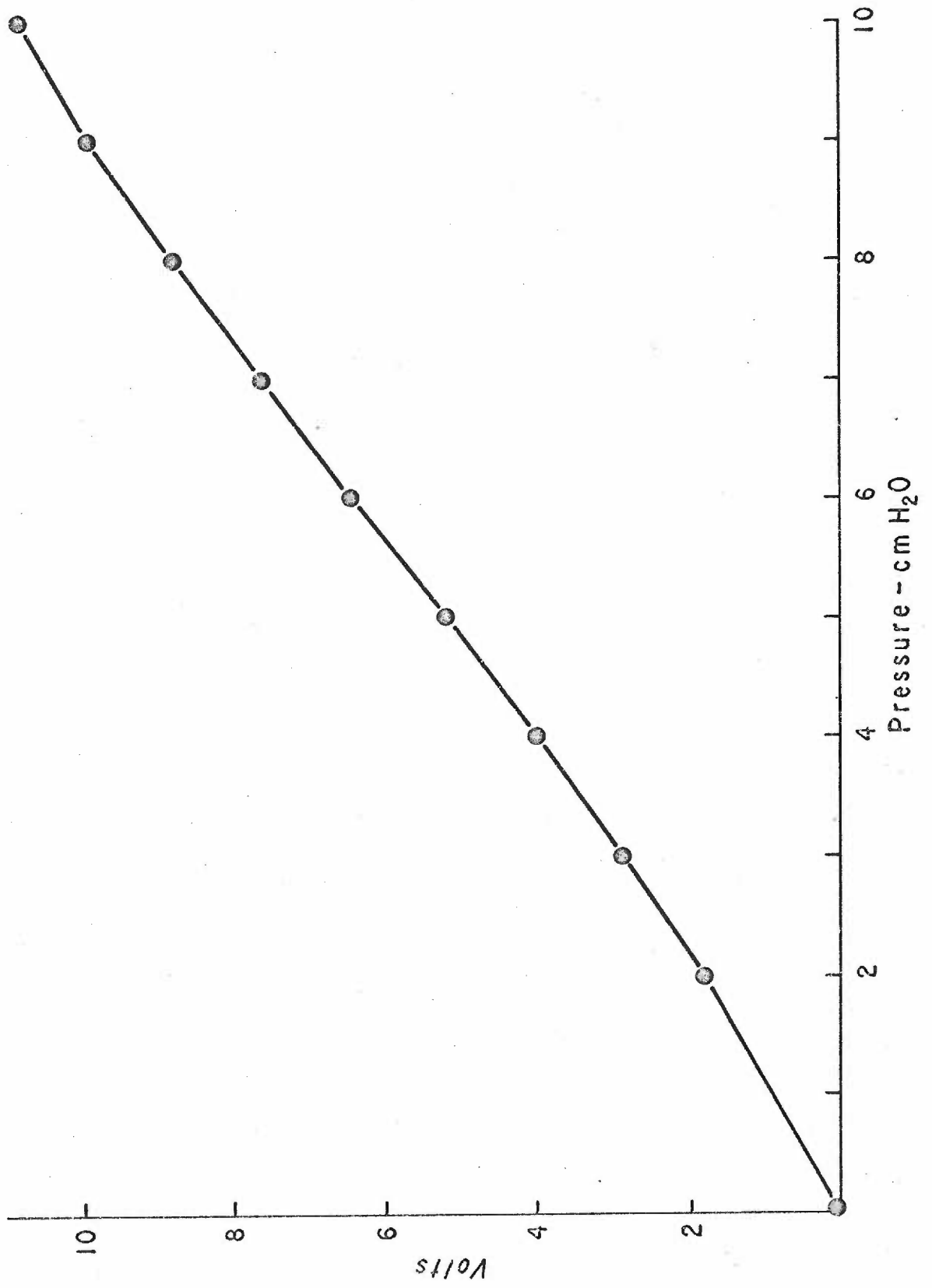
length of PE 320 tubing. Both tubing and transducer were fluid filled. The calibration curve for the pressure recording system is shown in figure 16.

The action potentials (approximately $100 \mu V$) were recorded by placing the nerve on two 0.007" diameter 90% platinum - 10% iridium electrodes. The electrodes were positioned with a micromanipulator. The electrodes were coupled to a Tektronix 122 preamplifier by way of shielded cable. The 122 was modified by replacing 12AU7 tubes with 12AT7 tubes which increased the gain to 5000 instead of the normal 1000. An 80-10K Hz bandpass was used.

Signal Processing

The output of the 122 preamplifier was fed to the input of a Tektronix 360 oscilloscope. The 360 was used for visual display of action potentials. Depending on the experimental protocol, amplified action potentials were fed via a T adapter from the 360 to either a Honeywell 8100 tape recorder for storage or a Tektronix 502 dual beam oscilloscope. The amplified pressure transducer signal was taken from pin J-1 of the Grass driver amplifier and filtered with a standard RC($f_1=23\text{Hz}$) low pass filter. The filtered signal was fed to either the tape recorder or the Tektronix 502 scope. An unfiltered pressure signal was fed to a second 360 scope for visual display. In some experiments volume signals from the Q unit were substituted

Figure 16. Calibration curve of pressure recording system.
Abscissa is pressure measured by water manometer
and ordinate is output voltage from Grass amplifier.



for pressure signals.

Simultaneous photographs of the action potentials and intrapulmonic pressure or pulmonary volume were obtained through the use of the Grass camera and the 502 scope. The horizontal amplifier of the oscilloscope was placed in the external mode and the horizontal input to the amplifier was grounded. The Grass camera was used in the moving mode so that Kodak Linographortho film passed behind the lens at a constant ($\pm 2\%$) rate. A dark red transparent plexiglass hood was placed between the scope face and camera lens so that photographs could be obtained in a lighted room.

The film speed for photography of action potentials from the face of the 502 was an indicated 2.5 cm/sec. This rate was checked by photographing pulses from a Tektronix 161 pulse generator which was triggered by a Tektronix 162 waveform generator. The true film speed (according to the 162) differed from the indicated film speed by 10%. The film speed varied less than 2% of the mean film speed. The deviation of the true value from the indicated value does not influence the experimental results as the results depend on a constant film speed.

Data Reduction

Discharge frequency of action potentials was determined in one of three ways. The first was the measurement of the reciprocal of

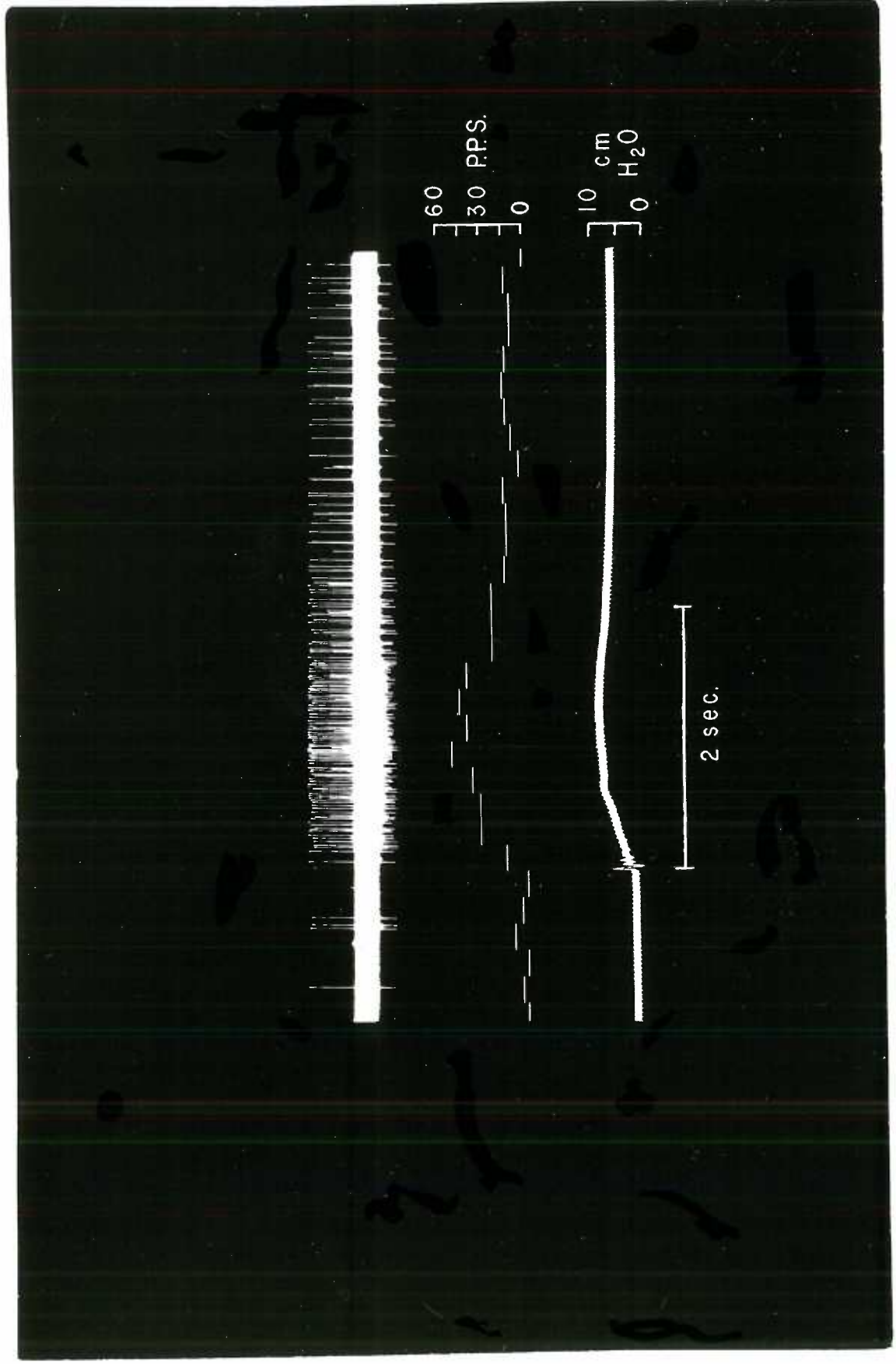
the interval between action potentials as they appeared on the photographic record. The second method allowed the determination of the instantaneous frequency of discharge; however this was done electronically. This second method is described in detail in the appendix. The third method involved the use of an E. A. I. 680 analog computer. The computer was patched (appendix) in such a fashion as to count the number of action potentials which occurred in successive short time intervals, typically 200 ms. The relationship between the action potentials and the computer output may be seen in figure 17.

Experimental Procedure

Resting or initial conditions were established by inflating the lung with Ringer's solution and allowing the elastic recoil of the lung to expel the fluid. Under these conditions the intrapulmonic pressure was equal to the vertical distance between the side arm and the fluid level in the culture dish multiplied by the specific gravity of the Ringer's solution. This pressure was typically 2.5 cm of water. The discharge under these conditions was taken as resting discharge. The P. E. tubing from the infusion pump was connected to the side arm fitting and the lung was experimentally inflated. The half-trapezoid waveforms used were a ramp of 0.34 ml/sec with a final volume of 0.2 ml, 0.4 ml, 0.6 ml, 0.8 ml, and

Figure 17. Relationship between action potential input and computer output.

Top line, action potentials; middle trace, computer output in pulses per second; bottom trace, intrapulmonic pressure. "Bin" width was 200 ms. Computer program is explained in the appendix.



1.0 ml, and also a final volume of 1.0 ml with a ramp of 0.14 ml/sec and 0.07 ml/sec. The duration of the waveform was varied throughout the study.

A very rapid half-trapezoid waveform volume change was introduced into the lung by disconnecting the connecting rod of the scotch yoke from the motor driven wheel and striking this rod with the palm of the hand. This method produced a near linear volume change of 0.5 ml with a ramp duration of less than 20 ms. This procedure was used to find the delay time for the "system." The significance of this delay will be presented in the results section.

Sinusoidal inflation of the lung was sometimes preceded by inflating the lung with a variable quantity of Ringer's solution. In one experiment 1.0 ml was the inflation volume. In four experiments an initial volume of 0.6 ml was used. The sinusoidal change in lung volume about this initial level was 0.5 ml and the frequencies used were approximately 0.2, 0.5, 1.0, and 2.0 Hz.

Miscellaneous Procedures

Following some experiments the conduction velocity as well as the lung volume at initial conditions was determined. The initial lung volume was determined by reestablishing initial conditions, removing the lung from the apparatus and weighing the lung with and without its fluid contents. The difference in weight in grams was

taken as the quantity of Ringer's solution in ml present in the lung under resting conditions.

Conduction velocity was determined for several fibers. Three Pt.-Ir. electrodes were used instead of the usual two. The most distal of the three electrodes provided one side of the differential input to two 122 preamplifiers. The middle electrode completed the input to one of the preamplifiers while the proximal electrode completed the input to the other preamplifier. The outputs of both preamplifiers were fed to a Tektronix dual trace 564 storage oscilloscope. A propagated action potential was first detected as the wave of depolarization arrived at the proximal electrode. This same action potential was detected somewhat later when it arrived at the middle electrode. The conduction velocity of the fiber in which the action potential was recorded was given by the interelectrode distance divided by the time required for transit between the two electrodes. The output of the 122's were simultaneously displayed on the face of the storage scope. One of the action potentials triggered the sweep and the distance between the peaks of the two action potential traces was measured and converted to a time value. Interelectrode distance was typically 1 mm.

Compliance values ($\Delta V/\Delta P$) for the lung were obtained from the half-trapezoid data and from a group of experiments with isolated frog lungs. The Grass polygraph output was used as the pressure

readout in the isolated lung experiments. The lungs were inflated with the Harvard infusion-withdrawal pump. Pressures were read to the nearest 0.5 cm of water which because of the variability between trials was considered to be sufficiently precise.

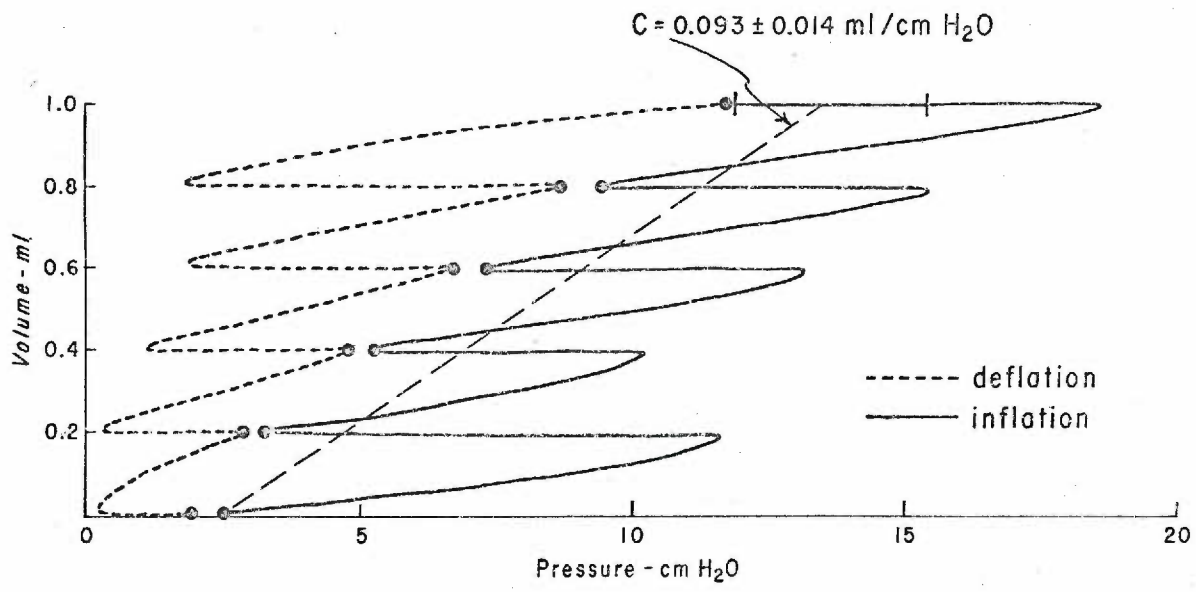
RESULTS

Pressure-Volume Characteristics of the Frog Lung

The pressure-volume characteristics of the frog lung were determined for several reasons. The pressure-volume relationships reflect some of the mechanical characteristics of lung tissue. In the Pacinian corpuscle and the Golgi tendon organ the mechanical behavior of the tissue surrounding the receptor has been shown to influence the response characteristics of the receptor. Thus a study of both mechanical properties of the lung and the response properties of the receptor might allow the testing of the possibility that a portion of the response characteristics of the receptor is due to mechanical filtering by the lung. In addition pulmonary pressure-volume characteristics were determined so results of pressure-volume measurements previously found in the frog (66, 68) and mammal (70) might be compared with the results found in this study.

The pressure-volume characteristics of the frog lung are summarized in figure 18. Following the initiation of a half-trapezoid volume change the intrapulmonic pressure rose from the initial pressure of 2.5 cm H₂O, reached a peak at the termination of the ramp portion of the waveform, decayed during the constant volume portion of the waveform, and then became stable about 40-60 seconds following the termination of the ramp. From the resting lung volume

Figure 18. Pressure-volume characteristics of the frog lung. Straight dashed line represents the mean compliance of nine frog lungs. Short vertical lines indicate one standard deviation of compliance. Each of the nine lungs p-v relationships was tested for linearity. Correlation coefficients ranged from 0.856 to 0.995 with degrees of freedom equal to three. Only one of the nine lungs had a nonlinear compliance relationship. The solid and the short dashed lines represent the pressure-volume behavior of a single lung. The experimental procedure is described in the text.



plus 0.2 ml a second half-trapezoid volume change was initiated and the intrapulmonic pressure rose and then fell. Following the half-trapezoid volume change from 0.8 to 1.0 ml the lung volume was decreased in 0.2 ml increments in a half-trapezoid fashion and the intrapulmonic pressure changed according to the dashed line. At a given lung volume the intrapulmonic pressure was always greater during lung inflation than during lung deflation. These results indicate hysteresis. Intrapulmonic pressure decrease during the inflation limb (pressure increase during the deflation limb) appeared to have at least two components. The initial decay had a rapid time course (time constant 0.2-0.6 sec) while the slower decay was essentially complete within one minute following the termination of the ramp. The rapid decay was not seen with every inflation as the magnitude of this component decreased with repetition of the inflation. In other words the rapid decay component was most easily seen in "fresh" lungs. On the basis of changes in intrapulmonic pressure without corresponding changes in lung volume there was seen in some lungs (figure 25) what was believed to be spontaneous smooth muscle activity.

The compliance of the lungs of nine frogs is shown as the straight dashed line in figure 18. The pressure measurements were determined immediately following the most rapid decay component. The compliance curve determined under these conditions was linear

($P < 0.001$) according to linear regression analysis (71). Initial lung volumes, smallest lung volumes necessary for discharge in the afferent fibers associated with receptors (thresholds), and conduction velocities in the afferents associated with the receptors were determined in numerous nerve-lung preparations. These parameters were investigated to determine if there was a correlation between receptor response and initial lung volume, threshold, or fiber conduction velocity. In the cat the threshold for the rapidly adapting pulmonary stretch receptor has been reported to be much greater than the lung volume (threshold) necessary to produce activity in the afferent fiber associated with the slowly adapting stretch receptor (56). Two types of mammalian muscle spindles, each with a characteristic response, may be differentiated on the basis of the conduction velocity in the afferent fiber associated with the particular receptor (31).

Initial Lung Volume

The initial lung volumes were determined in five frog lungs and ranged from 0.2-0.5 ml with a mean value of 0.36 ml. In subsequent sections of this thesis the term lung volume signifies the lung volume above initial lung volume.

Threshold

Twenty one of thirty receptors (70%) studied for threshold showed discharge during the resting conditions. The greatest discharge frequency recorded during the resting conditions was eight discharges per second. The remaining 30% of the receptors had a threshold ranging from 0.1 ml to 0.8 ml above resting lung volume. The volume at which discharge commenced (threshold) was dependent on the rate of inflation. Observed thresholds for discharge were generally greater for low inflation rates than for high inflation rates.

Conduction Velocity

Conduction velocity was determined for six fibers. The observed conduction velocities were 3, 4, 8, 10, 12, and 34 meters per second.

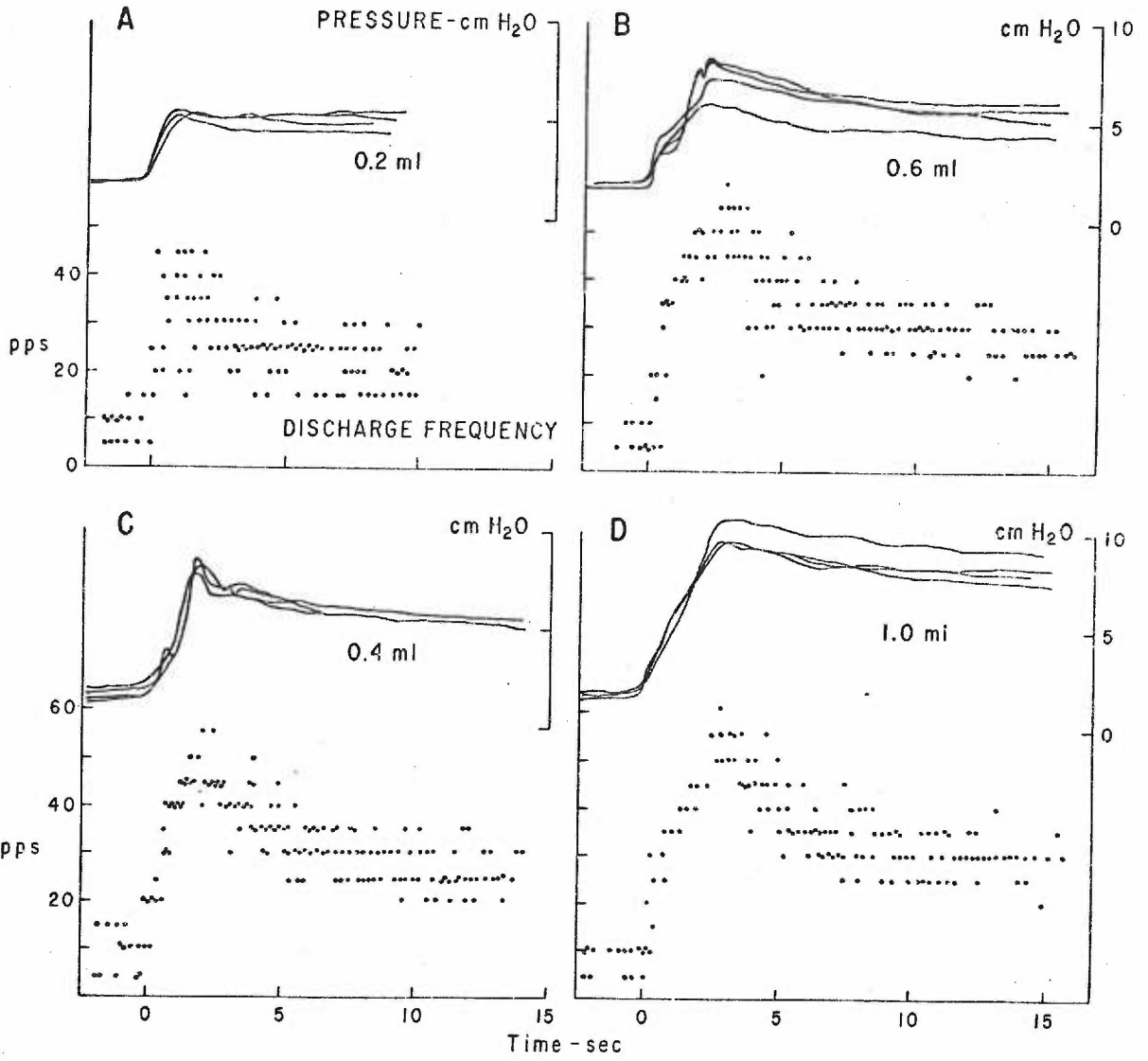
Discharge Patterns

Several hundred frog lungs were subjected to the half-trapezoid input and the resulting response was recorded from forty afferent fibers. On the basis of their discharge patterns, receptors were classified into three groups. The basis for grouping was as follows: Receptors which exhibited a proportional response had discharge frequencies which increased with the magnitude of the constant

volume portion of the waveform. Receptors which exhibited a rate response had discharge frequencies which increased as the slope of the half-trapezoid waveform increased. Figure 14 illustrates the three categories of receptors; those which exhibit rate responses, those which exhibit proportional responses, and those which exhibit both kinds of responses. Even with the classification of receptors into three groups according to their rate and proportional responses, there remained certain kinds of variability among receptors within a group. The pattern of frequency changes given by two receptors within a group often had identical time courses yet the magnitudes of the frequency changes differed. A second type of variability among receptors within a group was seen only in the rate plus proportional group. Two receptors with identical proportional responses had different rate responses and conversely two receptors with identical rate responses exhibited different proportional responses. Yet both receptors were grouped as rate plus proportional receptors. Thus considerable receptor variability accompanied the classification of receptors into one of three groups.

The variability of the response of a receptor to repeated trials is shown in figure 19. The receptor was subjected to five trials with a fifteen second interval between trials. The first of the five responses was discarded and the remaining four responses were superimposed. Although there was intertrial variability the receptor's

Figure 19. Intertrial variability of the response. Each dot represents the frequency of discharge during a 200 ms bin. The input waveform was a half-trapezoid volume change with a slope of 0.34 ml/sec and final volume indicated beneath the pressure traces. Experimental procedure is described in the text. Figure redrawn from polygraph record.



basic discharge pattern was preserved over these four trials.

Rate Receptor

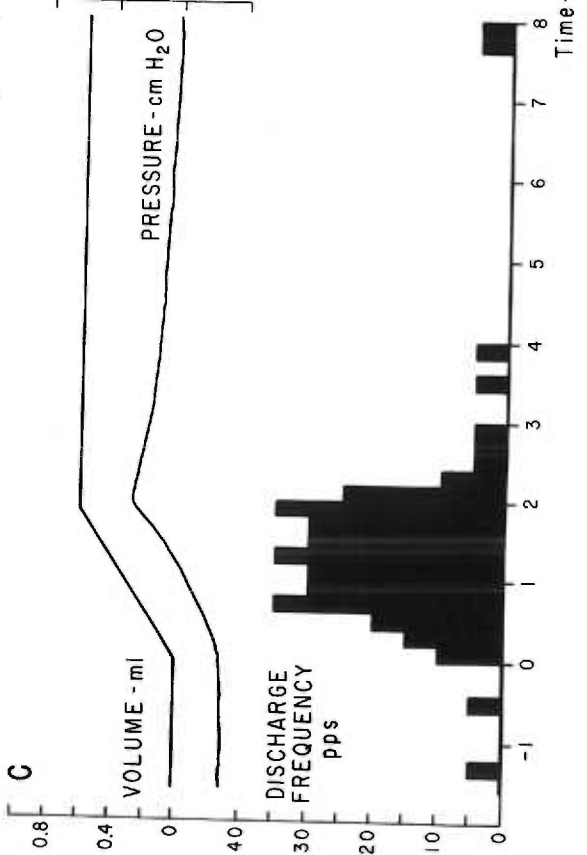
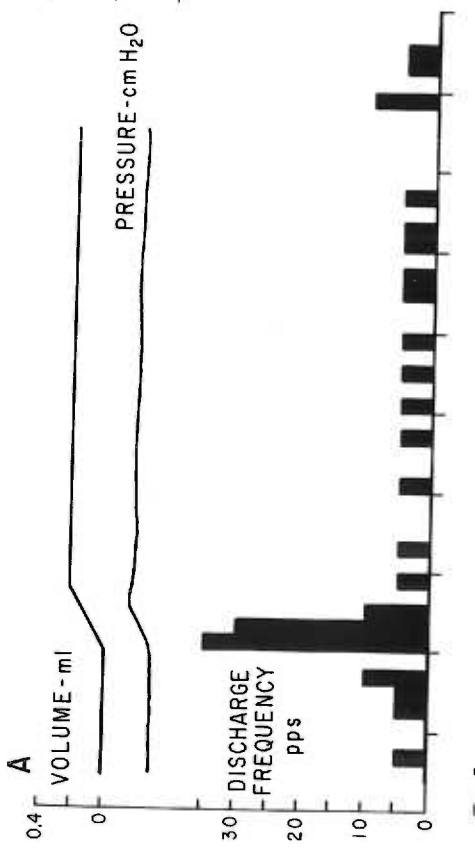
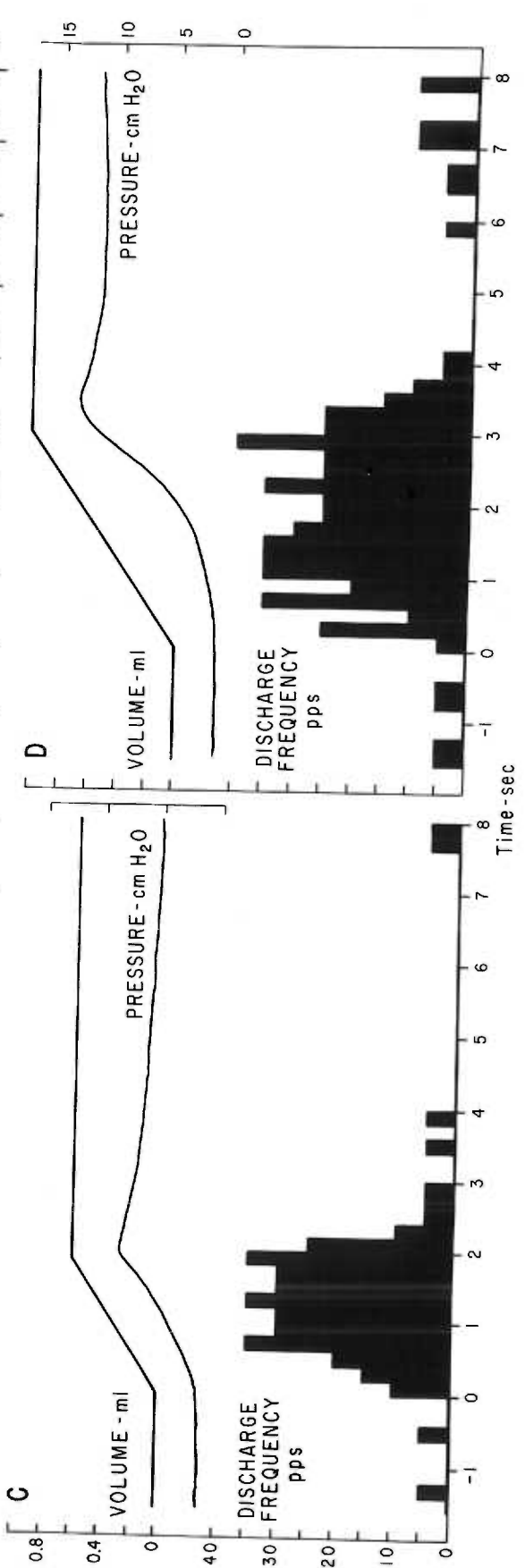
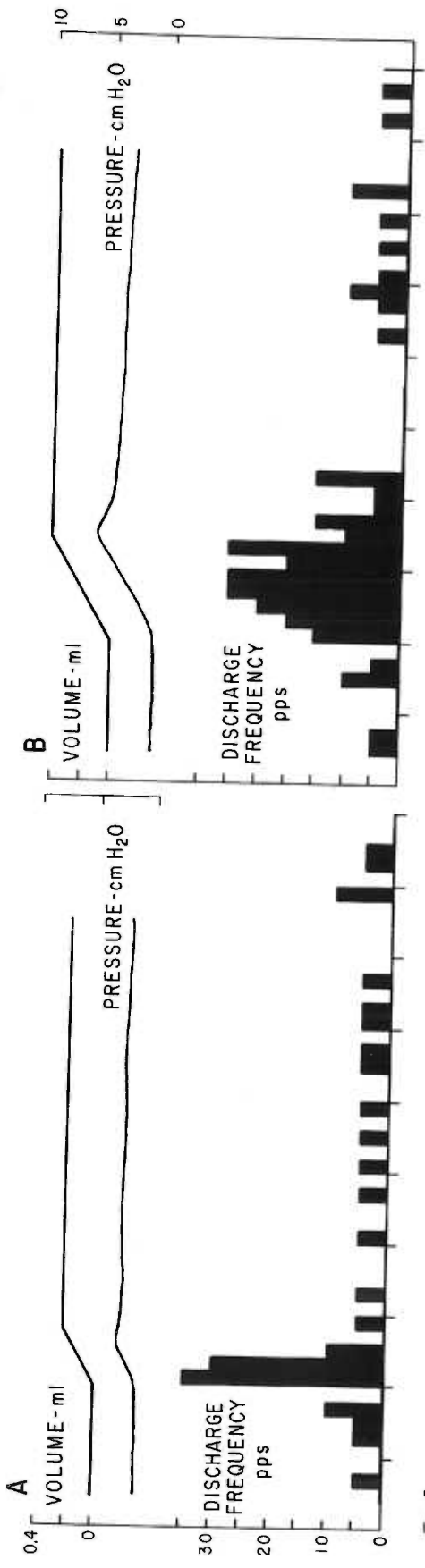
Figure 20 shows the characteristic discharge pattern of a rate receptor. Twenty eight percent of the forty receptors were classified as rate receptors. This particular receptor (figure 20) exhibited discharge activity during the resting condition. The discharge frequency increased abruptly with the onset of the input waveform, stabilized around 30-35 pulses per second for the duration of the ramp, and rapidly decreased to the preinflation level following the termination of the ramp portion of the waveform. Except for the duration of the activity, the receptor's response was independent of lung volume. Figure 21 illustrates the response of this same receptor to different rates of inflation. The discharge frequency appears to be directly related to the rate of inflation of the lung.

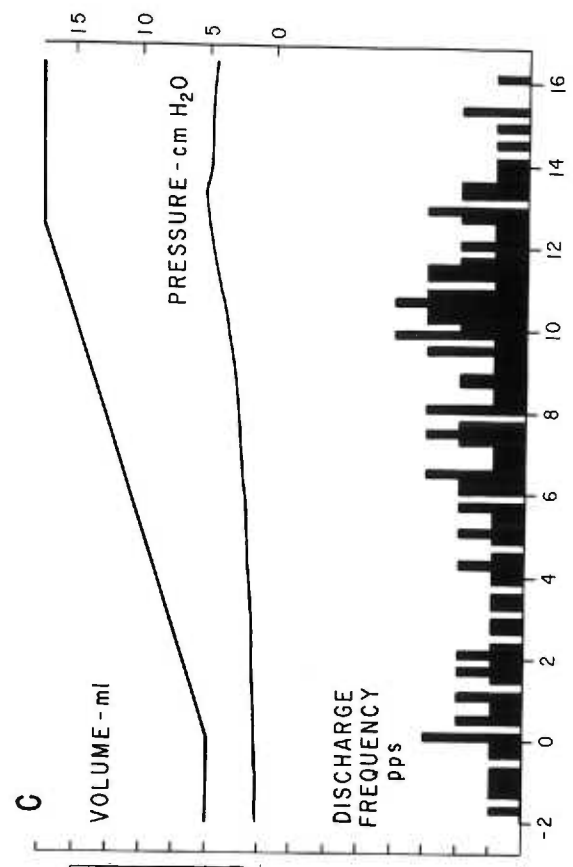
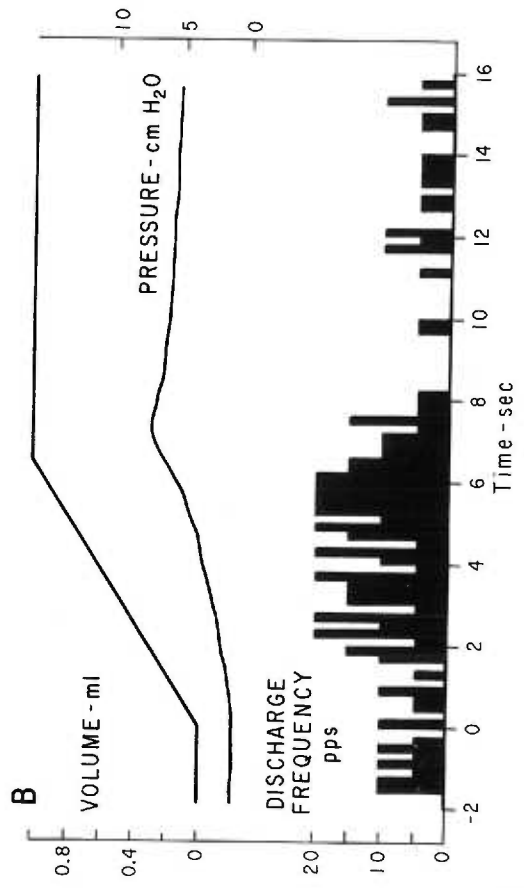
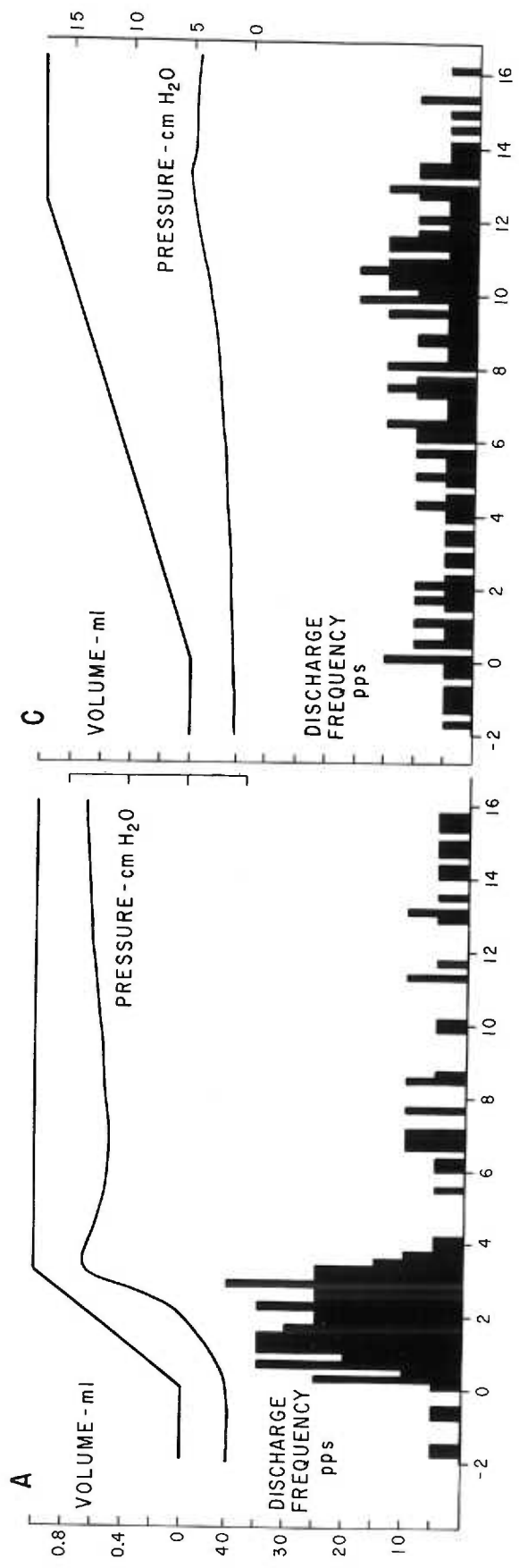
Rate Plus Proportional Receptor

The type of receptor most often encountered (52%) was the rate plus proportional receptor. The response of a rate plus proportional receptor is shown in figure 22. The peak discharge frequency which occurred at the termination of the ramp increased as the volume increased. The discharge which occurred during the plateau region of the waveform also increased with the final volume. The difference

Figure 20. Discharge pattern of rate receptor. The height of the black bars represents the number of action potentials which occurred within a 200 ms interval (bin). The discharge frequency (pps) is given by the number of action potentials which occur during a bin divided by the bin width. The rate of inflation was 0.34 ml sec. The final volume is indicated in the volume trace.

Figure was redrawn from a polygraph trace.





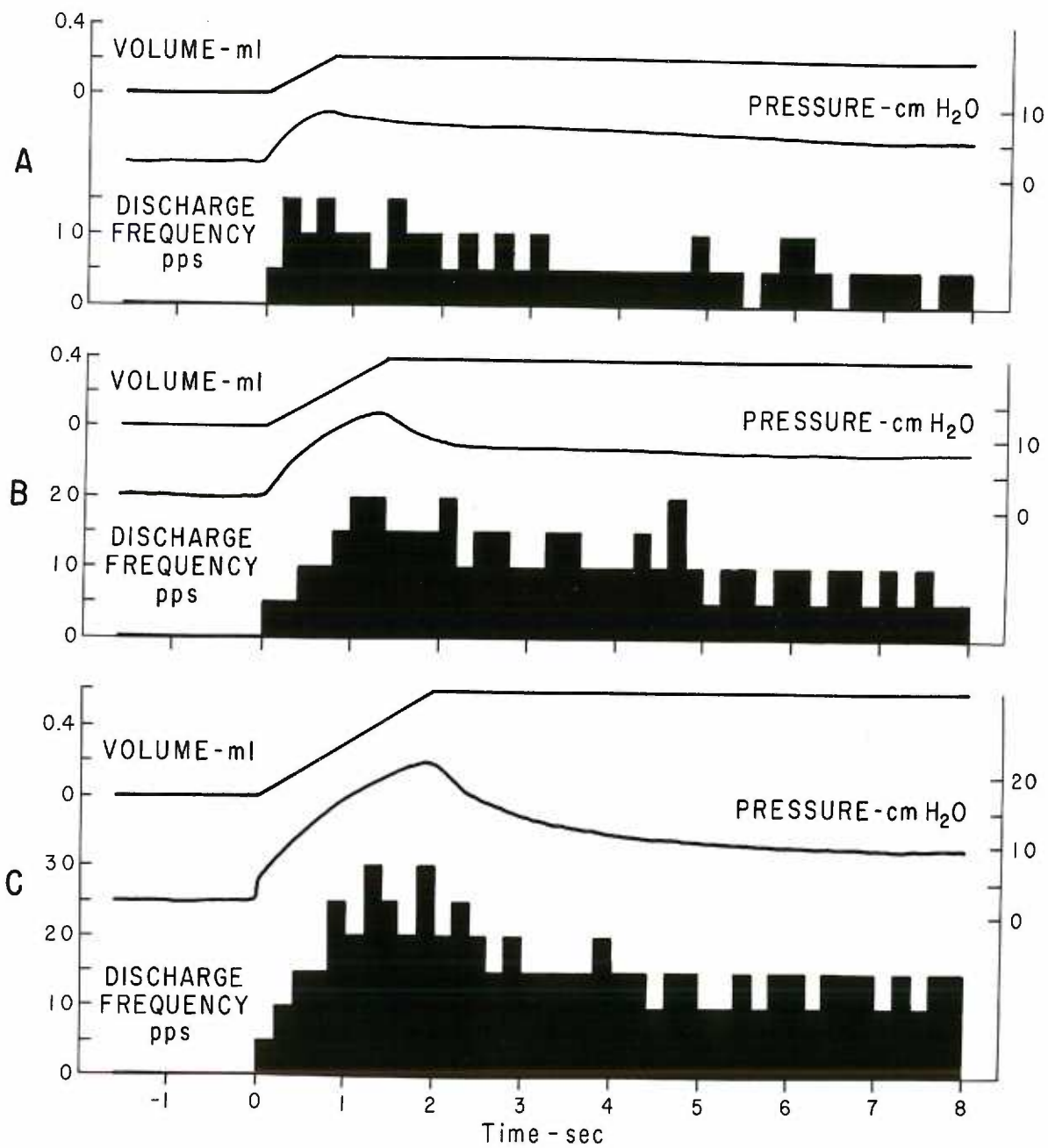


Figure 23. Discharge pattern of rate plus proportional receptor. Rate of inflation was 0.07, 0.14, and 0.34 ml/second in A, B, and C respectively. Final volume was 0.6 ml in all cases. Bin width was 200 ms. Note the decreasing threshold from A to C.

Figure redrawn from polygraph record.

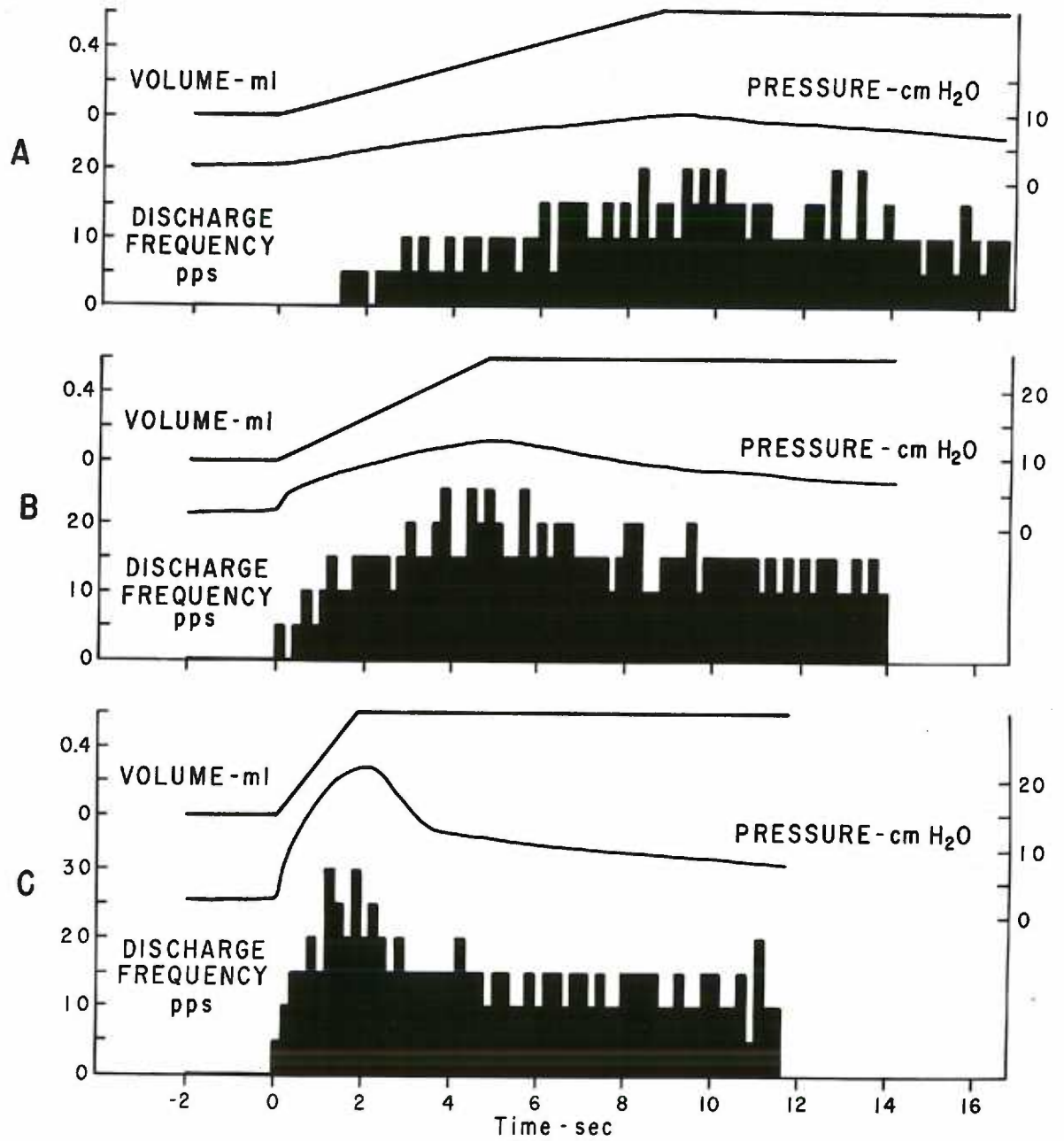


Figure 24. Discharge pattern of proportional receptor. In A, B, and C the rate of inflation was 0.34 ml/second. Inflation rate in D was 0.14 ml/second. Bin width was 200 ms.

Figure redrawn from polygraph record.

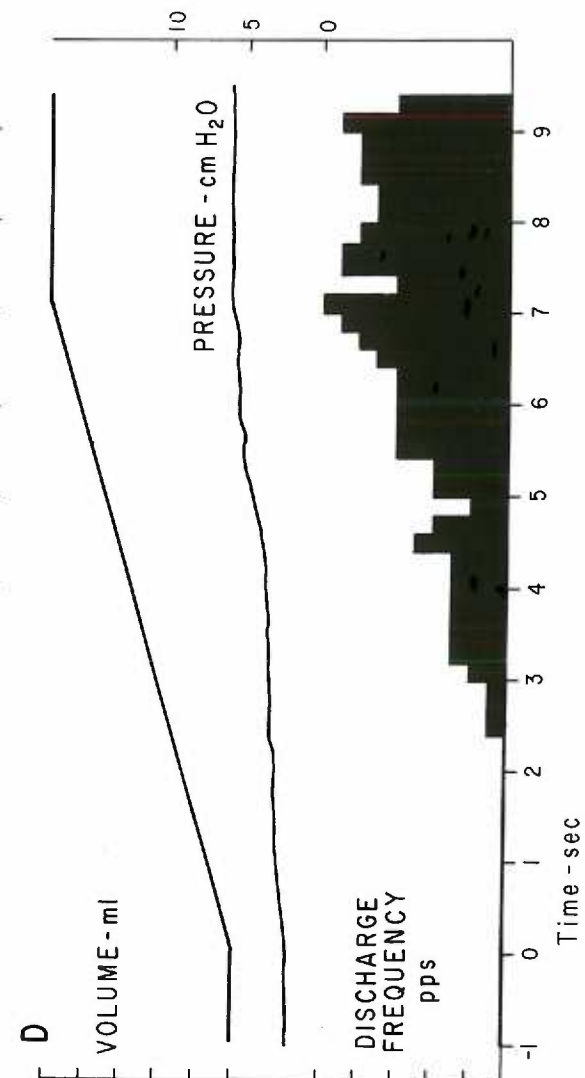
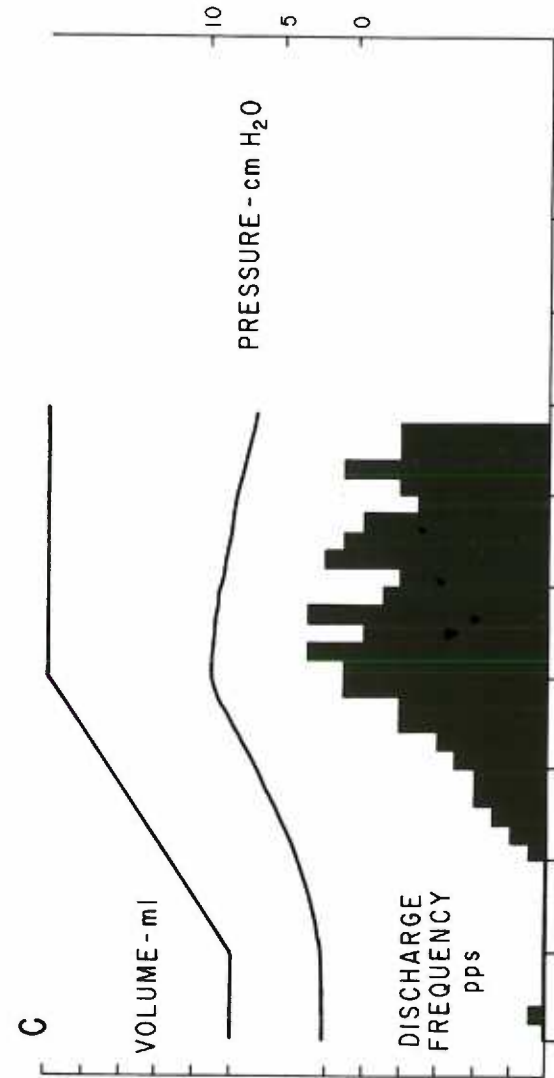
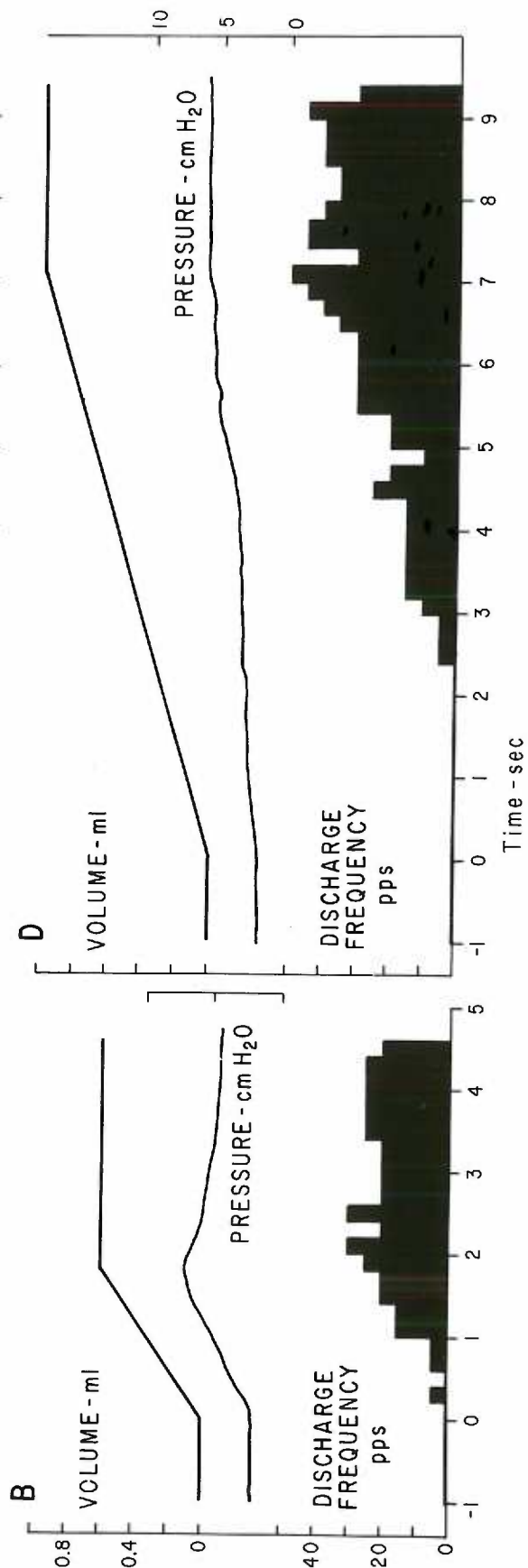
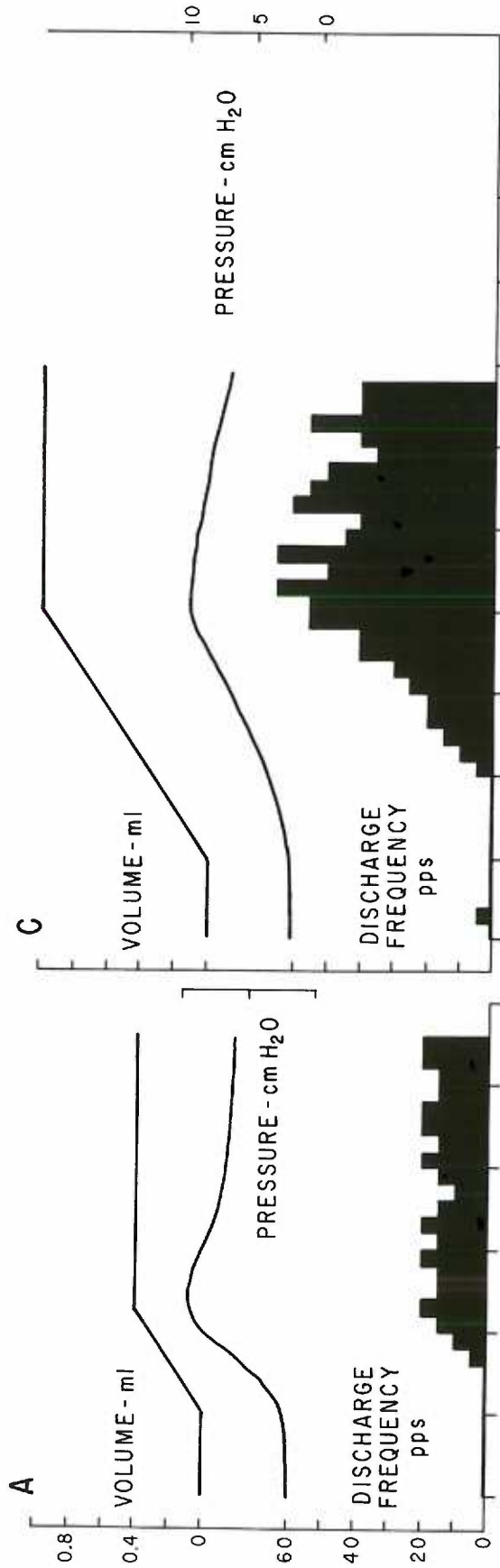
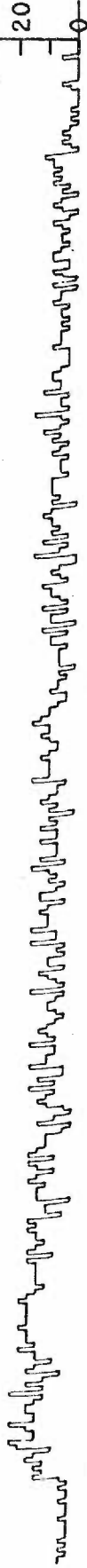


Figure 25. Discharge pattern of proportional receptor. Input waveform was half-trapezoid volume change of 0.34 ml/second ramp and final volume of one ml. Magnitude of the intrapulmonic pressure was not determined.

Figure is a photographic reproduction of a polygraph record.

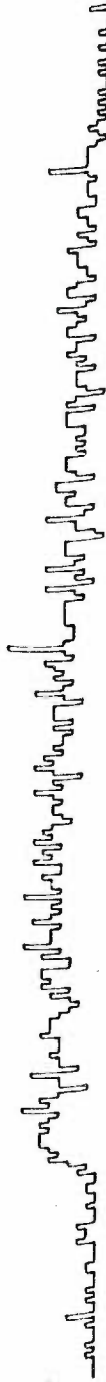
Discharge Frequency

pps
20



Pressure

10 sec

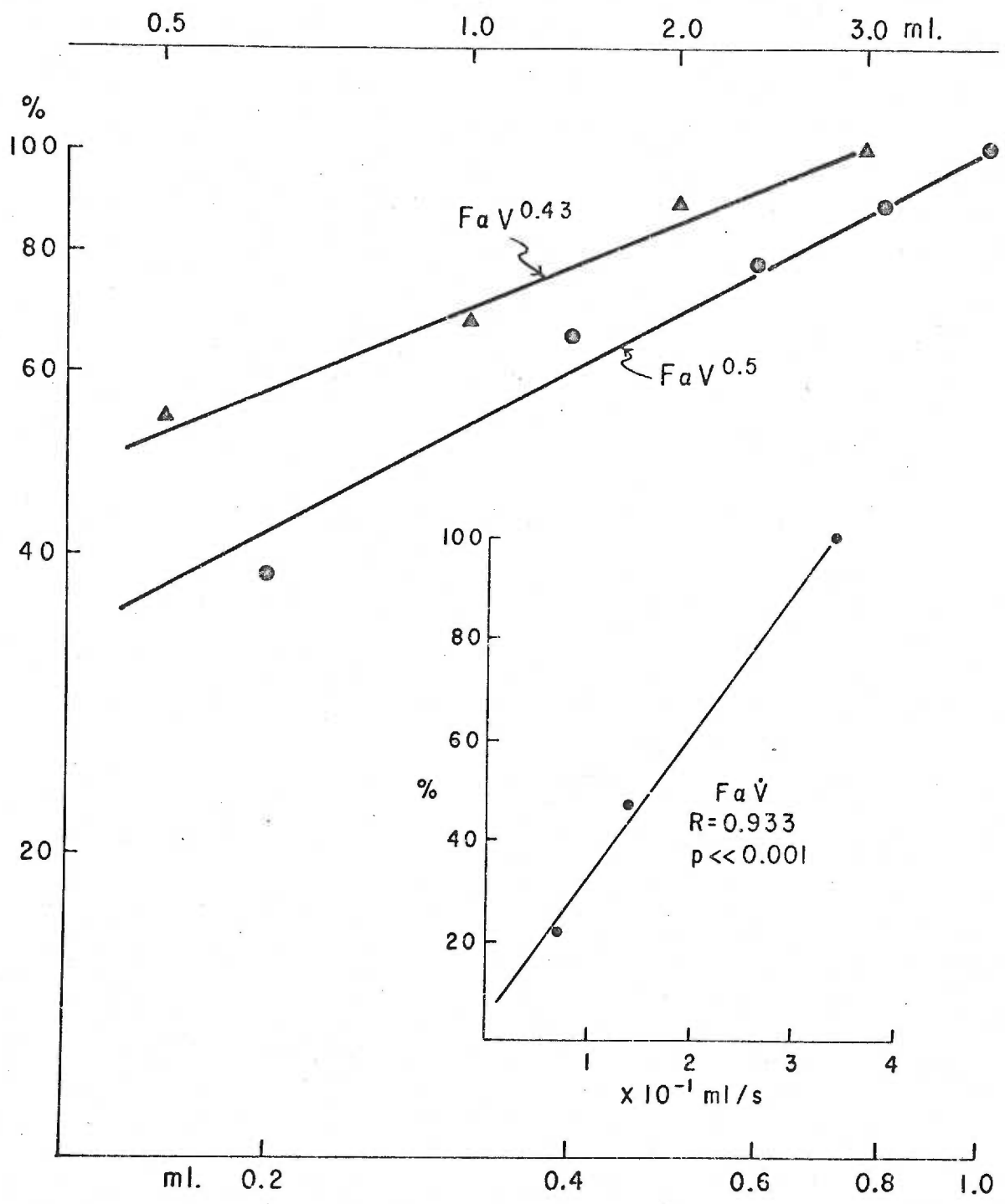


The volume waveforms in A and B were identical with a final volume of 1.0 ml. The greater pressure that occurred in B was probably caused by spontaneous smooth muscle activity. This figure suggests that at constant volume the discharge frequency varies directly with pressure. The A portion of the figure indicates that discharge frequency during sustained inflation does not remain constant or oscillate around a mean value but slowly decreases over an interval of approximately one minute and then attains a near constant value.

The Relationship Between Discharge Frequency and Lung Volume and Rate of Change of Lung Volume

The relationship between lung volume and discharge frequency was studied in those receptors which exhibited a proportional response i. e. rate plus proportional and proportional receptors. The proportional response is defined as the average frequency of discharge 3-5 seconds following the termination of the ramp minus the resting discharge frequency. A summary of these discharge frequency-volume relationships is shown in figure 26. The data for proportional responses were normalized: the frequency of discharge at 1.0 ml final volume was taken as 100%. The frequency of discharge at smaller lung volumes was calculated as a percentage of discharge frequency at the 1.0 ml volume. The solid dots in the figure represent the means of the normalized responses of six single

Figure 26. Rate and proportional responses of frog lung receptors. Inset shows the responses of six receptors which exhibited a rate response. Straight line determined by method of least squares (71). Note intercept of straight line near zero. Experimental procedure described in text. The frequency-volume relationship discharge of receptors which exhibited a proportional response is summarized in the log-log plot of normalized response versus change in lung volume. The filled circles represent the means of the normalized responses of six single units which exhibited a proportional response. The straight line through these points was drawn by visual inspection. The abscissa to be used with these points is the lower abscissa. Experimental procedure is described in the text. The triangles represent the normalized data from eight mass discharge recordings of Taglietti and Casella (68). Upper abscissa refers to the triangular data points and is also a logarithmic scale. Straight line through triangular points was drawn by visual inspection.



units which exhibited a proportional response. Under the conditions stated above the discharge frequency appears to be proportional to the square root of the volume. The triangles represent the means of the normalized responses of eight mass discharge recordings of Taglietti and Casella (59). Although the volumes used were different, the time during which discharge frequency was determined was similar to that used in this study. These data suggest the frequency of discharge is proportional to the 0.43 power of the volume.

In addition, the relationship between discharge frequency and rate of change of lung volume was studied in those receptors which exhibited rate responses namely rate and rate plus proportional receptors. A receptor's response to rate of change of lung volume is defined as the peak discharge frequency minus the average discharge frequency 3-5 seconds following the termination of the ramp. The rate responses of six receptors were determined and normalized with the response to 0.34 ml/sec taken as 100%. The data points are shown in the inset of figure 26. The data were subjected to linear regression analysis (71) the result of which indicated a linear relationship between discharge frequency and rate of change of lung volume.

Decay Times

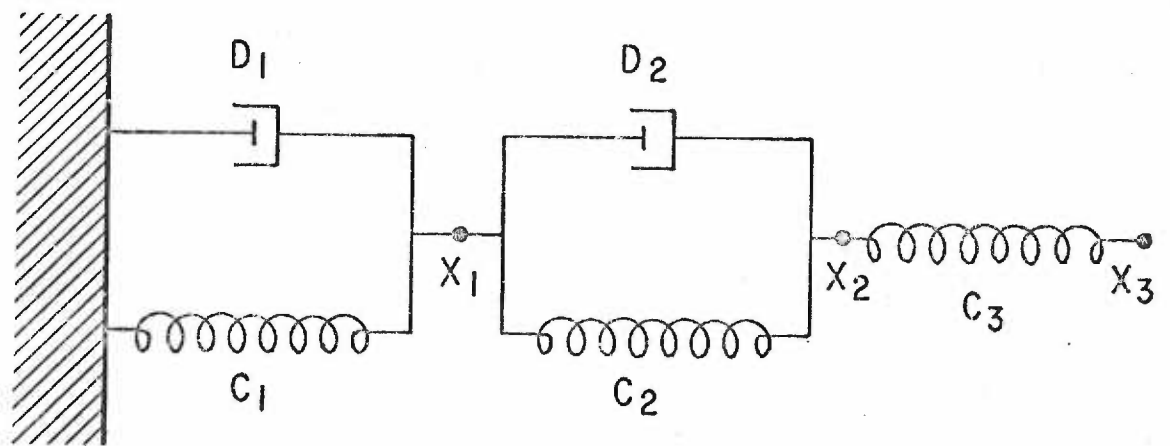
The time required for the discharge frequency to decay from

the observed value at the termination of the ramp to the region when this decay component was essentially complete was determined for eleven receptors. This time value ranged from one to three seconds with a mean of 1.5 seconds. Eight of the eleven receptors in which the measurement was determined showed a decay time of 1.0 seconds. The more rapid decay components approximated a simple exponential decay as the relationship between the change in discharge frequency and the logarithm of time was nearly linear throughout the time course of the decay. The slower decay component seen in figure 25 had a time course of about one minute. Because of spontaneous smooth muscle activity the slow decay component was not tested for linearity in a frequency-log time plot.

Model of the Three Receptor Types

On the basis of the three receptor responses (rate, rate plus proportional, and proportional) and the two decay terms (t. c. = 0.2 sec, t. c. = 10 sec) a model consisting of two springs and a dashpot and a low pass filter was developed to simulate the recorded responses of different fiber activities. The model is shown in figure 27. The input to the model consisted of a change in length X_3 which is the analog of changes in lung volume. The output of the model is the tension across spring three which is the analog of the frequency of discharge in the fiber associated with the receptor. The reader will recall the

Figure 27. Model of the frog lung receptor and surrounding tissue. Dashpot one and spring one represent the filtering characteristics of the lung tissue as a whole. Dashpot two and springs two and three represent the mechanical properties of the tissue immediately surrounding the receptor. The receptor is assumed to be a linear tension transducer which has an output proportional to the tension in spring three. The input to the model is an elongation applied at point X_3 .



similarity between the model shown in figure 27 and the model developed by Toyama (30) seen in figure 4. The differential equations which describe the model in figure 27 are given by:

$$1. \quad C_1 X_1 + D_1 (dX_1/dt) = C_2 (X_2 - X_1) + D_2 (dX_2/dt - dX_1/dt) = C_3 (X_3 - X_2).$$

C_1 is the spring coefficient and has the units of dynes/cm.

D_1 is the dashpot coefficient and has the units of dynes/cm/sec.

X_1 is a distance and has the units of cm; t represents time in seconds.

The patch diagram for the differential equations which describe the model is shown in figure 28. A comparator was used in the computer model to limit the output representing discharge frequency to non negative values.

Simulation

With the adjustment of C_1 , D_1 , and C_2 with $D_2=0.2$ dynes/cm/sec and $C_3=0.95$ dynes/cm the salient features of the rate, rate plus proportional, and proportional receptors could be simulated (figure 29) with the model shown in figure 27. The model mimics the rapid decay (t. c. =0.2) of the rate and rate plus proportional receptors and the slow decay (t. c. =10 sec) of the rate plus proportional and proportional receptors. In the rate plus proportional receptor model the coefficients were adjusted so the output during the initial portion of

Figure 28. Patch diagram for model shown in figure 27. Output was $X_3 - X_2$ for $X_3 - X_2 > 0$; and 0 for $X_3 - X_2 \leq 0$. Input was half-trapezoid or sinusoidal volume change.

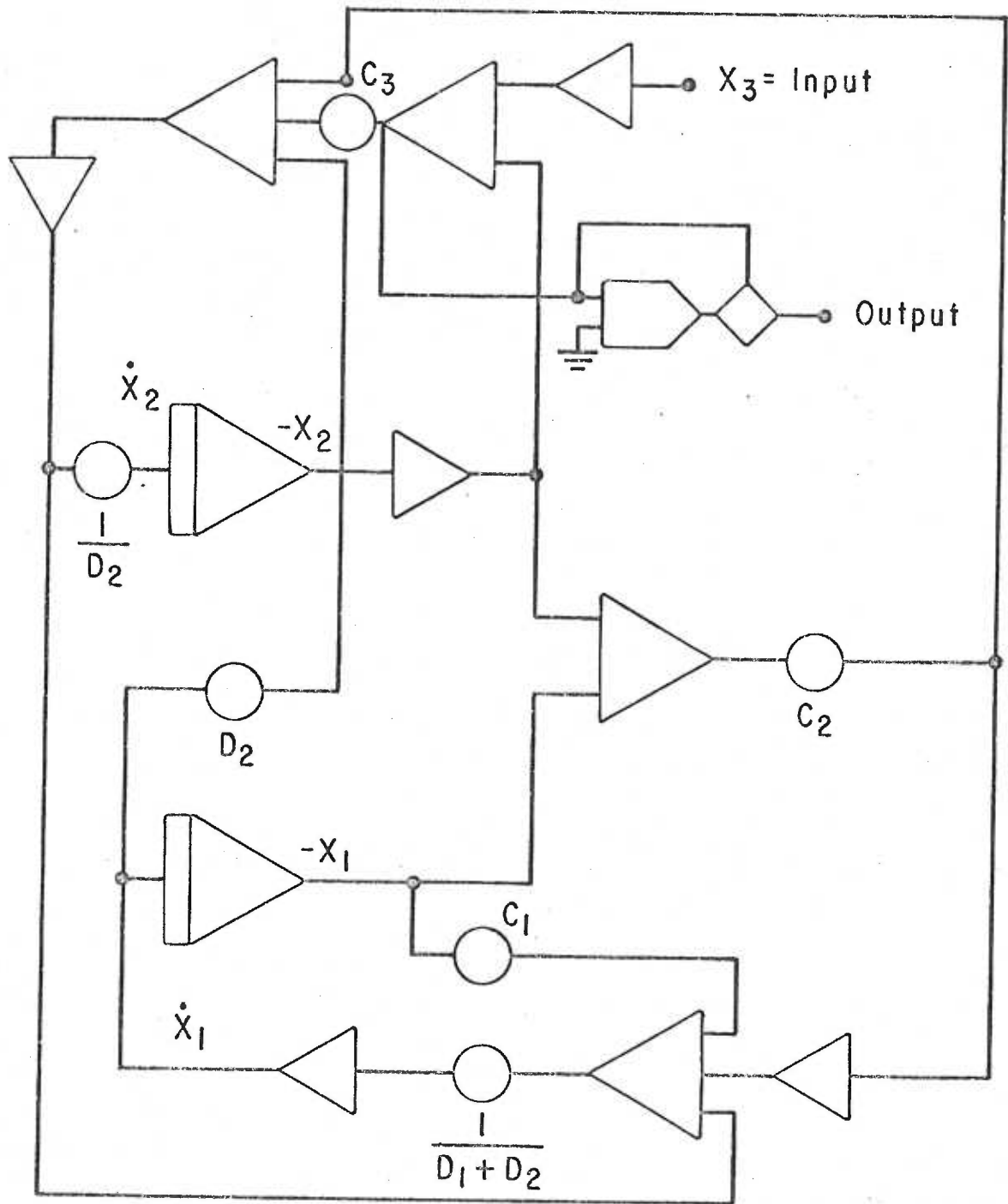
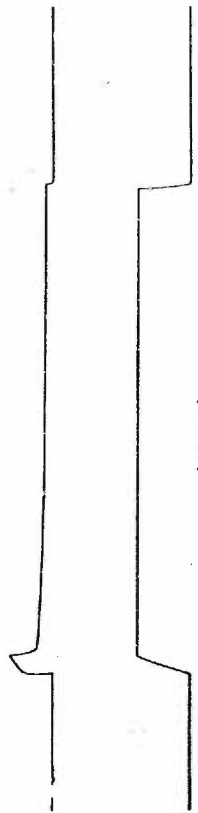


Figure 29. Model response to half-trapezoid volume change input. The simulated response is the upper trace. The input waveform is the lower trace. A, rate plus proportional receptor - final volume 1.0 ml - rate of inflation 0.34 ml second; B, rate plus proportional receptor final volume of 1.0 ml - rate of inflation from left to right was 0.07 to 0.14 to 0.34 ml/second; C, rate receptor - input waveform sequence same as B; D, proportional receptor - rate of inflation was 0.34 ml second, final volume from left to right was 0.2, 0.4, 0.6, 0.8, and 1.0 ml.

The coefficients used for simulation are as follows:

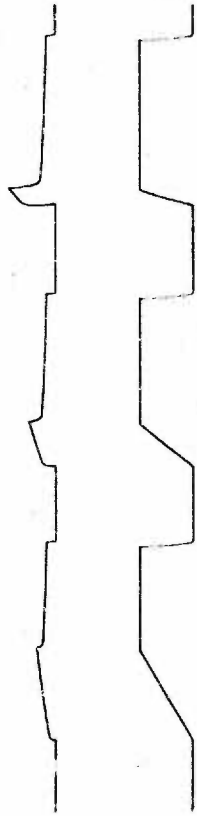
<u>Rate</u>	<u>Rate plus proportional</u>	<u>Proportional</u>
D_1 0.8	0.8	6.0
C_1 0.02	0.02	0.20
D_2 0.20	0.20	0.20
C_2 0.00	0.05	0.50
C_3 0.95	0.95	0.95

A



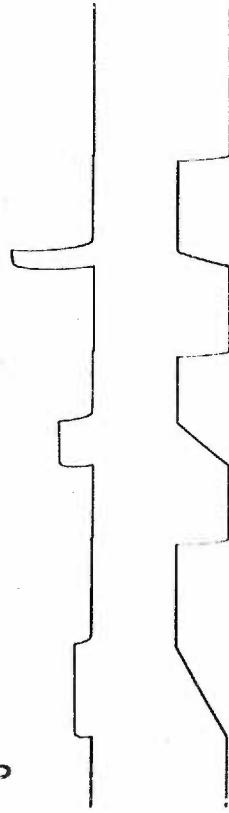
10 sec

B



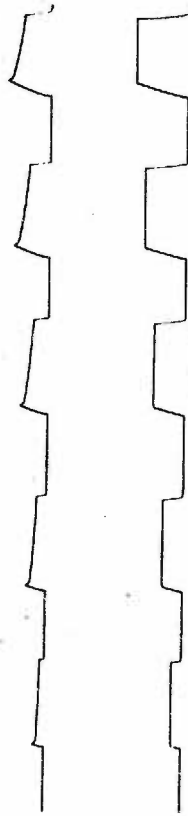
5 sec

C



5 sec

D



10 sec

the plateau was about 50% of the peak output (cf. figure 22 c). In the proportional receptor model the coefficients were adjusted so that the rate response was about 10% of the proportional response and the final output was about 50% of the output during the initial portion of the plateau (cf. figure 25A). (Even though receptors were classified as proportional receptors it was felt that in some receptors classified as such rate sensitivity was present. However, the sensitivity to rate of change of lung volume was small and was often obscured by arrhythmicity of discharge.) The model mimicked the linear relationship between discharge frequency and rate of lung inflation but failed to mimic the nonlinear relationship between discharge frequency and lung volume.

If spring one and dashpot one are omitted from the model shown in figure 27 the slow decay component of the responses of the rate plus proportional and the proportional receptors will no longer be mimicked. The remaining portion of the model can be used to simulate the responses of the three receptors just as the original model for short (1 sec following the ramp) time periods. The simplified model has the interesting property that with $C_3=0.95$ dynes/cm and $D_2=0.2$ dynes/cm/sec a C_2 of 0, 0.05, and 0.5 dynes/cm results in model simulation of a rate, rate plus proportional, and proportional response respectively. For reasons that will be presented later it is desirable to be able to change but a single coefficient (C_2) to change

the model from representing one receptor type to another. To allow such a change yet include the slow decay component two approaches may be taken. The first of these approaches is the development of a model consisting of springs and dashpots such that a change in the coefficient of a single spring with all other coefficients held constant allows the model to simulate the three responses. It was felt that the complexity of such a model did not warrant its use. The second approach is the lumping of spring one and dashpot one into a non-loading low pass filter so that the characteristics of the filter remained unaltered with changes in other portions of the model. If the second of the two approaches is taken the low pass filter may be described by its transfer function of

$$2. \quad 1/(S+0.1) \quad (72)$$

where S is the complex frequency domain and 0.1 is called a pole and is equal to the reciprocal of the time constant of the slow decay. The transfer function of the low pass filter multiplied by the transfer function of the abbreviated model gives the transfer function of the "conceptual" model. The transfer function of the abbreviated model is derived in the first page of the appendix and is given by:

$$3. \quad (S+b)/(S+a)$$

when $b=C_2/D_2$ and $a=(C_2+C_3)/D_2$. The reciprocal of the pole a is the

time constant for the rapid decay of the rate and rate plus proportional receptors and the ratio of the zero (b) to the pole (a) is directly related to the model's rate of change response. With $b/a=0$ ($C_2=0$) the model simulates a pure rate receptor; with $b/a=1$ the model simulates a pure proportional receptor. With $0 < b < a$ the model behaves as a rate plus proportional receptor with a smaller b associated with a greater rate response.

The results of the half-trapezoid input waveform studies indicated that the transfer functions of the proportional, rate, and rate plus proportional receptors were approximately and respectively:

4. $(S+2.5)/(S+0.1)(S+7.5)$
5. $(S)/(S+0.1)(S+5)$
6. $(S+0.25)/(S+0.1)(S+5)$

The transfer functions of the proportional and rate plus proportional receptors indicate a linear proportional response. The actual proportional response was nonlinear. The transfer functions also indicate that the response may take on negative values. The actual response can never be less than zero.

Sinusoidal Forcing

To determine the uniqueness of the transfer functions determined by half-trapezoidal volume changes, the lungs of frogs were

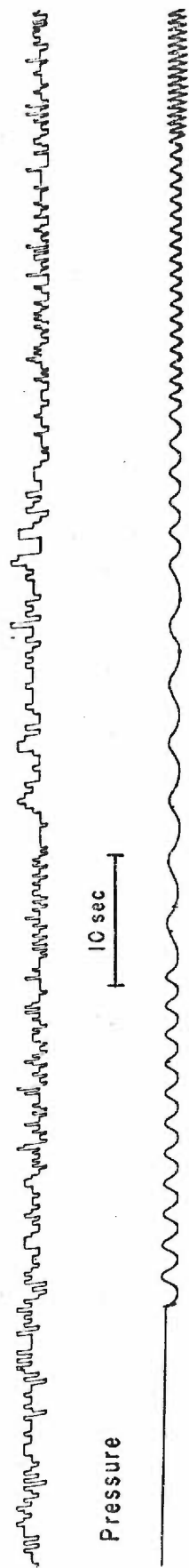
inflated sinusoidally and the afferent nerve activity was recorded. It was anticipated that the transfer functions of the three types of receptors could be determined from Bode plots which are generated as a result of data obtained through sinusoidal forcing. The responses of the three types of receptors to sinusoidal inflation are shown in figure 30. These data indicated: 1. averaging techniques would need to be employed to demonstrate whether the output was sinusoidal, 2. there was little change in the magnitude of the peak to peak responses between different frequencies of sinusoidal inflation. The half-trapezoid data indicated nonlinearity, thus a sinusoidal input would not necessarily be accompanied by a sinusoidal output. The above considerations prevented the use of the log magnitude-log frequency plot as a means of confirming the transfer functions determined with the half-trapezoid input. The half-trapezoid data did indicate linear rate sensitivity however. The linearity in the rate response allowed the generation of a phase angle-log frequency plot. The receptor's change in phase angle with frequency could be compared with those changes in phase angle which would occur if a system of known transfer function were forced over the same frequencies. Figure 31 shows the response of a receptor to sinusoidal inflation. The discharge occurs only during certain portions of the cycle. The portion of the cycle at which discharge commences is determined by both the receptor's rate and proportional sensitivities. However the change in

Figure 30. Receptor response to sinusoidal inflation. A, proportional receptor; B, Rate plus proportional receptor; C, Rate receptor. Volume change in all cases was 0.5 ml peak to peak. Preinflation volume in A was 1.0 ml. Preinflation volume in B and C was 0.6 ml. A flow sensitive artifact seen in the pressure record of A during high frequency inflation prevented the pressure recording from being used as a pump position reference signal. For that reason a pump position signal (volume) was used throughout the remainder of the study.

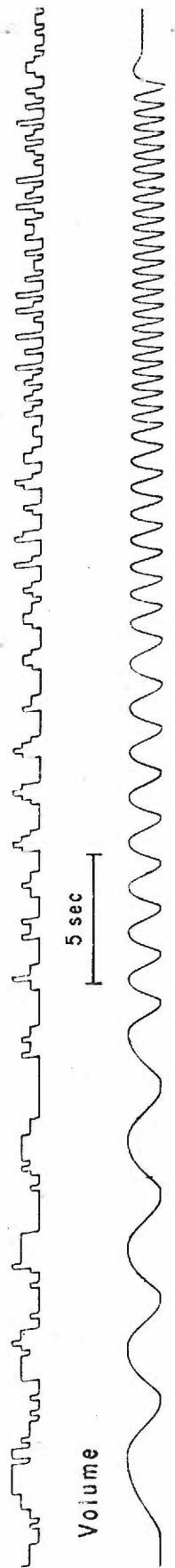
Figure is a photographic reproduction of the polygraph record.

Discharge Frequency

A



B



C

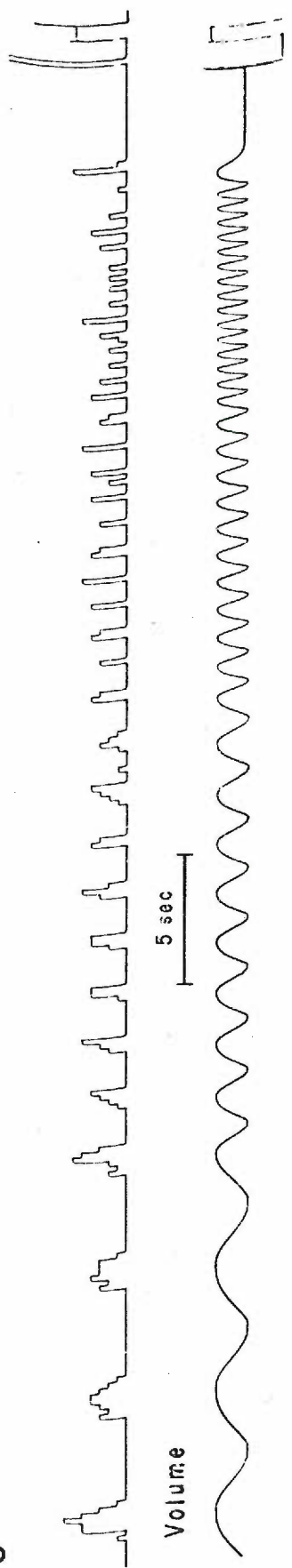
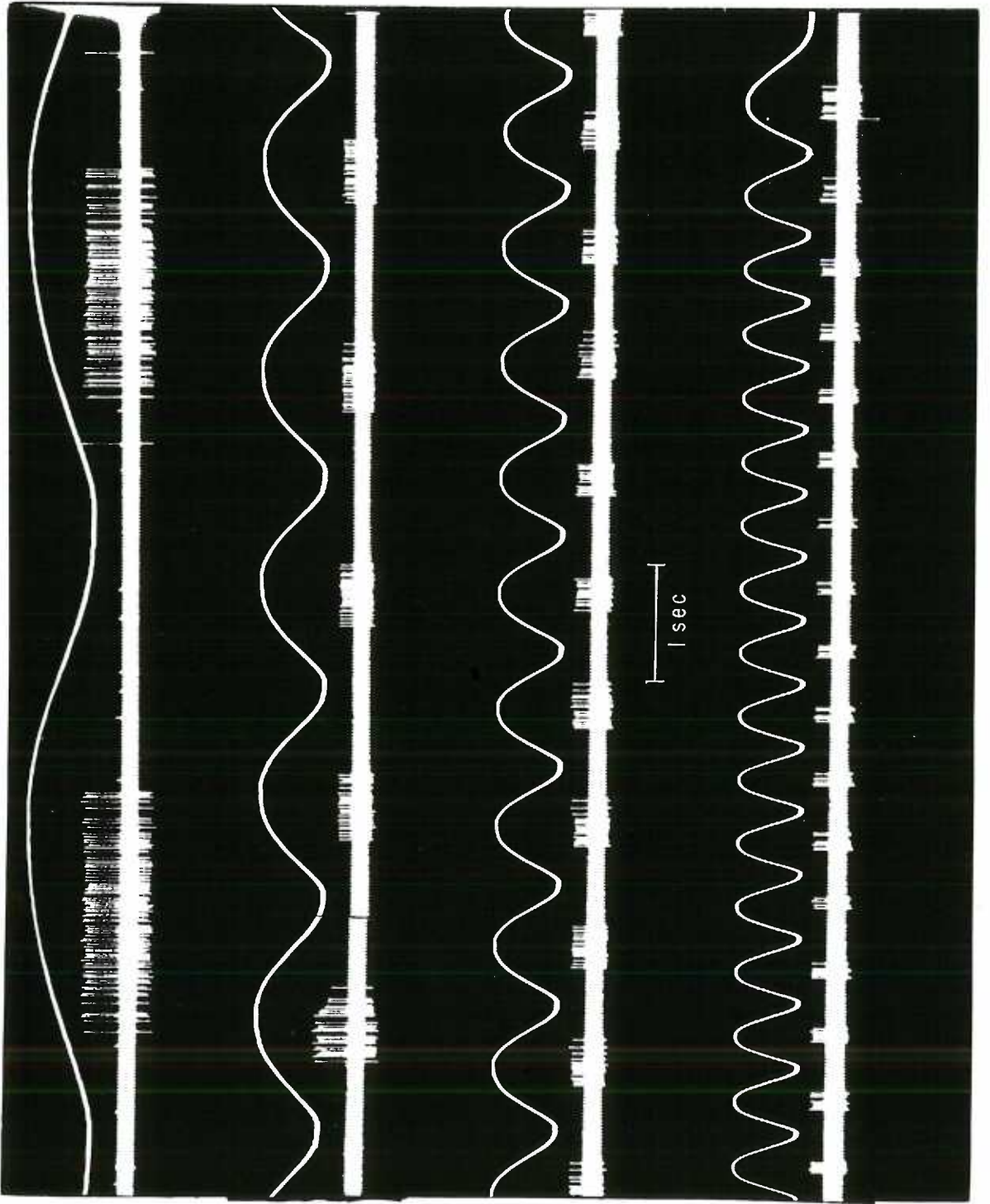


Figure 31. Rate plus proportional receptor response to sinusoidal inflation. Volume change was 0.5 ml. Preinflation volume was 0.6 ml. Frequency of inflation reading from top panel downward was approximately 0.2, 0.5, 1.0, and 2.0 Hz. The decreased amplitude of the action potentials occurred as a consequence of nerve movement on the recording electrode.



time of onset of discharge at different frequencies is dependent only on the rate sensitivity of the receptor provided that the peak to peak forcing volume remains unchanged. This change in onset of discharge may be expressed as a percentage of one cycle i. e. an angle or specifically phase angle.

It was felt that there would be a time delay between the volume change in the syringe and the appearance of discharge in the nerve associated with that volume change. Conduction of the pressure wave along the P. E. tubing and through the lung, establishment of a generator potential, and conduction of the action potential along the nerve to the recording electrodes are all contributors to this delay. Figure 32 shows the discharge of several fibers following rapid inflation of the lung. The latency of the response to the rapid half-trapezoid inflation was about 20 ms. This latency of 20 ms was seen in four lung-receptor preparations and was taken as the system delay. At low frequencies a 20 ms delay causes little error between the true onset of discharge and the observed onset of discharge. At higher frequencies (2 Hz) the time delay must be subtracted from the observed onset time to find the true onset time for discharge. If this correction is not made an error of 25% results.

The true onset times at different frequencies of sinusoidal inflation were determined for eleven receptors. The repeatability of these onset times is shown in table II. An additional six receptors

Figure 32. Mass discharge response to rapid half-trapezoidal inflation. Delay time was approximately 20 ms. Action potentials were retouched for photographic purposes. Discharge indicative of both rate and rate plus proportional receptors may be recognized in the figure.

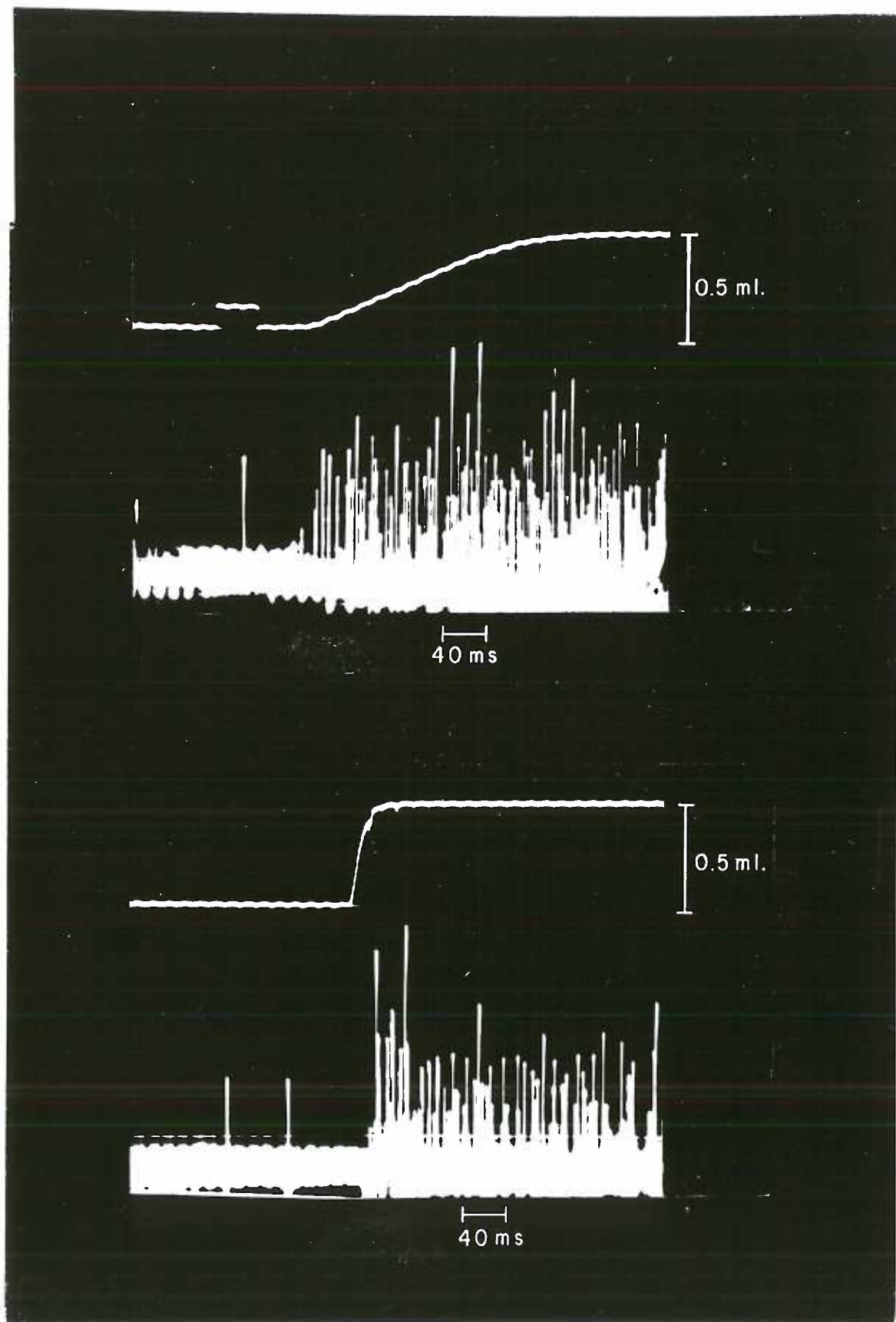


TABLE II

Repeatability of onset and cessation of discharge times during sinusoidal inflation of a typical receptor.

Period of Sinusoid	Onset of Discharge	Cessation of Discharge
14	5	9
14	5	9
14	5	10
14	4	9
14	5	8
14	4	9
14	5	9
27	8	14
27	8	14
26	8	13
25	8	13
25	9	14
25	8	14
25	8	15
45	13	23
45	16	21
44	16	24
44	16	24
44	14	26
43	14	24
44	15	23
119	24	66
118	27	65
119	26	65
121	27	66
120	26	58
119	30	70

Time units are in $1/25$ th's of a second. Due to time delay 20 ms must be subtracted from the onset and cessation times to arrive at true onset and cessation times. The receptor was a rate plus proportional receptor.

were studied but data from these receptors were not acceptable because of serious flow sensitive artifacts in the pressure recording (figure 30 A). Volume recordings were not available for these receptors. For the remaining eleven receptors the onset times were expressed as a percentage of the total cycle time and then converted into an angle. The data were normalized so that at the lowest frequency the phase angle was zero. The phase angle versus log frequency plots for the eleven receptors is shown in figure 32. Visual inspection of the phase angle data for the rate receptors and the rate plus proportional receptors indicated that the responses of the two groups did not differ. The single proportional receptor did however appear to undergo a lesser phase shift over the entire range of forcing frequencies. The data from rate plus proportional receptors and rate receptors were lumped and the means of the phase angles were determined at four different frequencies (figure 33). For purposes of comparison, a phase angle-log frequency relationship was constructed for a system with a transfer function of $(S+b)/(S+a)$ or $(S+b)/(S+a)(S+C)$ with $C \ll a$ (figure 34). The pole (a) was fixed while the zero (b) was varied from $0 \leq b/a \leq 0.7$. The experimental curve (figure 33) was superimposed on the theoretical curves to find the theoretical curve which best fit the experimental data. The position along the abscissa at which the best fit occurred determined the pole (a) while the best fitting b/a curve determined the zero (b). The

Figure 32. Phase angle data for eleven receptors. R, rate; P, proportional; R + P, rate plus proportional. Data points at 1.78 Hz for two receptors were discarded because of technical difficulties.

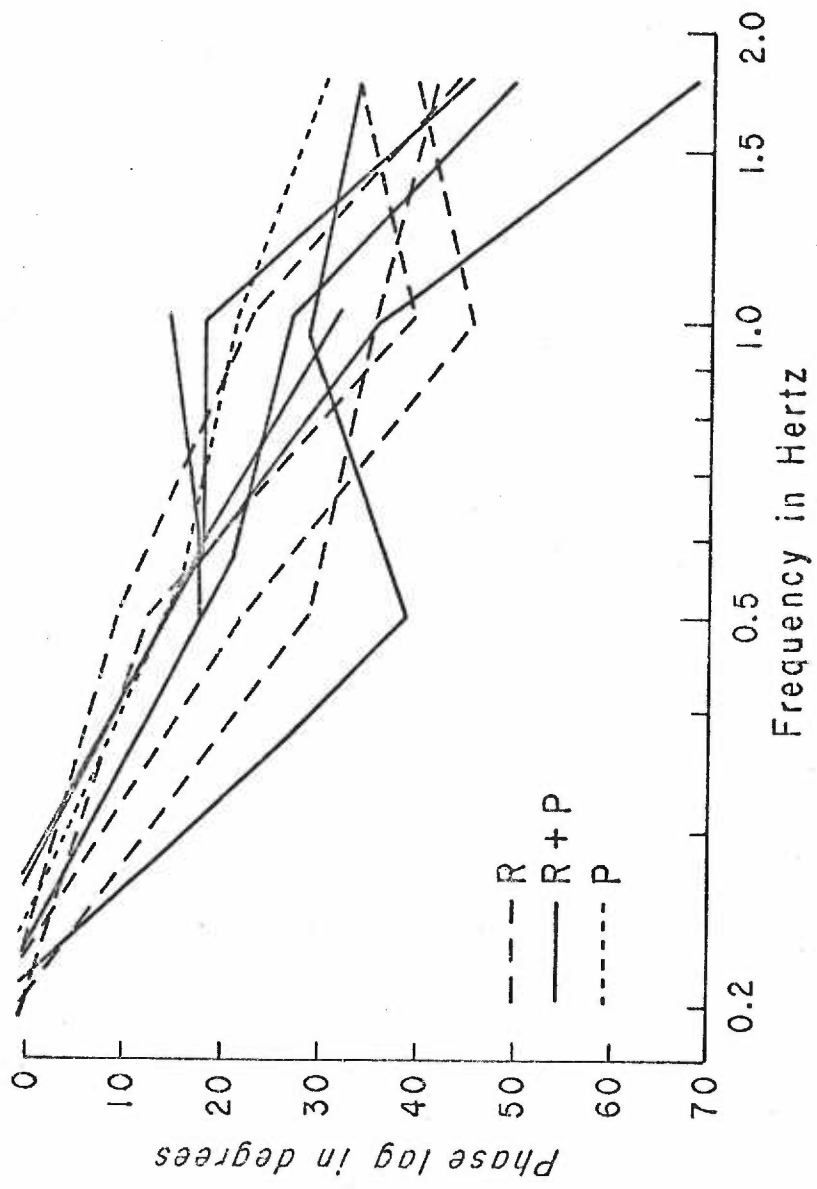


Figure 33. Phase angle data for rate and rate plus proportional receptors. Experimental curve represents mean phase angle for four rate receptors and four rate plus proportional receptors. Theoretical curve given by triangles is phase shift of a system with a transfer function given by $S/(S + 4)$. Theoretical curve given by open circles is phase shift of a system with a transfer function of $(S + 0.24)/(S + 4)$.

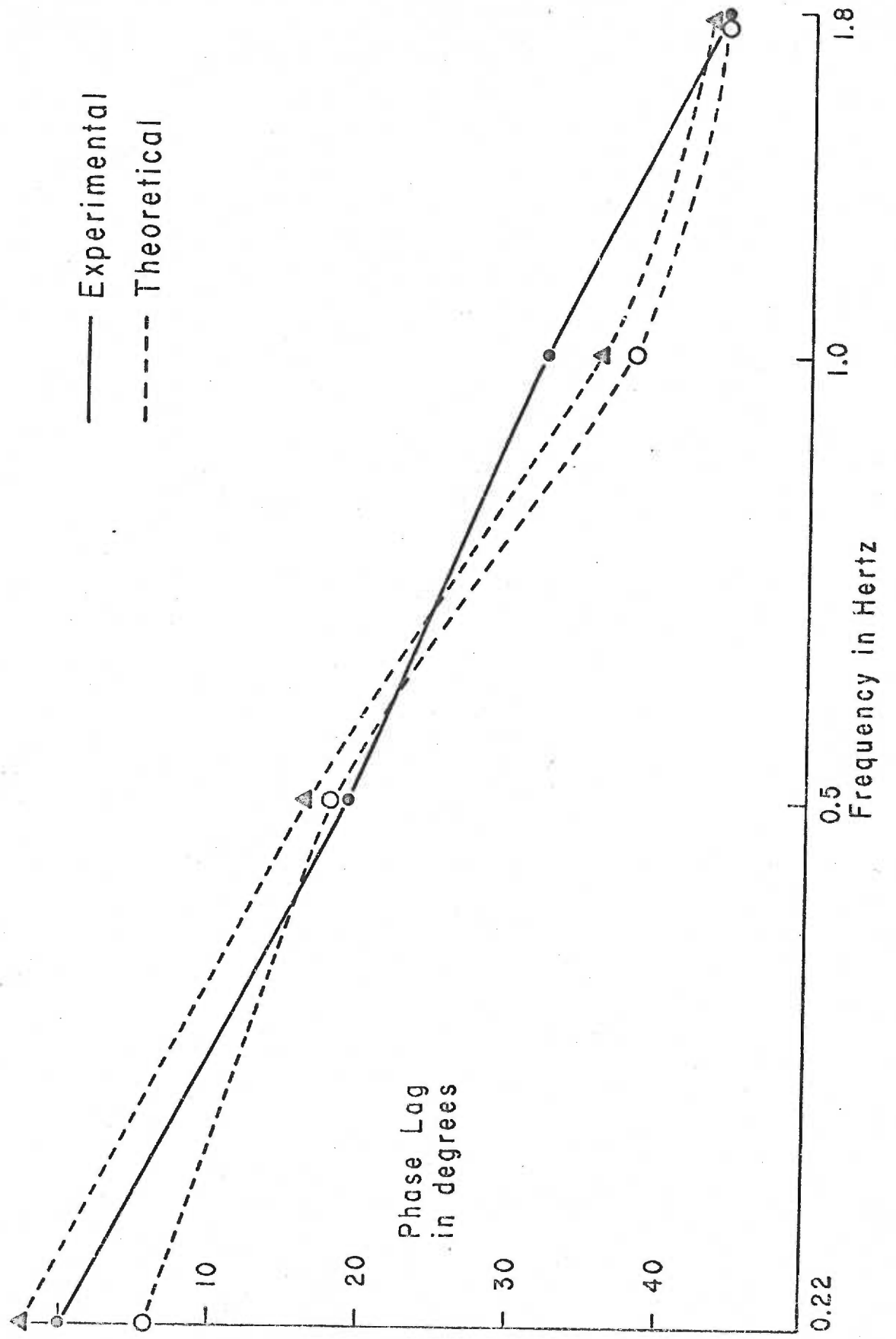


Figure 34. Phase angle versus frequency of a system with a transfer function of the form $(S + b)/(S + a)$.

curves generated from $S/S+4$ and $(S+0.24)/(S+4)$ provided the best fit between the theoretical and experimental curves.

Similar curve fitting was done for the phase angle data of the proportional receptor (figure 35). The best fitting curve was generated by $(S+0.7)/(S+2.3)$. The computer analog program was sinusoidally forced over the same frequency range as was the receptor. The onset times (figure 36) were determined and converted into phase angles. The phase angle-log frequency relationship for rate receptor model followed the curve generated by $S/(S+5)$ while the rate plus proportional model phase angle followed the $(S+0.25)/(S+5)$ phase angle-log frequency relationship. The phase angle for the proportional receptor model remained nearly constant over the entire frequency range. (Table III)

Figure 35. Phase angle data for proportional receptor. Theoretical curve is phase angle changes for system with a transfer function of $(S + 0.7)/(S + 2.5)$.

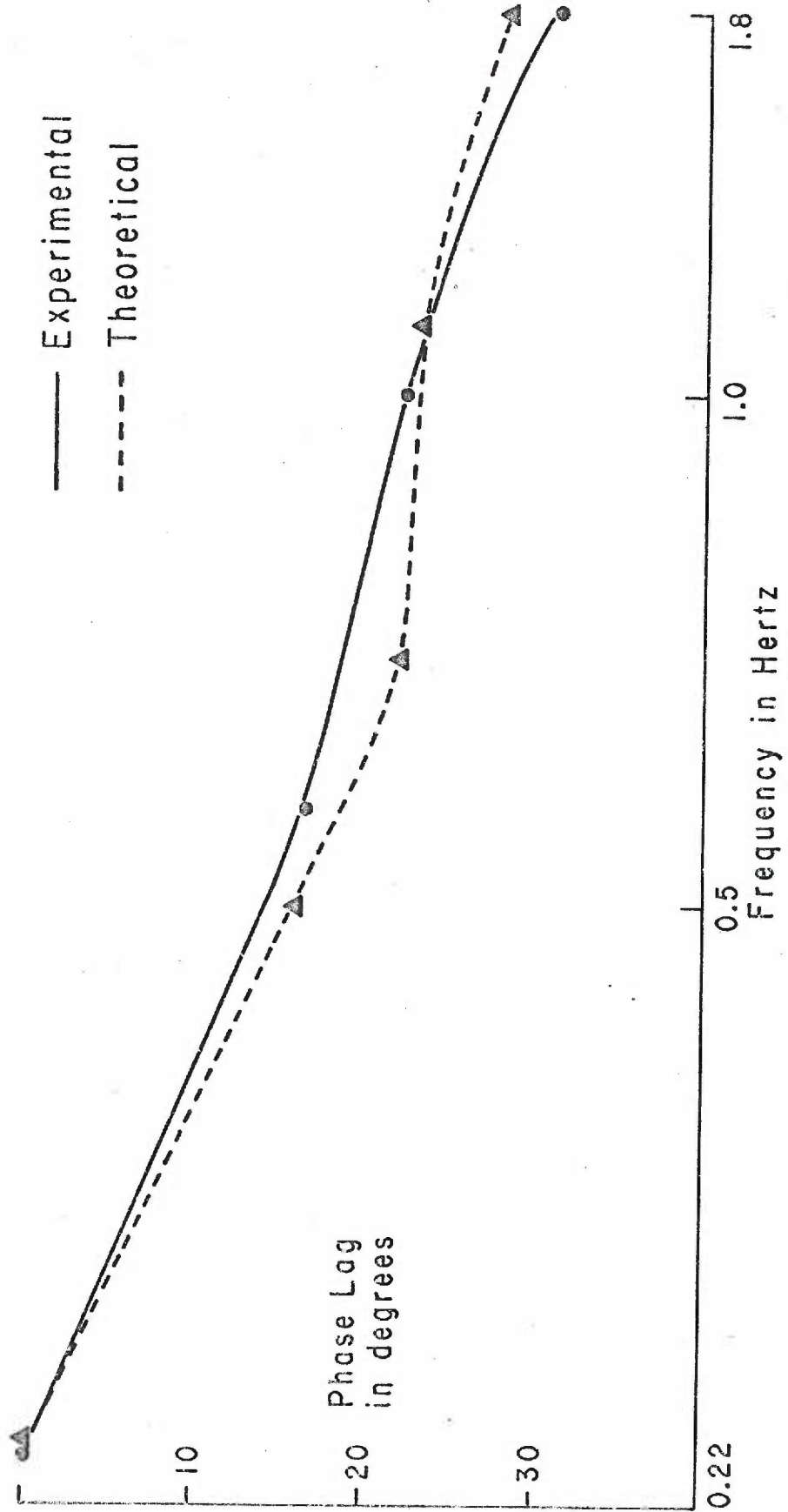
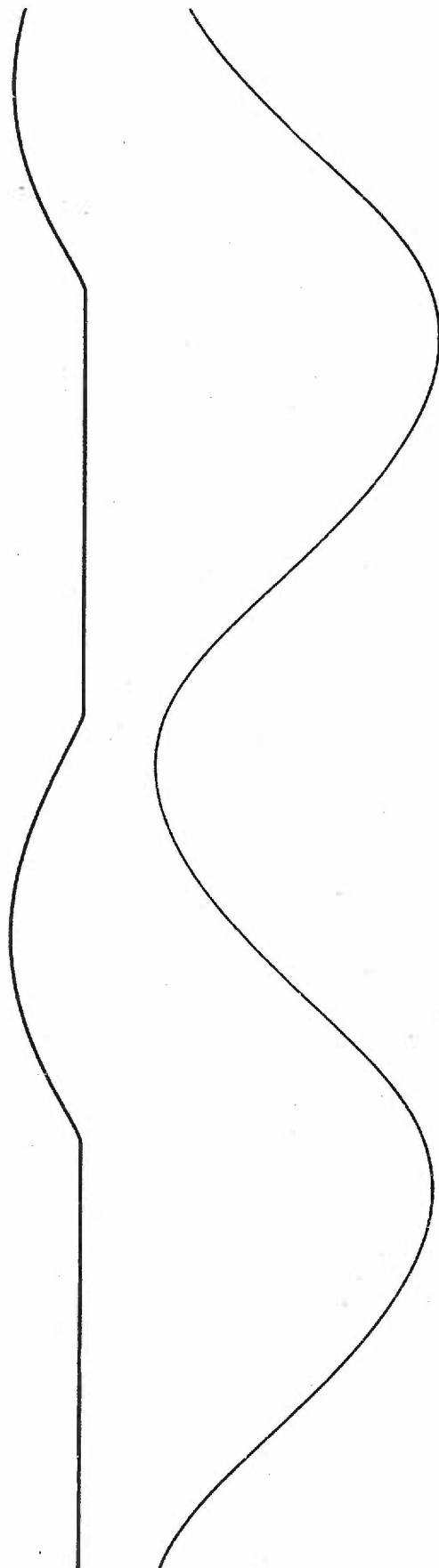


Figure 36. Model response to sinusoidal forcing. The model response shown in the figure is that of a rate receptor.

Figure is a photographic reproduction of a polygraph record.



1 sec

TABLE III

Phase relationship (lag) between simulated input and simulated output at different frequencies of sinusoidal model forcing. The term square root following the receptor type signifies the computer output (figure 28) was run through a square root diode function generator which took the square root of the output. + signs indicate phase lead (output leading input).

Receptor type:	0.2 Hertz	0.5 Hertz	1.0 Hertz	2.0 Hertz
Rate	0	15°	30°	50°
Rate square root	0	13°	27°	48°
Rate + proportional	0	10°	20°	40°
Rate + proportional square root	0	7°	18°	36°
Proportional	0	+8°	+15°	+10°
Proportional square root	0	+15°	+15°	+10°

DISCUSSION

Pressure Volume Characteristics

The pressure volume characteristics of the frog lung are in many respects similar to the pressure volume characteristics of the mammalian lung. Edmunds and Huber (70) found a rapid (1-2 sec) and slow (>30 sec) decline in transpulmonary pressure following rapid administrations of 100 ml of air into dog lungs. As in the frog, the magnitude of the rapidly decaying component of intrapulmonic pressure decreased with repeated inflations. These authors also found an increase in lung compliance with each of three trials subsequent to complete degassing of the lung. Taglietti and Casella (68) found that the compliance of the frog lung increased during the second of two runs in which the compliance was determined. The increased compliance was observed only if pulmonary volume during the trials exceeded 1.0 ml. In contrast, the results of this study indicated increasing lung compliance with repeated inflations to changes in lung volumes of less than 1.0 ml. The discrepancy between the results of this study and the observations of the Italian investigators might be explained by the species differences (R. pipiens vs. R. esculenta) or different experimental procedure (fluid vs. air inflation).

To explain the compliance-trial relationship in dog lungs Edmunds and Huber suggest ". . . surface-active alveolar lining

material may require occasional large inflations in order to maintain low surface tensions during subsequent deflations." According to this theory large inflations during the first trial enhance the ability of the alveolar lining material to reduce interfacial tension. Thus for a given intertrial volume surface forces in the subsequent trial are lowered, intrapulmonic pressure is lowered, and compliance is increased. However, the compliance-trial relationship was demonstrable in the frog lung during saline inflation when surface forces were absent. Thus it appears to be doubtful that the behavior of the surface active material is responsible for the changing behavior of the lung.

The rapid and slow decay components in intrapulmonic pressure were evident in the pressure recordings of Bonhoeffer and Kollat (66). The recordings during the first five seconds following inflation were not given in the Taglietti and Casella publication. However, the slow decay component was evident. The actual time courses of the two decay components could not be determined from the published reports of these investigators.

The lung compliance between changes in lung volumes of zero to 1.0 ml was 0.174 ± 0.03 according to Taglietti and Casella (68) while over this same range Bonhoeffer and Kollat (66) report a value of 0.333 ml/cm H₂O. The pressure-volume curves in both of these reports were not linear over this range of pulmonary volume. In

contrast the results of this study indicated a linear pressure-volume relationship over the same lung volumes. Also the lung compliance was found to be much smaller in magnitude (0.093 vs. 0.333 ml/cm H₂O). The high compliance values determined by Bonhoeffer and Kollat might be explained by their use of succinylcholine as an immobilizing agent. Carlson and Luckhart (69) demonstrated that vagus nerve section is accompanied by hypertonus in the pulmonary smooth muscle of the frog and this smooth muscle contraction tends to increase intrapulmonic pressure for a given pulmonary volume. Succinylcholine may cause relaxation of pulmonary smooth muscle (73). Thus succinylcholine could have the effect of increasing lung compliance by decreasing smooth muscle tension in the lung. The compliance value reported by the Italian investigators in relation to that observed in this study could be due to species differences. The low compliance values observed in this study could have resulted from the use of smaller lungs than the lungs used by the European investigators although there is no evidence for (or against) differences in lung size. Compliance of a viscus is dependent on the material of which the viscus is constructed as well as the size of the viscus (74).

The major portion of static pressure-volume hysteresis in the mammalian lung is caused by surface tension phenomena since saline inflation reduces the magnitude of the pressure-volume hysteresis

but does not obliterate the hysteresis (75). The residual static hysteresis (as opposed to the dynamic hysteresis caused by energy loss due to air flow and tissue inertia) has been studied by Hildebrandt (76). A model prompted this investigator to suggest ". . . as tissue is distorted some structural bonds rupture producing heat by process which is not time of rate (sic) dependent." The mechanisms which are responsible for hysteresis in the frog lung are unknown but the similarity between frog lung and mammalian lung in other pressure-volume characteristics suggests a common hysteresis producing mechanism, possibly the rupture of structural bonds within the lung tissue.

Threshold

Unlike the correlation between receptor type and threshold for receptors of the cat lung, the results of this study indicate that threshold for discharge could not be correlated with receptor type. Only one of nine receptors with no resting discharge had a threshold greater than 0.3 ml. This receptor was a proportional receptor. The remaining proportional receptors had thresholds of 0.1 ml or exhibited discharge during the resting conditions. Both rate and rate plus proportional receptors exhibited discharge during the resting condition. There were also rate and rate plus proportional receptors which had thresholds ranging from 0.1-0.3 ml. The lack of

correlation between receptor type and threshold is in contrast to the receptors of the mammalian lung where the rapidly adapting (rate) receptor has a greater threshold for discharge than the slowly adapting (rate plus proportional) receptor.

The apparent increase in threshold with decreased rates of inflation which was seen in several rate plus proportional receptors is similar in some respects to critical slope of the Pacinian corpuscle. The critical slope is the slowest rate at which focal pressure may be applied to the corpuscle during which time action potentials occur (77). The high pass filtering characteristics of the lamellae prevent inner core strain when rate of change of pressure is less than this "critical slope." The Pacinian corpuscle does not have a pressure threshold but instead has a rate of change of pressure threshold or the critical slope at which the pressure is increasing. The rate plus proportional receptor of the frog lung may have a volume threshold as well as a rate of change of volume threshold or critical slope. If the rate of change of volume exceeds the critical slope, discharge commences with inflation. If the critical slope is not exceeded (slower inflation rate) then the volume at which discharge commences will be determined by both the volume threshold and the rate of inflation, slower rates of inflation being associated with increased volume at which discharge is first seen.

Conduction Velocity

The accuracy of the conduction velocity determinations is unknown. Unless a precise measurement of the small interelectrode distance is accomplished, the deviation of the measured conduction velocity from the true value would be considerable. The interelectrode distance was typically 1 mm. However the Ringer's solution contact between the nerve and electrode could significantly reduce this distance (as a percent of total distance) and cause considerable error in the determination of the distance over which the action potential was thought to have traversed. The measured conduction velocities indicated an order of magnitude of 10^0 - 10^1 m/s for each of the three types of pulmonary stretch receptors. There was no correlation between conduction velocity and discharge pattern. However these findings must be interpreted in light of the questionable accuracy with which conduction velocity was determined.

Model

The model used to simulate the behavior of the frog lung receptor was chosen for several reasons. Excepting the low pass filter, the model had been established in the literature. Toyama (30) had successfully used the model (with different coefficients) to describe the behavior of the frog toe muscle spindle receptor. Hildebrandt

(76) incorporated the model in a larger more complex model which described the pressure-volume behavior of mammalian lungs. Sedlin (78) likewise incorporated the model in a larger model to describe stress-strain characteristics of bone. The elements (spring, dashpot) in the model have physical analogs e. g. tissue elasticity and viscosity. A model which has physical analogs might be used to better understand the processes underlying the transduction of mechanical energy into electrical energy. To illustrate this point two models (although not explicitly stated as models) have been proposed for the crayfish stretch receptor. Both models adequately relate output to input. The first model (39) employs processes such as a fractional differentiation which are not encountered in the physical world. The second model (43, 79), as the model in this study, consists of springs and dashpots which represent mechanical filtering or mechanical differentiation, all processes which are known to occur in the physical world. The model developed for the frog lung receptor is not an unique model; other models could be constructed to describe the behavior of the receptor. The particular model employed has the advantage that the model components represent physical processes which are known or which are thought to occur in the events leading to reception of mechanical changes.

It was stated before that there was not a "tight" grouping of receptors in each of the three categories i. e. there was intragroup

$(s+2.5)/(s+7.5)$ (neglecting the low pass filter which does not influence changes in phase angle in the high frequency range). The discrepancy between the predicted and the observed transfer function lies in the position of the pole. The ratio of the zero to the pole is in both cases about 0.3. The observed pole is about one third of the predicted pole (2.5/7.5). The pole determines the rapid decay portion of the discharge pattern in response to half-trapezoid inflation. The time constant for this decay was said to have varied between 0.2 and 0.6 seconds, the majority of receptors showing an 0.2 second time constant. The reciprocal of this time constant is the pole. The discrepancy between the predicted and the observed response of the single proportional response could be explained on the basis of the departure from the most frequently encountered time constant (pole) to a larger rarely encountered time constant. The time constant was not measured for this particular receptor. However it is likely that this receptor represents a departure from the norm in that the value of its pole is atypical. The similarity between the phase shift behavior of the rate and rate plus proportional receptors was both predicted and observed. However at frequencies lower than those used in this study (0.2 Hz) the phase shift characteristics of these two groups would differ markedly. Below 0.2 Hz the phase angle of the rate receptor response would remain unchanged yet the rate plus proportional receptor response would undergo a ninety degree phase

shift. The changes in onset of the model output were in agreement with the phase angle-log frequency relationships which result from the theoretical behavior of the model. Close agreement between the two supports the contention that change in onset of discharge is equivalent to changes in phase angle. It may be argued that the onset phase-angle relationship would not hold in a nonlinear system. To test this objection the computer output was fed to a square root diode function generator. The proportional response of the model was then directly proportional to the square root of the volume. The rate response was no longer linear. However, deviation from linearity was small. The onset times of the nonlinear model were different from the onset times of the linear model. However, the changes in onset time with frequency were very similar. Equating changes in onset of discharge (expressed as an angle) with phase angle appeared to be justified for the lung receptor system.

Components of the Response and Their Origin

The slow decay component (1 min) seen in the intrapulmonic pressure and in discharge frequency suggests a causal relation between the two. The slow decrease in intrapulmonic pressure at constant volume is not unlike the phenomenon of receptive relaxation (80) of other viscera. The cause of the phenomenon is unknown. The decrease in pressure at constant volume causes (in the absence of

major changes in surface area) a decrease in tension in the wall of the lung. The decreased tension causes decreased strain in the membrane of the receptor which leads to a decrease in the frequency of discharge in the primary afferent fiber. The low pass filter component of the model represents those properties of lung tissue which are responsible for receptive relaxation.

The rapid decay (time constant ~ 0.2 sec) in discharge frequency which is seen in the rate plus proportional receptors' response is sometimes evident in the pressure recordings. The component of the response is represented in the model as the combination of springs two and three and dashpot two. It is suggested that this component of the response is due to the visco-elastic properties of the lung tissue immediately surrounding the nerve endings which constitute the receptor. Since this rapid transient response of the receptor is not dependent on similar transients in the pressure recordings, it is probable that the mechanical properties of the lung as a whole are not responsible for this component of the receptors' response. Further support for this argument is that all three responses may be generated by changing but a single component in the model, the compliance of spring two. Anatomical findings indicate receptor location in epithelial and subepithelial tissue. Abundance of elastin, collagen, and smooth muscle fibers in the connective tissue matrix of the lung (81) suggest viscous forces would arise as a consequence of lung

inflation. It is suggested that as the lung is being inflated the epithelial tissue elongates more than its "fair share" because the tension in the connective tissue has a viscous as well as an elastic component. When inflation is terminated viscous forces diminish with time toward zero, connective tissue elongates, and epithelial tissue tension (and length) decreases. It is also suggested that epithelial tissue in close proximity to the connective tissue undergoes a lesser overshoot in tension than epithelial tissue which borders the lung interior. The position of the receptor within the lung tissue could determine the response characteristics of the receptor; superficial receptors being rate receptors and receptors lying in the deeper structures of the lung being closer to proportional receptors.

The locations of the various types of receptors within the lung tissue which have been proposed in this study are the same locations which Widdecombe (57) proposed for the rapidly adapting and slowly adapting receptors of the cat lung. Widdecombe proposed a deep, possibly smooth muscle locus for the slowly adapting stretch receptor of the cat. The proportional and rate plus proportional receptors of the frog lung probably have a subepithelial locus. According to the adaptation terminology the proportional and rate plus proportional receptors are slowly adapting receptors. Widdecombe proposed a superficial, epithelial locus for the rapidly adapting stretch receptor of the cat lung. The rate (rapidly adapting) receptor of the frog lung

probably has a superficial locus.

Matthews (28) in his studies of the muscle spindle was one of the first investigators to propose that mechanical filtering by surrounding tissue could explain the response characteristics of mechanoreceptors. Toyama (30), Houk (42), and Angers (82) adopted and expanded Matthew's proposition in that they developed visco-elastic models of the muscle spindle and the surrounding muscle tissue which simulated the actual recorded responses from the spindle afferents. However, none of these investigators determined the actual visco-elastic properties of the surrounding tissue. In contrast Loewenstein and Mendelson (35) and Hubbard (27) investigated the mechanical properties of the lamellar tissue of the Pacinian corpuscle and found these visco-elastic properties were necessary and sufficient to explain the response characteristics of the corpuscle. As in this study Houk (37) found in the tendon organ a slow decay component in both the receptor response and the tension in the surrounding tissue following a rapid increase in the length of the surrounding tissue. The decay in discharge frequency was thought to have been a direct result of the decreasing tissue tension. In contrast to Houk's study, both the rapid decay component of the receptor response and the tissue tension was seen in this study. A study of a mechanoreceptor found in frog skin which employed such techniques as mechanical stimulation, electrical stimulation, selective enzymic

destruction of tissue and modeling prompted Catton and Petoe (83) to suggest that the response characteristics of this mechanoreceptor could be explained by the visco-elastic characteristics of the surrounding tissue. Thus the results of this study combined with the findings of others strongly suggest that the characteristic response of a mechanoreceptor is in part, if not wholly, determined by the mechanical properties of the tissue surrounding the receptor. It is suggested that the behavior of the pulmonary mechanoreceptor of the frog is in part determined by the mechanical properties of the lung as a whole. The mechanical (visco-elastic) properties of the lung tissue immediately surrounding the nerve endings determine the receptor's ability to function as a rate, rate plus proportional, or proportional receptor.

SUMMARY AND CONCLUSIONS

The pressure-volume characteristics of the frog lung were studied and were similar in many respects to the pressure-volume characteristics of the mammalian lung.

The discharge frequency of single afferent fibers associated with pulmonary tension receptors was studied during half-trapezoidal and sinusoidal inflation of the lung. On the basis of their response characteristics, receptors were classified as either rate, rate plus proportional, or proportional receptors. A linear approximation of the transfer function of each of these three groups was given by

$$\frac{S}{(S + 5)(S + 0.1)}, \quad \frac{(S + 0.24)}{(S + 5)(S + 0.1)}, \quad \text{and} \quad \frac{(S + 2.5)}{(S + 7.5)(S + 0.1)}$$

respectively.

The term $(S + 0.1)$ was thought to have resulted as a consequence of the filtering properties of the lung as a whole. The remaining terms were thought to result as a consequence of the viscoelastic properties of the tissue immediately surrounding the receptor. There was no need to postulate different nerve endings between groups as the location of a single type of nerve ending within the lung tissue was sufficient to explain the three types of responses.

BIBLIOGRAPHY

1. Ruch, T. C. & Fulton, J. F. (Ed.) *Medical Physiology and Biophysics*. Philadelphia and London: W. B. Saunders Company, 1960. (page 502)
2. Ruch, T. C., & Patton, H. D. (Ed.) *Physiology and Biophysics*. Philadelphia and London: W. B. Saunders Company, 1965. (page 95)
3. Ruch, T. C. & Patton, H. D. (Ed.) *Physiology and Biophysics*. Philadelphia and London: W. B. Saunders Company, 1965. (page 96)
4. Terzuolo, C. A., & Washizu, Y. Relation between stimulus strength, generator potential and impulse frequency in stretch receptor of crustacea. *J. Neurophysiol.*, 1962. 25, 56-66.
5. Katz, B. Depolarization of sensory terminals and initiation of impulses in the muscle spindle. *J. Physiol. (London)*, 1950. 111, 261-282.
6. Loewenstein, W. R. The generation of electric activity in a nerve ending. *Ann. N. Y. Acad. Sci.* 1958. 81, 367-387.
7. Sherrington, C. S. *The integrative action of the nervous system*. New Haven: Yale University Press, 1906. (page 12)
8. Dodt, E., & Zotterman, Y. Mode of action of warm receptors. *Acta. Physiol. Scand.* 1952. 26, 345-357.
9. Granit, R. *Sensory mechanisms of the retina*. London, New York, and Toronto: Geoffrey Cumberlege Oxford University Press, 1947.
10. Bronk, D. W., & Stella, G. Afferent impulses in the carotid sinus nerve. *J. Cell. Comp. Physiol.* 1932. 1, 113-130.
11. Davis, H. Excitation of auditory receptors. In J. Field, H. W. Magoun, & V. E. Hall (Ed.) *Handbook of physiology*. Vol. I, Section 1. Washington, D. C.: American Physiological Society, 1959.
12. Hornbein, T., & Roos, A. Specificity of H⁺ ion concentration

- as a carotid chemoreceptor stimulus. *J. Appl. Physiol.* 1963. 18, 580-584.
13. Adrian, E. D., & Zotterman, Y. The impulses produced by sensory endings. *J. Physiol. (London)*, 1926. 61, 151-171.
 14. Hagiwara, S., Kusano, K., & Negishi, K. Physiological properties of electroreceptors of some gymnotids. *J. Neurophysiol.*, 1962. 25, 430-449.
 15. Granit, R. The colour receptors of the mammalian retina. *J. Neurophysiol.*, 1945. 8, 195-210.
 16. MacNichol, E. F. Visual pigments of single primate cones. *Science*, 1964. 143, 1181-1183.
 17. Ruch, T. C., & Patton, H. D. (Ed.) *Physiology and Biophysics*. Philadelphia and London: W. B. Saunders Company, 1965. (page 420)
 18. Skoglund, S. Anatomical and physiological studies of knee joint innervation in the cat. *Acta Physiol. Scand.*, 1956. Suppl. 124.
 19. Gray, E. G. The spindle and extrafusal innervation of a frog muscle. *Proc. Roy. Soc. [Biol.]*, 1956. 146, 416-430.
 20. Hodgkin, A. L. The local electric changes associated with repetitive action in a non-medullated axon. *J. Physiol. (London)*, 1948. 107, 165-181.
 21. Diamond, J., Gray, J. A. B., & Inman, D. R. The relation between receptor potentials and the concentration of sodium ions. *J. Physiol. (London)*, 1958. 142, 382-394.
 22. Loewenstein, W. R. Biological transducers. *Scientific American*, 1960. 203, 98-108.
 23. Edwards, C., & Ottoson, D. The site of impulse initiation in a nerve cell of a crustacean stretch receptor. *J. Physiol. (London)*, 1958. 143, 138-148.
 24. Eyzaguirre, C., & Kuffler, S. W. Processes of excitation in the dendrites and in the soma of single isolated sensory nerve cells of the lobster and crayfish. *J. Gen. Physiol.*, 1955. 39, 87-119.

25. Julian, F. J., & Goldman, D. E. The effects of mechanical stimulation on some electrical properties of axons. *J. Gen. Physiol.*, 1962. 46, 297-313.
26. Goldman, D. E. The transducer action of mechanoreceptor membranes. *Cold Spring Harbor Symposia on Quantitative Biology*, 1965. 30, 56-68.
27. Hubbard, S. J. A study of rapid mechanical events in a mechanoreceptor. *J. Physiol. (London)*, 1958. 198-218.
28. Matthews, B. H. C. Nerve endings in mammalian muscle. *J. Physiol. (London)*, 1933. 78, 1-53.
29. Katz, B. Sensory terminations in the muscle spindle of the frog. *J. Physiol. (London)*, 1960. 152, 13-14P.
30. Toyama, K. An analysis of impulse discharges from the spindle receptor. *Jap. J. Physiol.*, 1966. 16, 113-125.
31. Matthews, P. B. C. Muscle spindles and their motor control. *Physiol. Rev.*, 1964. 44, 219-288.
32. Schäfer, S. The acceleration response of primary muscle spindle endings to ramp stretch of extrafusal muscle. *Experientia*, 1967. 23, 1026-1027.
33. Gray, J. A. B., & Sato, M. Properties of the receptor potential in Pacinian corpuscles. *J. Physiol. (London)*, 1953. 122, 610-636.
34. Loewenstein, W. R. Facets of a transducer process. *Cold Spring Harbor Symposia on Quantitative Biology*, 1965. 30, 29-43.
35. Mendelson, M., & Loewenstein, W. R. Mechanisms of receptor adaptation. *Science*, 1964. 144, 554-555.
36. Houk, J. C., & Simon, W. Responses of Golgi tendon organs to forces applied to muscle tendon. *J. Neurophysiology*, 1967. 30, 1466-1481.
37. Houk, J. C. A viscoelastic interaction which produces one component of adaptation in responses of Golgi tendon organs. *J. Neurophysiol.*, 1967. 30, 1482-1493.

38. Houk, J. C., & Henneman, E. Responses of Golgi tendon organs to active contractions of the soleus muscle of the cat. *J. Neurophysiol.* 1967. 30, 466-481.
39. Brown, M. C., & Stein, R. B. Quantitative studies on the slowly adapting stretch receptor of the crayfish. *Kybernetik*, 1966. 3, 175-185.
40. Chapman, K. M., & Smith, R. S. A linear transfer function underlying impulse frequency modulation in a cockroach mechanoreceptor. *Nature*, 1963. 197, 699-700.
41. Pringle, J. W. S., & Wilson, V. J. The response of a sense organ to a harmonic stimulus. *J. Exp. Biol.*, 1952. 29, 220-234.
42. Houk, J. C. A mathematical model of the stretch reflex in human muscle systems. Unpublished master's dissertation, M. I. T., 1964.
43. Borsellino, A., Poppele, R. E., & Terzuolo, C. A. Transfer functions of the slowly adapting stretch receptor organ of crustacea. *Cold Spring Harbor Symposia on Quantitative Biology*, 1965. 30, 581-586.
44. Spickler, J. W., & Kezdi, P. Dynamic response characteristics of carotid sinus baroreceptors. *Amer. J. Physiol.*, 1967. 212, 472-476.
45. Sagawa, K., Ross, J. M., & Guyton, A. C. Quantitation of cerebral ischemic pressor response in dogs. *Amer. J. Physiol.*, 1961. 200, 1164-1168.
46. Levison, W. H., Barnett, G. O., & Jackson, W. D. Nonlinear analysis of the baroreceptor reflex system. *Circulation Research*, 1966. 18, 673-682.
47. Hering, E., & Breuer, J. Die Selbststeuerung der Athmung durch den Nervus vagus. *Sitzber. Akad. Wiss. Wien.*, 1868. 57, 672-677. According to Widdecombe, J. G. Respiratory reflexes. In Fenn, W. O., & Rahn, H. (Ed.). *Handbook of physiology*. Vol. I, Section 3. Washington, D. C.: American Physiological Society, 1964.
48. Breuer, J. Die Selbststeuerung der Atmung durch den Nervus

- vagus. Sitzber. Akad. Wiss. Wien., 1868. 58, 909-937.
According to Widdecombe, J.G. Respiratory reflexes. In
Fenn, W.O., & Rahn, H. (Ed.). Handbook of physiology.
Vol. I, Section 3. Washington, D.C.: American Physiological
Society, 1964.
49. Anrep, G.V., & Samaan, A. Double vagotomy in relation to
respiration. *J. Physiol. (London)*, 1933. 77, 1-15.
 50. Hammouda, M., Samaan, A., & Wilson, W.H. The origin of
the inflation and deflation pulmonary reflexes. *J. Physiol.*
(London), 1943. 101, 446-459.
 51. Einthoven, W. On vagus currents examined with the string
galvanometer. *Quart. J. Exp. Physiol.*, 1908. 1, 243-245.
 52. Lewandowski, M. Ueber Schwankungen des Vagusstromes
bei Volumänderungen der Lunge. *Pflueger. Arch. Ges.*
Physiol. 1898. 73, 288-296.
 53. Alcock, N.H., & Seeman, J. Ueber die negative Schwankung
in den Lungenfasern des Vagus. *Pflueger. Arch. Ges.*
Physiol., 1905. 108, 426-446.
 54. Adrian, E.D. Afferent impulses in the vagus and their effect
on respiration. *J. Physiol. (London)*, 1933. 79, 332-358.
 55. Davis, H.L., Fowler, W.S., & Lambert, E.H. Effect of
volume and rate of inflation and deflation on transpulmonary
pressure and response of pulmonary stretch receptors.
Amer. J. Physiol., 1956. 187, 558-566.
 56. Knowlton, G.C., & Larrabee, M.G. A unitary analysis of
pulmonary volume receptors. *Amer. J. Physiol.*, 1946.
147, 100-114.
 57. Widdecombe, J.G. Respiratory reflexes from the trachea
and bronchi of the cat. *J. Physiol. (London)*, 1954. 123,
55-104.
 58. Larsell, O., & Dow, R.S. The innervation of the human lung.
Amer. J. Anat., 1933. 52, 125-146.
 59. Elftman, A.G. The afferent and parasympathetic innervation
of the lungs and trachea of the dog. *Amer. J. Anat.*, 1943.
72, 1-28.

60. Head, H. On the regulation of respiration. *J. Physiol.* (London), 1889. 10, 1-70; 279-290.
61. Wolff, M. Uber Ehrlich'sche Methylenblaufarbung und uber Lage und Bau einiger peripherer Nervenendigungen. *Arch. Anat. Entwickl.*, 1902. 5, 155-183.
62. Cuccati, G. Sopra il distribuimento e la terminazione delle fibre nervee nei polmoni della Rana temporaria. *Internat. Mschr. Anat. Physiol.*, 1888. 5, 194-203. According to Wolff (60).
63. Gaupp, E. (Ed.). A. Eckers u. R. Wierdersheims Anatomie des Frosches. Vol. III. Braunschweig: Vieweg, 1904. (pages 198-199)
64. Carlson, A. J., & Luckhardt, A. B. Studies on the visceral sensory nervous system. I. Lung automatism and lung reflexes in the frog (R. pipiens and R. catesbiana). *Amer. J. Physiol.*, 1920. 54, 55-95.
65. Neil, E., Ström, L., & Zotterman, Y. Action potential studies of afferent fibers in the IXth and Xth cranial nerves of the frog. *Acta. Physiol. Scand.*, 1950. 20, 338-350.
66. Bonhoeffer, K., & Kolatatz, T. Druckvolumendiagramm und Dehnungreceptoren der Froschlunge. *Pfluger. Arch. Ges. Physiol.* 1958. 265, 477-484.
67. Kilburn, K.H. Mucociliary clearance from bullfrog (Rana catesbiana). *J. Appl. Physiol.*, 1967. 23, 804-810.
68. Taglietti, V., & Casella, C. Stretch receptor stimulation in frog's lungs. *Pfluger. Arch. Ges. Physiol.*, 1966. 292, 297-308.
69. Pattle, R.E. Surface lining of lung alveoli. *Physiol. Rev.*, 1965. 45, 48-79.
70. Edmunds, L.H., & Huber, G.L. Pulmonary artery occlusion. I. Volume-pressure relationships and alveolar bubble stability. *J. Appl. Physiol.*, 1967. 22, 990-1001.
71. Thompson, R.F. A brief outline of some statistical methods used in medicine. Portland: University of Oregon Medical

- School, Dept. of Public Health and Preventive Medicine, 1963. (pages 7-8)
72. Milhorn, H. T. The application of control theory to physiological systems. Philadelphia: W. B. Saunders, 1966. (page 108)
 73. Goodman, L. S., & Gillman, A. (Ed.) The pharmacological basis of therapeutics. New York: The Macmillan Company, 1965. (page 607)
 74. Agostoni, E., & Mead, J. Statics of the respiratory system. In Fenn, W. O., & Rahn, H. (Ed.) Handbook of physiology. Vol. I, section 3. Washington, D. C.: American Physiological Society, 1964. (page 400)
 75. Agostoni, E., & Mead, J. Statics of the respiratory system. In Fenn, W. O., & Rahn, H. (Ed.) Handbook of physiology. Vol. I, section 3. Washington, D. C.: American Physiological Society, 1964. (page 400)
 76. Hildebrandt, J. Model describing static hysteresis component of PV loops. *The physiologist*, 1967. 10, 201. (Abstract)
 77. Gray, J. A. B., & Matthews, P. B. C. A comparison of the adaptation of the Pacinian corpuscle with the accommodation of its own axon. *J. Physiol. (London)*, 1951. 114, 454-464.
 78. Sedlin, E. D. A rheologic model for cortical bone. *Acta Orthopaedica Scandinavia*, 1965. Supplementum 83.
 79. Knox, C. K. Simulation of the transfer function of a crustacean muscle bundle. *Simulation*, 1968. 10, 93-96.
 80. Davenport, H. W. *Physiology of the digestive tract*. (2nd Ed.) Chicago: Year Book Medical Publishers Inc., 1966. (pages 47-48)
 81. Okada, Y., Ishiko, S., Daido, S., Kim, J., & Ikeda, S. Comparative morphology of the lung with special reference to the alveolar epithelial cells. I. Lung of the amphibia. *Acta Tuberc. Jap.*, 1962. 11, 63-72.
 82. Angers, D. Modéle mécanique de fuseau neuro-musculaire de-efferenté: terminaisons primaires et secondaires. *Compt. Rend. Acad. Sci., Paris*, 1965. 261, 2255-2258.

83. Catton, W. T., & Petoe, N. A visco-elastic theory of mechanoreceptor adaptation. *J. Physiol. (London)*, 1966. 187, 35-49.
84. Kay, R. H. Reciprocal time meter. *Electronic Engineering*, 1965. 37, 543-545.
85. Matthews, P. B. C. The differentiation of two types of fusimotor fibre by their effects on the dynamic response of the muscle spindle primary endings. *Quart. J. Exp. Physiol.*, 1962. 47, 324-333.

APPENDIX

APPENDIX

Justification of Toyama's Model - see page 22

The position of the right hand side of the series spring (spring one) is stationary. The position of the left hand side is given by x_1 . The length of the parallel arrangement of spring two and dashpot is given by $x_2 - x_1$. For case one the output is proportional to the tension in spring one.

Case one:

1. $(X_2 - X_1)(C_2 + sD) = X_1 C_1$.
2. $X_2(C_2 + sD) = X_1(C_1 + C_2 + sD)$.
3. $(C_2 + sD)/(C_1 + C_2 + sD) = X_1/X_2$

For the second case where the output is derived from both springs, let a be the contribution of spring two to the output and $1 - a$ be the contribution from spring one.

Case two:

4. $(X_2 - X_1)(C_2 + sD) = X_1 C_1$.
5. $(X_2 = X_1) = X_1 C_1 / (C_2 + sD)$.
6. $a(X_2 - X_1) + (1 - a)X_1 = [aC_1 X_1 / (C_2 + sD)] + (1 - a)X_1$.
7. $[a(X_2 - X_1) + (1 - a)X_1] / X_2 = \frac{X_1(aC_1 + C_2 + sD - aC_2 - asD)}{X_2(C_2 + sD)}$

From equation 3 (X_1/X_2) the T. F. equals

$$8. [aC_1 + sD - asD + C_2(1 - a)] / (C_1 + C_2 + sD).$$

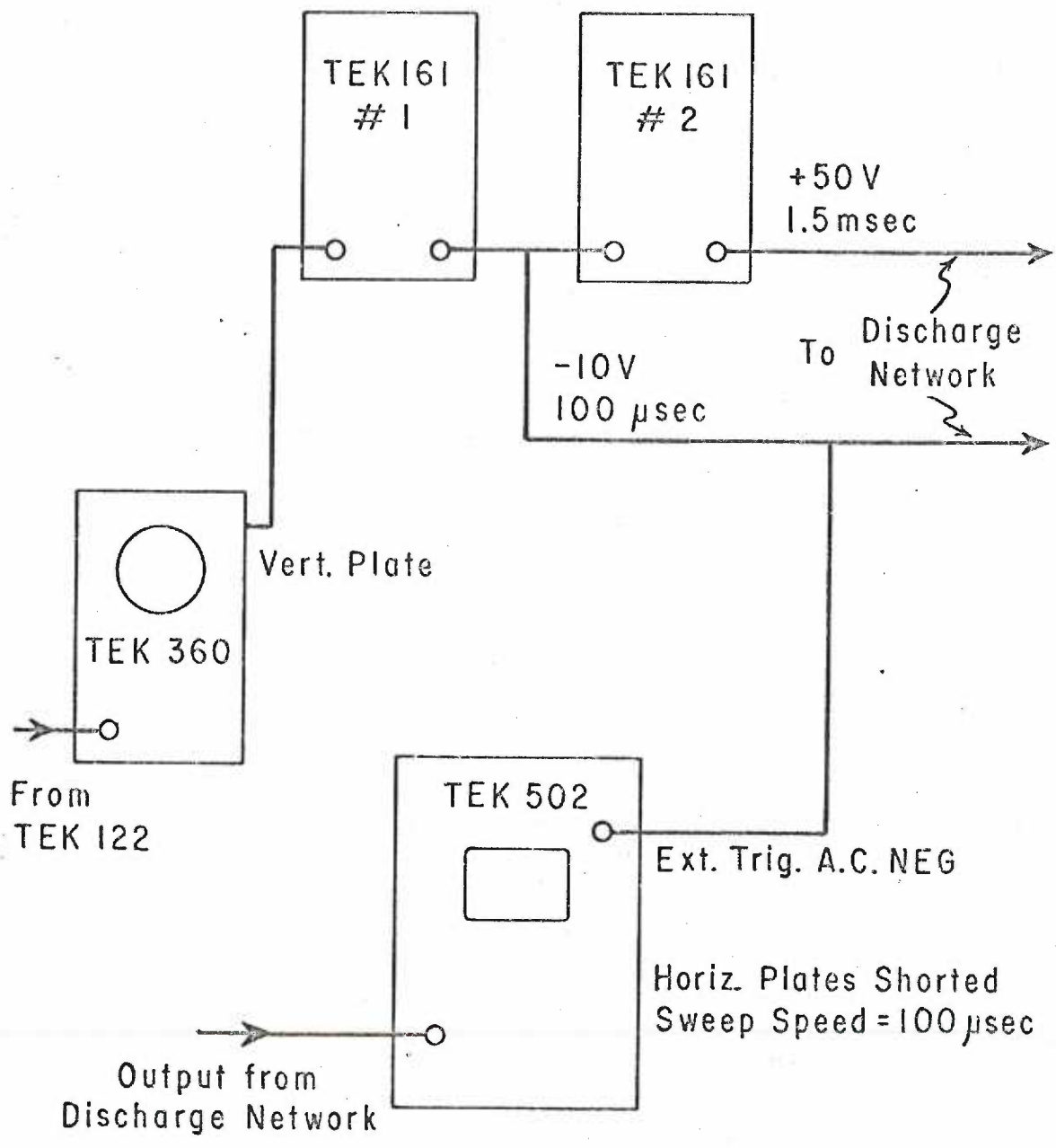
The C_2 in the first case is equivalent to $[aC_1 + C_2(1 - a)]$ in the second case and D in the first case is equivalent to $D(1 - a)$ in the second case. Thus a suitable change in coefficients allows equivalence of the two models.

Instantaneous Frequency Meter - see page 67

The instantaneous frequency meter was developed by R. H. Kay (84) for P. B. C. Matthews. The device determined the reciprocal of the time interval between successive action potentials. The principle of operation was based on the generation of a segment of a rectangular hyperbola $V = K/T$ where V and T are voltage and time respectively and K is a constant. The meter described in the following was an extensive modification of the meter developed by Kay.

Amplified action potentials of a magnitude sufficient to trigger a Tektronix 161 pulse generator were taken from the vertical deflection plate of the Tektronix 360 scope. The voltage of these action potentials was approximately 5-10 volts with a D. C. level of 100 volts. The action potentials led from the plate of the 360 were capacitatively coupled (600 V, 0.1 μ F) to the positive pulse input of the 161 pulse generator #1 (figure 37). Each action potential triggered a negative 10V, 100 μ s pulse from the 161. The first 161

Figure 37. Triggering system for instantaneous frequency meter.



pulse provided trailing edge triggering to the second 161 pulse generator which charged the discharge network with, 150 ms, positive 50V pulse. The discharge network's (figure 38) output across the discharge capacitor decayed according to $V = K/T$. Each action potential caused recharging of the discharge network from the voltage which remained across the capacitor as a result of the preceding action potential. The output of the discharge network was fed via a 10x probe to the Tektronix 502 scope. The horizontal plates of the 502 were shorted to keep the "trace" in the center of the scope face. The scope was triggered by the pulse of the first 161 pulse generator so that there was a brightening of the spot on the scope face for the duration of the $100\mu\text{s}$ "sweep." The scope face was photographed with the Grass camera. Thus the film record consisted of a number of dots corresponding to the occurrence of the action potentials (figure 39). The height of the dot above the base line was determined by the voltage level across the discharge capacitor when the first 161 pulsed. The voltage level was given by $V = K/T$, that is the reciprocal of the interval between the action potential which triggered the 161 and the preceding triggering action potential. The output of the first 161 was also used to turn off the transistor shown in the discharge network. When this transistor was turned off the network decayed with a very slow time constant. This slow time constant was necessary during the read-out of high frequency discharge.

Figure 38. Discharge network for instantaneous frequency meter.

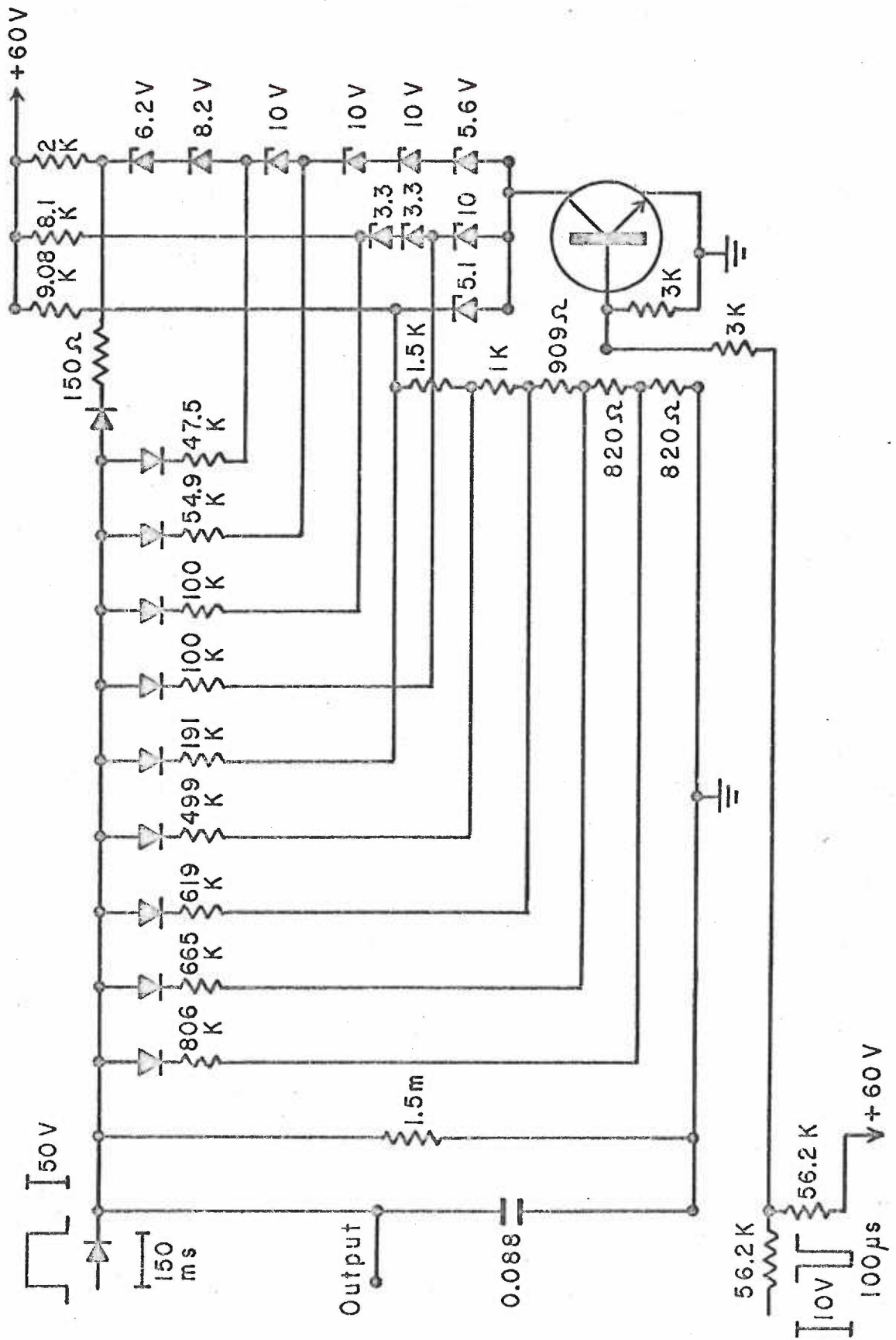
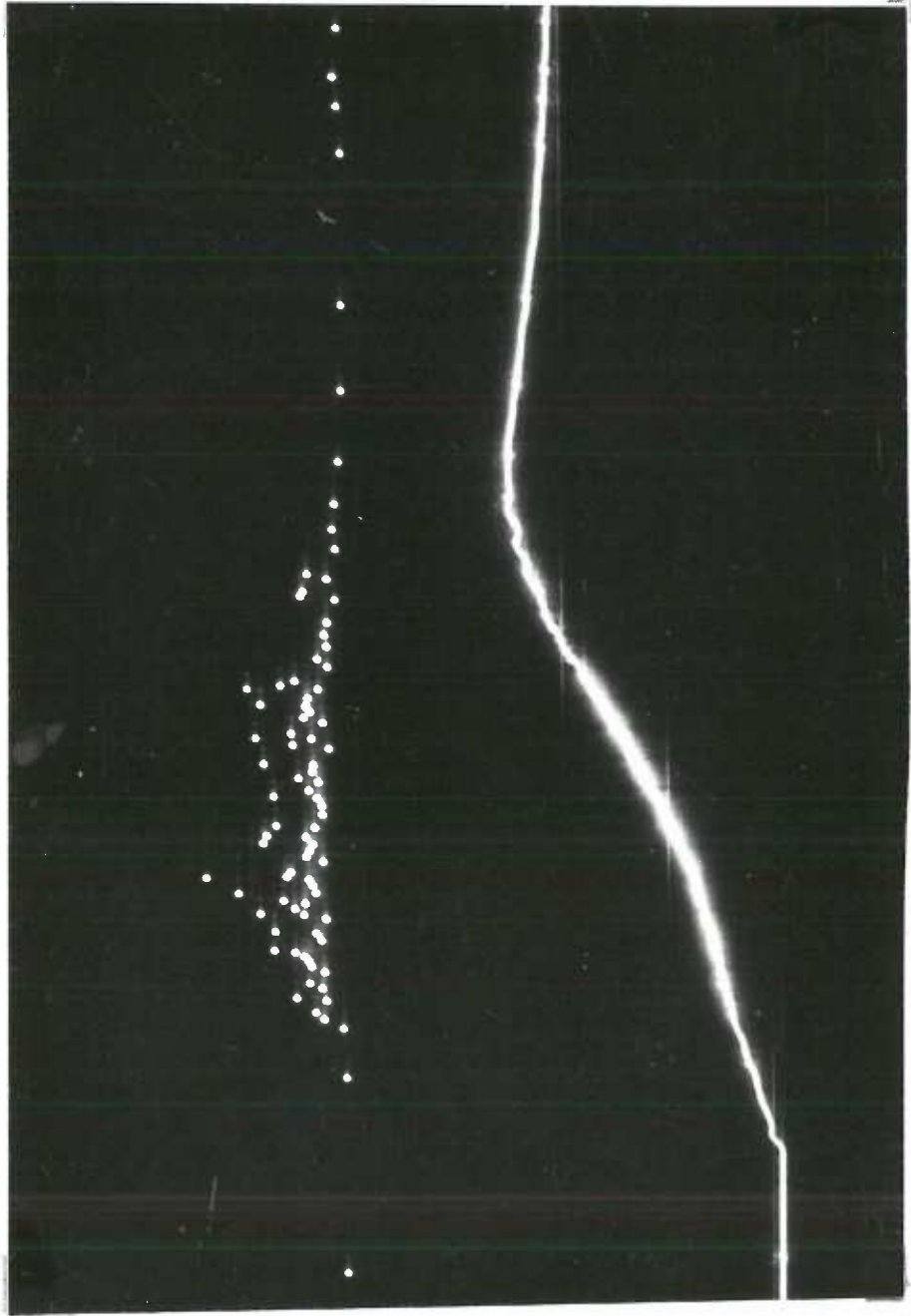


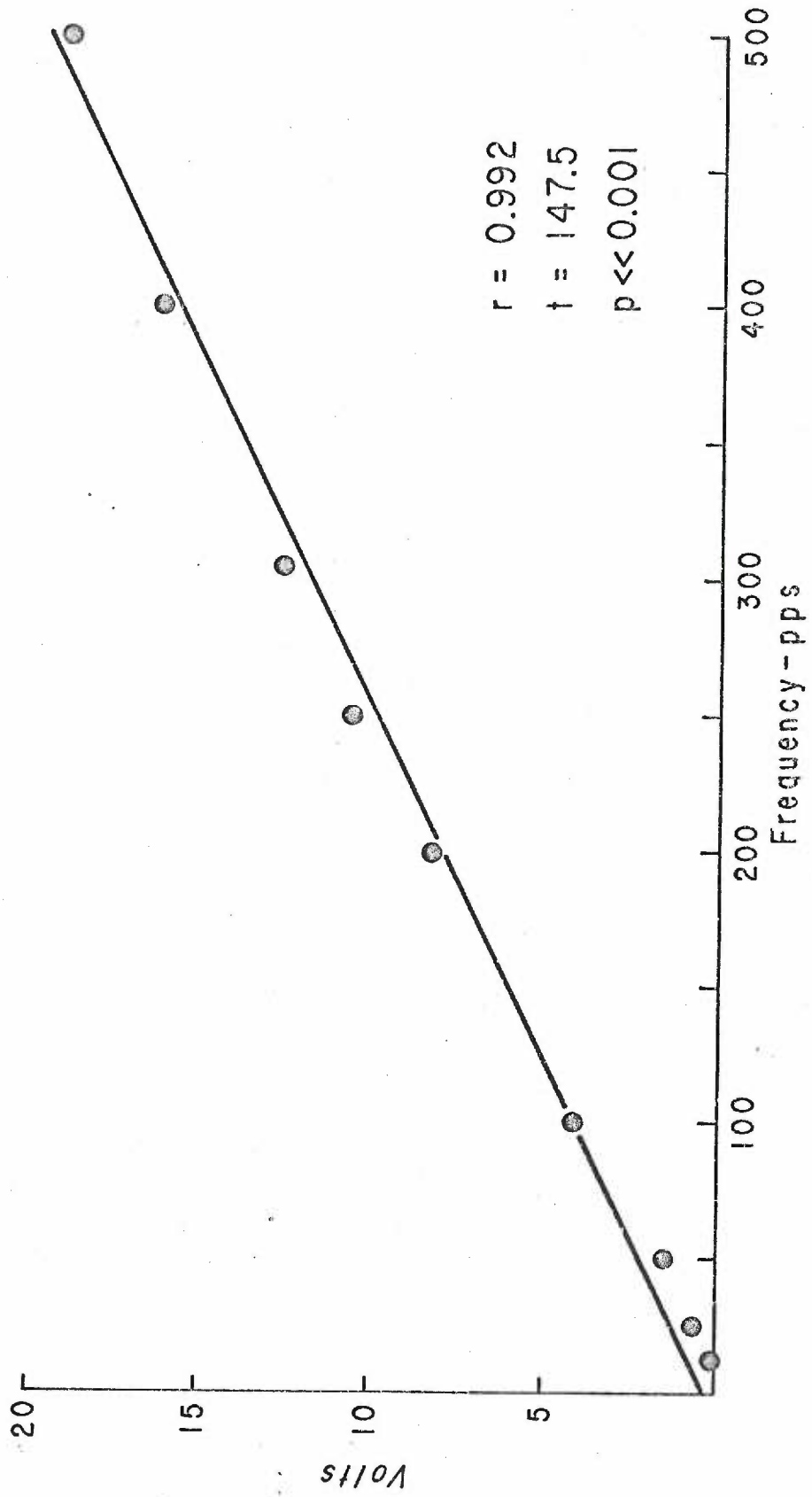
Figure 39. Recording of nerve discharge using instantaneous frequency meter. Top trace, output from meter; bottom trace, record of intrapulmonic pressure. The height of each dot is inversely proportional to the time elapsed from the preceding dot.



Otherwise the dot appeared as a short vertical line on the film record. The relationship between discharge frequency and voltage output of the instantaneous frequency meter is shown in figure 40.

Electronic calculation of reciprocal time has several distinct advantages over hand measurement of discharge frequency, the most important of which is the amount of time necessary for data reduction. A second advantage is an order of magnitude reduction in the amount of photographic film needed for a given experiment. The instantaneous frequency meter has several undesirable features. Amplified action potentials are used to trigger the meter. During the course of an experiment the magnitude of action potentials may diminish to the extent that action potentials are no longer registered. Excessive electrical noise generated during an experiment may cause triggering of the meter and thus obscure the action potential interval data. Although the instantaneous frequency meter has been used in studies dealing with other receptor organs, the measurement of instantaneous frequency of discharge in the frog lung receptor is not desirable. The discharge of the frog lung receptor is not nearly as rhythmic as the discharge in the muscle spindle for example. An instantaneous frequency versus time curve of a muscle spindle is a smooth, continuous curve (85) whereas the curve for the frog lung receptor is irregular and "jumpy." A second electronic method was devised to smooth the response curve of the frog lung receptor. In

Figure 40. Calibration curve for instantaneous frequency meter. Filled circles are experimental points; straight line determined by method of least squares (71); abscissa, pps (pulses per second); ordinate, discharge network output.



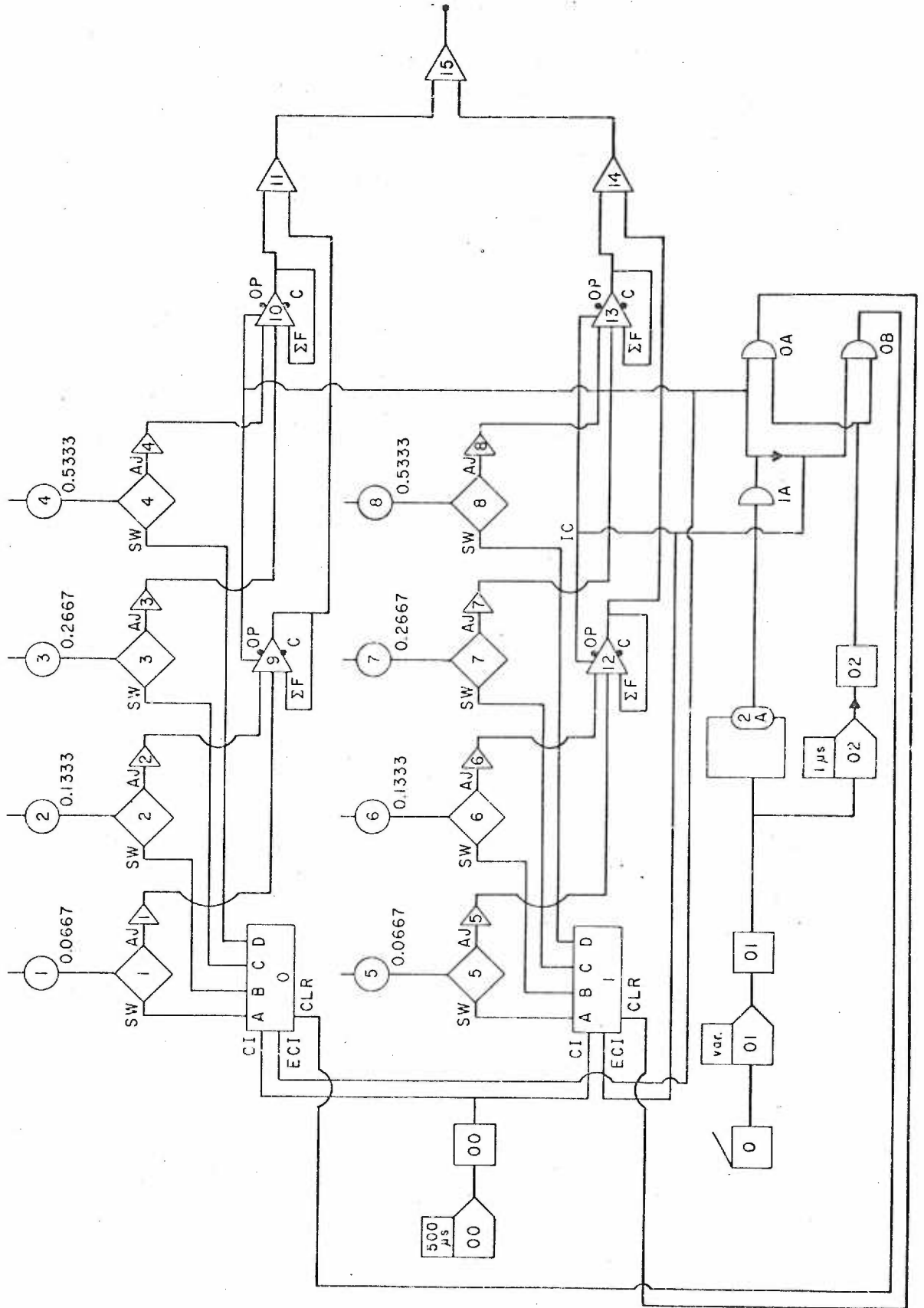
this second method which used the E. A. I. 680 computer the time precision associated with instantaneous frequency was sacrificed for a smoother response curve.

Response Histogram - see page 67

The computer method allowed the determination of the number of action potentials which occurred during successive short time intervals or bins. The relationship between action potentials and computer output is shown in figure 17. Prior to computer analysis the tape recorded action potentials were played back through a Tektronix type 564 storage oscilloscope. Single sweeps were stored and the criteria of constant spike height and discharge rhythmicity were applied to the action potential trace as a check for unitary discharge. Not infrequently two or more active units could be identified on the storage scope face. If one of these units had a spike height much greater than the remaining units and the signal to noise ratio was reasonable, then a 161 pulse generator could be adjusted to trigger on one spike. This 161 pulse generator was the input device to the computer. The patch diagram is shown in figure 41. Amplified action potentials triggered the pulse generator which provided a rectangular pulse of +5 volts and 300μ s duration to monostable 00 which after each pulse was allowed to run for a period of 500μ s. The output from monostable 00 was differentiated by differentiator 00 which

Figure 41. Patch diagram for action potential counting.

Diagram is explained in the text.



produced a positive $1 \mu s$ signal called a "blip" which incremented either register 0 or register 1 depending on which of the two was in the enable state which corresponded to true or high logic at its enable carry input (ECI). These registers were programmed to count for one bin width and hold for one bin width and subsequently clear and repeat the cycle. When one register was counting the other was holding and vice versa.

Push button 0, when engaged, provided a true input to monostable 01 whose cycling time was adjustable from $1 \mu s$ to 10 sec and determined bin width. Differentiator 01 produced a blip synchronous with the beginning of each bin. Each of the blips changed the output of relay 2A from true to false or false to true. The output of relay 2A determined the output of AND gate 1A, true produced true and false produced false. AND gate 1A also had a negative output such that when its output was true, its negative output was false and vice versa. The output of AND gate 1A provided the ECI input to register 0 and the negative output the ECI input to register 1, thus when register 0 was enabled, register 1 was holding and when register 0 was holding, register 1 was enabled.

The blip from differentiator 01 cycled monostable 02 for $1 \mu s$ and differentiator 02 produced a blip as the output from monostable 02 fell from true to false. This $1 \mu s$ delay allowed sufficient time for relay 2A and AND gate 1A to change state. When the output of

AND gate 1A went true register 0 changed from enable to hold and register 1 from hold to enable but less than $1 \mu\text{s}$ later the blip from differentiator 02 provided one of the inputs to AND gates 0A and 0B. The other input to 0A was true and the other input to 0B was false. Thus 0A provided a blip to clear the input of register 1 and reset the register to zero. So the two registers operated 180 degrees out of phase and were cleared and enabled and then held with a period determined by monostable 01. Each of the flip flops contained in the registers could with high logic activate an electronic switch which provided the potentiometer voltage to combination amplifiers which were in turn used as switches. When the output of AND gate 1A was true amplifiers 12 and 13 were in the operating mode and amplifiers 9 and 10 were in initial condition mode. Therefore the contents of register 0 was being read by amplifier 15 only when register 0 was in the hold state, so amplifier 15 alternately sampled the output from register 0 and register 1.

The computer readout was the Grass polygraph with a 5 P1 preamplifier. The amplifier input switch was placed in the DC 1 megaohm position and a X100 input probe was utilized.

between the discharge frequency just before the termination of the ramp (peak frequency) and a few seconds following the ramp was nearly the same (5-10 pps) for all three volumes. This difference represents the receptor's response to rate of change of volume.

Figure 23 illustrates the response of this same unit to changes in the rate of inflation with a constant final volume. As the rate of inflation was increased, the magnitude of the difference between peak and plateau frequency of discharge increased. Figure 23 also illustrates the dependence of "threshold" on rate of inflation. The volume at which discharge commenced was greater at the lowest inflation rate than at the highest inflation rate.

Proportional Receptor

Twenty percent of the forty receptors studied exhibited a discharge pattern that was indicative of a proportional receptor. The response of one of the eight proportional receptors is shown in figure 24. The discharge frequency increased progressively during the ramp. There was little decay in frequency of discharge following transition from constant rate of change to constant volume. The discharge frequency during the constant volume portion of the waveform varied directly with the final volume. The basic discharge pattern was not altered by slower (D) rates of inflation. Figure 25 illustrates the proportional receptor's response to sustained inflation.